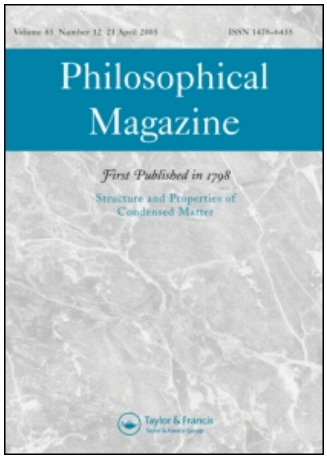

Philosophical Magazine
First published in 1798
Publication details, including instructions for authors and subscription information:
http://www.informaworld.com/smpp/title~content=t713695589

Conjectures on the exact solution of three-dimensional (3D) simple orthorhombic Ising lattices

Z-D Zhang [a]
[a] Shenyang National Laboratory for Materials Science, Institute of Metal Research and International Centre for Materials Physics, Chinese Academy of Sciences, Shenyang 110016, China

Online Publication Date: 01 December 2007
To cite this Article: Zhang, Z-D (2007) 'Conjectures on the exact solution of three-dimensional (3D) simple orthorhombic Ising lattices', Philosophical Magazine, 87:34, 5309 - 5419
To link to this article: DOI: 10.1080/14786430701646325
URL: http://dx.doi.org/10.1080/14786430701646325

Philosophical Magazine,
Vol. 87, No. 34, 1 December 2007, 5309–5419

Conjectures on the exact solution of three-dimensional (3D) simple orthorhombic Ising lattices

Z.-D. ZHANG*

Shenyang National Laboratory for Materials Science,
Institute of Metal Research and International Centre for Materials Physics,
Chinese Academy of Sciences, 72 Wenhua Road, Shenyang 110016, China

(*Received 28 June 2007; in final form 21 August 2007*)

We report conjectures on the three-dimensional (3D) Ising model of simple orthorhombic lattices, together with details of calculations for a putative exact solution. Two conjectures, an additional rotation in the fourth curled-up dimension and weight factors on the eigenvectors, are proposed to serve as a boundary condition to deal with the topologic problem of the 3D Ising model. The partition function of the 3D simple orthorhombic Ising model is evaluated by spinor analysis, employing these conjectures. Based on the validity of the conjectures, the critical temperature of the simple orthorhombic Ising lattices could be determined by the relation of $KK^* = KK' + KK'' + K'K''$ or $\sinh 2K \cdot \sinh 2(K' + K'' + (K'K''/K)) = 1$. For a simple cubic Ising lattice, the critical point is putatively determined to locate exactly at the golden ratio $x_c = e^{-2K_c} = ((\sqrt{5} - 1)/2)$, as derived from $K^* = 3K$ or $\sinh 2K \cdot \sinh 6K = 1$. If the conjectures would be true, the specific heat of the simple orthorhombic Ising system would show a logarithmic singularity at the critical point of the phase transition. The spontaneous magnetization of the simple orthorhombic Ising ferromagnet is derived explicitly by the perturbation procedure, following the conjectures. The spin correlation functions are discussed on the terms of the Pfaffians, by defining the effective skew-symmetric matrix A_{eff}. The true range κ_x of the correlation and the susceptibility of the simple orthorhombic Ising system are determined by procedures similar to those used for the two-dimensional Ising system. The putative critical exponents derived explicitly for the simple orthorhombic Ising lattices are $\alpha = 0$, $\beta = 3/8$, $\gamma = 5/4$, $\delta = 13/3$, $\eta = 1/8$ and $\nu = 2/3$, showing the universality behaviour and satisfying the scaling laws. The cooperative phenomena near the critical point are studied and the results based on the conjectures are compared with those of approximation methods and experimental findings. The putative solutions have been judged by several criteria. The deviations of the approximation results and the experimental data from the solutions are interpreted. Based on the solution, it is found that the 3D-to-2D crossover phenomenon differs with the 2D-to-1D crossover phenomenon and there is a gradual crossover of the exponents from the 3D to the 2D values. Special attention is also paid to the extra energy caused by the introduction of the fourth curled-up dimension and the states at/near infinite temperature revealed by the weight factors of the eigenvectors. The physics beyond the conjectures and the existence of the extra dimension are discussed. The present work is not only significant for statistical and condensed matter physics, but also fill the gap between the quantum field theory, cosmology theory, high-energy particle physics, graph theory and computer science.

*Email: zdzhang@imr.ac.cn

Philosophical Magazine
ISSN 1478–6435 print/ISSN 1478–6443 online © 2007 Taylor & Francis
http://www.tandf.co.uk/journals
DOI: 10.1080/14786430701646325

1. Introduction

The Ising model is of considerable physical significance and value in uncovering principles in the physical world [1]. It was conceived as a description of magnetism in crystalline materials, but is also applicable to phenomena as diverse as the order–disorder transformation in alloys [2–7], transition of liquid helium to its suprafluid state, freezing and evaporation of liquids, the behaviour of glassy substances and even the folding of protein molecules into their biologically active forms. In accordance with the Yang and Lee's theorems [8, 9], the problem of an Ising model in a magnetic field is mathematically equivalent to a lattice gas. The widespread interest in the Ising model is primarily derived from the fact that it is one of the simplest examples describing a system of interacting particles (or atoms or spins). The Ising model is an excellent test case for any new approximation method of investigating systems of interacting particles, especially in understanding the cooperative phenomena and critical behaviour at/near the critical point of a continuous phase transition. Furthermore, the 3D Ising model can serve as a testing model for the evolution of a system of interacting particles (or spins) from infinite temperature down to zero, as it is possible to see the analogy of temperature in the thermodynamics to a variable of time in the dynamics. Therefore, the exact solutions are helpful in understanding the evolution of an equilibrium infinite system, not only for a magnet but also for the Universe. In addition, the formal theory of equilibrium phase transitions has found applications in problems such as continuous quantum phase transitions [10, 11], constructing field and string theories of elementary particles, the transition to chaos in dynamical systems, the long-time behaviour of systems out of equilibrium and dynamic critical phenomena [12].

It is well understood that only the exact solution of a system of interacting particles can be used to fully reveal the cooperative phenomena and critical behaviour at/near the critical point. The two-dimensional (2D) Ising model is one of the few examples solved explicitly [13]. The partition function for the 2D Ising model was evaluated exactly by Onsager [13] using the approach introduced by Kramer and Wannier [14, 15], and Montroll [16]. Later, the problem was solved exactly by a simple and elegant spinor analysis developed by Kaufman and Onsager [17–19]. The temperature dependence of magnetization of a square, rectangular or triangular Ising magnet was calculated by Yang [20], Chang [21] and Potts [22], respectively, using a perturbation method. Newell [23] showed the equalization between a cylindrical crystal studied by Onsager and Kaufman [13, 17–19] and a screw crystal studied by Kramers and Wannier [14, 15]. The statistical mechanics of 2D Ising triangular, honeycomb and Kagomé nets was resolved by various authors [24–38]. A general lattice–statistical model, which included soluble 2D models of phase transitions, such as the ice model [39, 40], hydrogen-bonded ferroelectrics and antiferroelectrics models [41–51], has been proposed [52]. Only a limited number of three-dimensional (3D) systems have been solved, including the four-spin interaction Ising model solved by Suzuki [53], the Zamolodchikov model [54] solved by Barter [55] and its N-state extension by Bazhanov and Baxter [56], the 3D dimer model solved by Huang *et al*. [57]. However, the Suzuki model is actually a 2D system [53, 57], while the Zamolodchikov model and its extension involve unphysical negative Boltzmann weights [55–57]. The Huang *et al*. [57] 3D dimer model,

consisting of layered honeycomb dimer lattices with a specific layer–layer interaction, is the only solvable 3D lattice model with physical Boltzmann weights, but describes dimer configurations in which dimers are confined in planes. As a consequence, the critical behaviour of this 3D dimer model is essentially two-dimensional [58].

The exact solution of the 3D Ising model presents fundamental difficulties. The most reliable information on the behaviour of the 3D Ising model has been provided by exact series expansions of the partition function at low and high temperatures [59–125] and by renormalization group theory near the critical point [126–191] and Monte Carlo simulations [154–186]. Although the region near the critical point has been explored by various approximation methods and its physical properties have been determined numerically with high precision [59–191], to date, physicists have failed to provide the exact mathematical solution for the 3D Ising model. It is clear that the 3D Ising model cannot be exactly solved within the framework of the procedure for solving the 2D Ising lattice, which is disappointing for 3D physicists.

The difficulty in solving the 3D Ising model is evident as it is much more complicated than the 2D Ising model, which is already complex. Attempts to apply the algebraic method used for solving the 2D model to the 3D problem are seriously hindered at an early stage because the operators generate Lie algebras so large as to be of little value [59]. All previous algebraic methods have taken advantage of special properties of the operators and it was not possible to generalize them in any significant way to deal with the 3D Ising system successfully [59]. No spinors, Lie algebras or other specialized algebraic techniques of the type used in the matrix method are required in the combinatorial method, developed by Kac and Ward [60]. However, the combinatorial method introduces some problems in topology that have not been rigorously resolved. This combinatorial method of counting the closed graph cannot be adapted in any obvious way to the 3D problem, as the peculiar topological property of a polygon in three dimensions does not divide the space into an 'inside and outside' [59]. Realizing the numerous problems, many authors have tried various methods to generate approximation results, such as series expansions [61–125], renormalization group and Monte Carlo techniques [126–207], among others. However, any approximation method cannot provide exact information at/near the critical point since, whenever the thermodynamic functions have an essential singularity, it is difficult to perform any computation by successive approximation because the convergence by analytic functions in such cases is notoriously slow [13].

In this work, we shall try to derive a putative exact solution to the 3D Ising model, which must exist in nature, on simple orthorhombic lattices. A completely new mathematical technique must be developed to overcome the various difficulties. This novel mathematical technique must be outside the boundary of previous methods, although we have to follow the processes developed by Onsager, Kaufman and Yang, among others [13, 17–20]. The partition function of the simple orthorhombic Ising model will be evaluated by spinor analysis by introducing two conjectures employing an additional rotation in the fourth curled-up dimension and weight factors on the eigenvectors. These conjectures serve as boundary conditions to deal with the topologic problem of the 3D Ising model so that its

partition function could be evaluated successfully. By introducing the conjectures, a simple and beautiful solution emerges from a complicated system, automatically and spontaneously. The solutions will be compared with the results of various approximations and experiments. The putative exact solutions have been judged by several criteria. The deviations of approximation results and experimental data from the putative solutions are interpreted. The physics beyond the conjectures and the existence of the extra dimension are discussed. The simple and elegant results suggest that the target has been accurately achieved. Nevertheless, it should be emphasized that the validity of the putative solutions depends on the conjectures. In section 2, the simple orthorhombic Ising model will be described briefly and the matrix problem set up. In section 3, the partition function of the simple orthorhombic Ising model will be evaluated by spinor analysis with the help of two conjectures and the specific heat of the simple orthorhombic Ising system will be studied. In section 4, the spontaneous magnetization of the simple orthorhombic Ising magnet will be derived by the perturbation procedure, based on the validity of the conjectures. In sections 5 and 6, the correlation function and susceptibility will be investigated. In section 7, the critical exponents at/near the critical point will be compared with the results of previous approximations and experiments. Sections 8 and 9 contain the discussions and summary. Evaluation of the weight factors are performed in Appendices A and B, respectively, for the simple cubic lattice and the simple orthorhombic lattice. The purpose of the article is to present the calculation procedure and final results of our solutions in comparison with other approximation methods and the experimental data, not to a comprehension review of all advances in the Ising model, which is beyond the scope of this article. Readers interested in advances in various approximation techniques, such as the series expansions, Monte Carlo simulations and the renormalization group techniques, etc., as well as in the experiments, are referred to existing reviews [59, 103–107, 141–144, 149, 152–160, 192–202, 208–225] and references therein.

2. Model and setting up the matrix problem

A system similar to most real systems in 3D, where the atoms occupy blocks on a 3D lattice, like a collection of stacked boxes, was used to establish a 3D Ising model. Our physical model is a simple orthorhombic lattice with m rows and n sites per row in one of l planes. Each site in the lattice could be indexed by (i, j, k) for its location in the coordinate system (rows, column, plane). These sites are occupied by two kinds of constituent atoms, each of which can have its magnetic pole pointing in one of two opposite orientations. In our 3D Ising model of spin 1/2, only interactions between the nearest neighbour atoms are taken into account. Within one plane, the energy of interaction is $+J$ between unlike neighbours in a row, and $+J'$ between unlike neighbours in a column; but $-J$ or $-J'$ between like neighbours in a row or column, respectively. The energy is $+J''$ (or $-J''$) for interaction between unlike (or like) neighbours connecting two neighbouring planes. The unlike or like neighbours correspond to the anti-parallel or parallel arrangement of neighbouring spins. Clearly, our simple orthorhombic Ising model is an extension of the

rectangular Ising model dealt with by Onsager [13] and Kaufman [17]. The Hamiltonian of the 3D Ising model on simple orthorhombic lattices is written as:

$$\widehat{H} = -J\sum_{\tau=1}^{n}\sum_{\rho=1}^{m}\sum_{\delta=1}^{l} s_{\rho,\delta}^{(\tau)} s_{\rho,\delta}^{(\tau+1)} - J'\sum_{\tau=1}^{n}\sum_{\rho=1}^{m}\sum_{\delta=1}^{l} s_{\rho,\delta}^{(\tau)} s_{\rho+1,\delta}^{(\tau)} - J''\sum_{\tau=1}^{n}\sum_{\rho=1}^{m}\sum_{\delta=1}^{l} s_{\rho,\delta}^{(\tau)} s_{\rho,\delta+1}^{(\tau)}. \quad (1)$$

The probability of finding the simple orthorhombic Ising lattices in a given configuration, at temperature T, is proportional to $\exp\{-E_c/k_B T\}$, where E_c is the total energy of the configuration and k_B is the Boltzmann constant. The exponent appearing in the expression for the probability is always of the form:

$$\frac{(n_c \cdot J + n_c' \cdot J' + n_c'' \cdot J'')}{k_B T}.$$

Here n_c, n_c' and n_c'' are integers depending on the configuration of the lattice. Again, it is convenient to introduce variables $K \equiv (J/k_B T)$, $K' \equiv (J'/k_B T)$ and $K'' \equiv (J''/k_B T)$ instead of J, J' and J''. Note that the notation K is the same as H in studies of Onsager and Kaufman [13, 17, 18] and Yang [20]. Then, the probability of a configuration reads as:

$$\frac{1}{Z}\exp\{n_c K + n_c' K' + n_c'' K''\}$$

where Z is the partition function for the lattice:

$$Z = \sum_{\text{all configurations}} e^{n_c K + n_c' K' + n_c'' K''}. \quad (2)$$

The thermodynamic functions for the simple orthorhombic Ising model can be found from knowledge of Z but, unfortunately, the problem is much more complex than the case of a 2D Ising model, since the number of terms in Z is $2^{m \cdot n \cdot l}$. Following the procedure developed by Kaufman [17], we also introduce the fiction of spin attributed to each atom. All atoms of one type will be given the spin $+1$, the others a spin -1. So, the interaction between two neighbouring atoms with spins μ, μ' is: $-\mu\ \mu' K$ (or $-\mu\ \mu' K'$ or $-\mu\ \mu' K''$) for row (or column or plane) neighbours. The configurations of the magnet can now be specified either by stating the value of μ at each site of the magnet or by considering the row configurations. The latter is more convenient. Since within one plane there are n atoms in a row and there are l planes, there are $2^{n \cdot l}$ possible configurations, $1 \le \nu \le 2^{n \cdot l}$. Then, the configuration of the simple orthorhombic Ising model is given by the set $\{\nu_1, \nu_1, \ldots, \nu_m\}$.

The energy due to interactions within the ith row in all the planes is denoted by $E'(\nu_i)$; the energy due to interaction between two adjacent rows in all the planes by $E(\nu_i, \nu_{i+1})$; the energy due to interaction between two ith rows in two adjacent planes by $E''(\nu_i)$. As a result, the energy of a configuration of the crystal is represented as:

$$E_c = \sum_{i=1}^{m} E'(\nu_i) + \sum_{i=1}^{m} E''(\nu_i) + \sum_{i=1}^{m} E(\nu_i, \nu_{i+1}). \quad (3)$$

For the purpose of symmetry, it is assumed that the mth row in each plane of the crystal interacts with the first row in that plane. Thus, we actually apply the cylindrical crystal model preferred by Onsager [13] and Kaufman [17], in which we wrap our crystal on cylinders. However, in the present 3D case, there are l coaxial cylinders corresponding to l planes, while in the 2D case there is only a cylinder. Making the abbreviations:

$$(V_1)_{\nu_i\nu_{i+1}} \equiv \exp\left\{\frac{-E(\nu_i, \nu_{i+1})}{k_B T}\right\}, \tag{4a}$$

$$(V_2)_{\nu_i\nu_i} \equiv \exp\left\{\frac{-E'(\nu_i)}{k_B T}\right\}, \tag{4b}$$

$$(V_3)_{\nu_i\nu_i} \equiv \exp\left\{\frac{-E''(\nu_i)}{k_B T}\right\}, \tag{4c}$$

one finds that the probability of a configuration is proportional to

$$\begin{aligned} e^{-E_c/k_B T} = {} & (V_3)_{\nu_1\nu_1}(V_2)_{\nu_1\nu_1}(V_1)_{\nu_1\nu_2}(V_3)_{\nu_2\nu_2}(V_2)_{\nu_2\nu_2}(V_1)_{\nu_2\nu_3} \times \cdots \\ & \times (V_3)_{\nu_m\nu_m}(V_2)_{\nu_m\nu_m}(V_1)_{\nu_m\nu_1}. \end{aligned} \tag{5}$$

Therefore, the partition function becomes:

$$\begin{aligned} Z = {} & \sum_{\nu_1,\nu_2,\ldots\nu_m} (V_3)_{\nu_1\nu_1}(V_2)_{\nu_1\nu_1}(V_1)_{\nu_1\nu_2}\ldots(V_3)_{\nu_m\nu_m}(V_2)_{\nu_m\nu_m}(V_1)_{\nu_m\nu_1} \\ \equiv {} & \operatorname{trace}(V_3 V_2 V_1)^m. \end{aligned} \tag{6}$$

Since for each i: $1 \le \nu_i \le 2^{n \cdot l}$, we find that $\mathbf{V_1}$, $\mathbf{V_2}$ and $\mathbf{V_3}$ are $2^{n \cdot l}$-dimensional matrices and $\mathbf{V_2}$ and $\mathbf{V_3}$ are diagonal. $\mathbf{V_1}$, $\mathbf{V_2}$ and $\mathbf{V_3}$ can be given explicitly as:

$$V_3 = \exp\left\{K'' \cdot \sum_{r=1}^{n}\sum_{s=1}^{l} s''_{r,s}s''_{r,s+1}\right\} \equiv \exp\{K'' \cdot A''\}, \tag{7a}$$

$$V_2 = \exp\left\{K' \cdot \sum_{s=1}^{l}\sum_{r=1}^{n} s'_{r,s}s'_{r+1,s}\right\} \equiv \exp\{K' \cdot A'\}, \tag{7b}$$

$$V_1 = (2\sinh 2K)^{n \cdot l/2} \cdot \exp\left\{K^* \cdot \sum_{s=1}^{l}\sum_{r=1}^{n} C_{r,s}\right\}. \tag{7c}$$

Here $\mathbf{s''_{r,s}}$, $\mathbf{s'_{r,s}}$ and $\mathbf{C_{r,s}}$ are $2^{n \cdot l}$-dimensional quaternion matrices:

$$s''_{r,s} \equiv 1 \otimes 1 \otimes \cdots \otimes 1 \otimes s'' \otimes 1 \otimes \cdots \otimes 1, \tag{8a}$$

$$s'_{r,s} \equiv 1 \otimes 1 \otimes \cdots \otimes 1 \otimes s' \otimes 1 \otimes \cdots \otimes 1, \tag{8b}$$

$$C_{r,s} \equiv 1 \otimes 1 \otimes \cdots \otimes 1 \otimes C \otimes 1 \otimes \cdots \otimes 1, \tag{8c}$$

there are $n \cdot l$ factors in each direct-product, with $\mathbf{s}''$, $\mathbf{s}'$ and $\mathbf{C}$ appearing in the (r, s)th position. $\mathbf{s}''$, $\mathbf{s}'$ and $\mathbf{C}$ are generators of the Pauli spin matrices:

$$s'' \equiv \begin{bmatrix} 0 & -1 \\ 1 & 0 \end{bmatrix}, \; s' \equiv \begin{bmatrix} 1 & 0 \\ 0 & -1 \end{bmatrix}, \; C \equiv \begin{bmatrix} 0 & 1 \\ 1 & 0 \end{bmatrix}, \; 1 = \begin{pmatrix} 1 & 0 \\ 0 & 1 \end{pmatrix}. \tag{9}$$

K^* is defined by

$$e^{-2K} \equiv \tanh K^*. \tag{10}$$

Here, for simplicity, at the beginning of diagonalization procedure, we set up the largest only among K, K′ and K″ as the standard axis for defining K^*. This specialization will be discussed in detail later.

We redefine $\mathbf{V_1}$ to remove the scalar coefficient:

$$V_1 \equiv \exp\left\{ K^* \cdot \sum_{s=1}^{l} \sum_{r=1}^{n} C_{r,s} \right\} \equiv \exp\{K^* \cdot B\}. \tag{11}$$

Then, the partition function is reduced to

$$Z = (2 \sinh 2K)^{(m \cdot n \cdot l)/2} \cdot \text{trace}\,(V_3 V_2 V_1)^m \equiv (2 \sinh 2K)^{(m \cdot n \cdot l)/2} \cdot \sum_{i=1}^{2^{n \cdot l}} \lambda_i^m. \tag{12}$$

where λ_i are the eigenvalues of $\mathbf{V} \equiv \mathbf{V_3} \cdot \mathbf{V_2} \cdot \mathbf{V_1}$.

3. Partition function

In this section, we shall try to evaluate the partition function of the 3D simple orthorhombic Ising crystal by the spinor analysis developed by Kaufman [17] and by introducing two conjectures.

Before dealing with the problem, one needs to analyze the root of the difficulties with the 3D Ising model and the essential difference between the 2D and 3D models. Obviously, the 2D is flat, whereas the 3D has the additional third dimension. The essential difference between the 2D and 3D Ising models is more complex – the key is the difference in topology – the pattern of connections between the nearest-neighbour sites. After comparing the formulae in section 2 with those for the 2D Ising model [17], one finds that, in the 3D case, many of the bonds are nonplanar. These bonds in the 3D Ising model cross over with those in other planes, whereas a 2D rectangular (and even triangular or hexagonal) lattice can always be drawn without crossings, except for a 2D lattice with the next nearest neighbours plus the nearest neighbours [59]. A 2D triangular net can be transformed from a square net with an additional interaction along one of the diagonals [59]. Unfortunately, it has not been possible to solve the case of the interactions along both diagonals for the 2D models. Indeed, no cases that have been solved exactly involve interactions with such crossings. This topological distinction seems to be at the root of all the difficulties with the 3D Ising lattice where the topology of closed paths involve knots [59].

3.1. *Representation of V via spin matrices*

It is clear that matrices of the type $\exp(\mathrm{a}'' \cdot \mathbf{s}''_{\mathbf{r,s}}\mathbf{s}''_{\mathbf{r,s+1}})$, $\exp(\mathrm{a}' \cdot \mathbf{s}'_{\mathbf{r,s}}\mathbf{s}'_{\mathbf{r+1,s}})$, $\exp(\mathrm{b} \cdot \mathbf{C}_{\mathbf{r,s}})$, and their products, form a $2^{n \cdot l}$-dimensional representation of the group of rotations in $2n \cdot l$ dimensions. Thus, the matrix $\mathbf{V}$ itself is the representative of some such rotations.

We start with a set of $2n \cdot l$ quantities $\mathbf{\Gamma_k}$:

$$\begin{aligned}\Gamma_{2r-1} &\equiv C \times C \times \cdots \times s \times 1 \times 1 \times \cdots \equiv P_r,\\ \Gamma_{2r} &\equiv -C \times C \times \cdots \times \mathrm{i}sC \times 1 \times 1 \times \cdots \equiv Q_r, \quad 1 \le r \le nl,\end{aligned} \tag{13}$$

where $n \cdot l$ factors appear in each product; $\mathbf{s}$ or $\mathrm{i}\mathbf{sC}$ appears in the rth place. The $\mathbf{\Gamma_k}$ are $2^{n \cdot l}$-dimensional matrices, which obey the commutation rules

$$\Gamma_k^2 = 1, \Gamma_k \Gamma_l = -\Gamma_l \Gamma_k, (1 \le k, l, \le 2n \cdot l). \tag{14}$$

All possible product of the $\Gamma_{\mathbf{k}}$ form a set of $2^{2n \cdot l}$ matrices, so that any $2^{n \cdot l}$-dimensional matrix can be written as a linear combination of these base matrices. Following the work of Kaufman [17], the matrices $\mathbf{V_1}$, $\mathbf{V_2}$ and $\mathbf{V_3}$ can be represented in terms of the base matrices as:

$$V_3 = \prod_{r=1}^{n} \prod_{s=1}^{l-1} \exp\{-iK'' P_{r,s+1} Q_{r,s}\} \cdot \exp\{iK'' P_{r,1} Q_{r,l} U''_r\}; \tag{15a}$$

$$V_2 = \prod_{s=1}^{l} \prod_{r=1}^{n-1} \exp\{-iK' P_{r+1,s} Q_{r,s}\} \cdot \exp\{iK' P_{1,s} Q_{n,s} U'_s\}; \tag{15b}$$

$$V_1 = \prod_{s=1}^{l} \prod_{r=1}^{n} \exp\{iK^* \cdot P_{r,s} Q_{r,s}\}. \tag{15c}$$

since

$$C_{r,s} = iP_{r,s}Q_{r,s} = 1 \times 1 \times \cdots \times C \times 1 \times \cdots, \tag{16a}$$

$$s'_{r,s} = C_{1,s} C_{2,s} \ldots C_{r-1,s} P_{r,s} = 1 \times 1 \times \cdots \times s \times 1 \times \cdots, \tag{16b}$$

$$s''_{r,s} = C_{r,1} C_{r,2} \ldots C_{r,s-1} P_{r,s} = 1 \times 1 \times \cdots \times \mathrm{i}sC \times 1 \times \cdots. \tag{16c}$$

The end factors in equations (15a) and (15b) differ from others, which originate from the boundary conditions. As mentioned above, it is clear from these boundary conditions that in the 3D Ising model, many of the bonds are nonplanar and that these bonds cross over those in other planes.

We have [17]: if the set $\mathbf{\Gamma_k}$ is a matrix realization of the commutation rules of (14), all the sets $\mathbf{S\Gamma_k S^{-1}}$ will be also realizations of (14). If both sets of matrices, $\mathbf{\Gamma_k}$ and $\mathbf{\Gamma_k^*}$, obey the commutation rules of (14), a transformation $\mathbf{S}$ can be found, such that $\mathbf{\Gamma_k^* = S\Gamma_k S^{-1}}$. The immediate consequences are: two relations between two sets of matrices, $\mathbf{\Gamma_k}$ and $\mathbf{\Gamma_k^*}$, both obeying the commutation rules of (14), can be referred as a rotation in $2n \cdot l$ space and its spin representation in $2^{n \cdot l}$ space of the rotation in $2n \cdot l$ space. If there is a rotation in $2n \cdot l$ space, one can always find a spin representation in $2^{n \cdot l}$ space for the rotation in $2n \cdot l$ space.

Compared with the 2D Ising model, our 3D model is much more complex, topologically, i.e. the knots of interactions between the sites. In what follows, we shall introduce a novel transformation to remove the crossover of the nonplanar bonds to overcome the topologic difficulty of the 3D Ising model, which is the key to solving this problem. We need to find a transformation representing rotations, which must remove simultaneously the crossings of connections for the interactions J' and J'' between neighbours in the lattice, while rearranging elements in matrix $\mathbf{V}$. It is necessary to introduce a conjecture as follow:

Conjecture 1: *The topologic problem of a 3D Ising system can be solved by introducing an additional rotation in a four-dimensional (4D) space, since the knots in a 3D space can be opened by a rotation in a 4D space. One can find a spin representation in $2^{n\cdot l\cdot o}$-space for this additional rotation in $2n\cdot l\cdot o$-space with $o=(n\cdot l)^{1/2}$. Meanwhile, the matrices $\boldsymbol{V}_1$, $\boldsymbol{V}_2$ and $\boldsymbol{V}_3$ have to be represented and rearranged, also in the $2n\cdot l\cdot o$-space.*

This additional rotation in the $2n\cdot l\cdot o$-space appears in $\mathbf{V}$ as an additional matrix $\mathbf{V}_4'$:

$$V_4' = \prod_{t=1}^{n\cdot l\cdot o-1} \exp\{-iK''' P_{t+1} Q_t\} \cdot \exp\{iK''' P_1 Q_{n\cdot l\cdot o} U\}. \tag{17}$$

with:

$$K''' = \frac{K'K''}{K} \text{ for } K \neq 0, \tag{18}$$

considering the symmetry of the system and the topologic problem. The form of $(K'K''/K)$ stands for crossings and/or knots in the 3D Ising model. The introduction of the additional dimension can be treated as a boundary condition to deal with the topologic problem and the non-local behaviour in the 3D physical system. This procedure is similar to the introduction of the well-known Born–Kármán periodic boundary condition for dealing with the energy band of an infinite crystal with free boundary in solid-state physics. In the thermodynamic limit ($N\to\infty$), the periodic boundary condition is equalized mathematically to the free boundary. In our case, the special boundary condition, introduced with the additional rotation, is equalized mathematically to the free boundary of the 3D model in the thermodynamic limit. In mathematics, there are many similar techniques, such as first to rent something and then to pay it back. The 3D Ising model has to be considered within a $(3+1)$-dimensional frame owing to the known topologic problem of the 3D model. The introduction of an additional rotation in an additional dimension properly considered an important hidden intrinsic property, i.e. the topologic knots of interacting spins and, thus, the non-local behaviour of the 3D model.

It is important to ensure that K''' is not larger than K' or K'', since the additional rotation is performed in a curled-up dimension. It would be unreasonable if the strength of rotation or interaction in the curled-up dimension were larger than that in the normal dimensions. This verifies the necessity of taking the

crystallographic axis with the largest exchange interaction as the standard axis for initiating the procedure. Namely, the conditions of $K \geq K'$ and $K \geq K''$ should be valid, as we start our procedure by defining K^* by $e^{-2K} = \tanh K^*$. Meanwhile, the matrices $\mathbf{V_1}$, $\mathbf{V_2}$ and $\mathbf{V_3}$ could be represented and rearranged also in the $2n \cdot l \cdot o$ space as:

$$V_3' = \prod_{t=1}^{n \cdot l \cdot o - 1} \exp\{-iK'' P_{t+1} Q_t\} \cdot \exp\{iK'' P_1 Q_{n \cdot l \cdot o} U\}; \tag{19a}$$

$$V_2' = \prod_{t=1}^{n \cdot l \cdot o - 1} \exp\{-iK' P_{t+1} Q_t\} \cdot \exp\{iK' P_1 Q_{n \cdot l \cdot o} U\}; \tag{19b}$$

$$V_1' = \prod_{t=1}^{n \cdot l \cdot o} \exp\{iK^* \cdot P_t Q_t\}. \tag{19c}$$

It is clear that the additional rotation in the $2n \cdot l \cdot o$-space (i.e. $2(n \cdot l)^{3/2}$, owing to $\mathrm{o} = (n \cdot l)^{1/2}$) with the spin representation in the $2^{n \cdot l \cdot o}$ (i.e.$2^{(n \cdot l)^{3/2}}$)-space, extends the original rotations in the $2n \cdot l$-space with the spin representations in the $2^{n \cdot l}$-space to be those in the $2n \cdot l \cdot o$-space with the spin representations in the $2^{n \cdot l \cdot o}$-space. The operators of the 3D Ising lattice generate a very large Lie algebra – so large, in fact, that it cannot be dealt with in the frame of the spin representations in the $2^{n \cdot l}$-space, but only in the $2^{n \cdot l \cdot o}$-space. The three groups of $2^{n \cdot l} \times 2^{n \cdot l}$ matrices $\mathbf{C}_{\alpha\beta}$, $\mathbf{s}'_{\alpha\beta}$, $\mathbf{s}''_{\alpha\beta}$ ($\alpha = 1, 2, \ldots n$; $\beta = 1, 2, \ldots l$) in equation (8) are extended to be:

$$C_t = iP_t Q_t = 1 \times 1 \times \cdots \times C \times 1 \times \cdots, \tag{20a}$$

$$s_t' = C_1 C_2 \ldots C_{t-1} P_t = 1 \times 1 \times \cdots \times s \times 1 \times \cdots, \tag{20b}$$

$$s_t'' = C_1 C_2 \ldots C_{t-1} P_t = 1 \times 1 \times \cdots \times \mathrm{is}C \times 1 \times \cdots. \tag{20c}$$

Here $\mathbf{C}$, $\mathbf{s}$ and $\mathbf{isC}$ are located on the position of the ηth factor ($\eta = 1, 2, \ldots, n \cdot l \cdot o$) of the $2^{n \cdot l \cdot o} \times 2^{n \cdot l \cdot o}$ (i.e. $2^{(n \cdot l)^{3/2}} \times 2^{(n \cdot l)^{3/2}}$ due to $\mathrm{o} = (n \cdot l)^{1/2}$) spin matrices. By doing so, we have performed the transformations of $n \to n^{3/2}$ and $\mathrm{i} \to i^{3/2}$ on the lattice.

The problem is to evaluate the eigenvalues of the new matrices $V' \equiv V_4' \cdot V_3' \cdot V_2' \cdot V_1'$. The new matrices $\mathbf{V}'$ are much larger than the original **V matrix**, with an additional energy of interaction $J''' = (J'J'')/J$ along an additional curled-up dimension. It is noticed that, as $J''' \to 0$ (i.e. one of J' and J'' approaches zero), the model turns automatically back to the 2D model. The appearance of $\mathbf{V}_4'$ in the $\mathbf{V}'$ and the extension of the space for the spin representations of $\mathbf{V_1}$, $\mathbf{V_2}$ and $\mathbf{V_3}$ should not change the values for the maximal eigenvalues of matrix $\mathbf{V}$. However, it over-estimates the total free energy of the system. To compensate for this, one needs to introduce another new conjecture, **Conjecture 2** (as proposed below), of the weight factors on the eigenvectors. Furthermore, when necessary, one could perform the transformations of $n \to n^{2/3}$ and $l \to l^{2/3}$ to transform the $2^{n \cdot l \cdot o} \times 2^{n \cdot l \cdot o}$ (i.e. $2^{(n \cdot l)^{3/2}} \times 2^{(n \cdot l)^{3/2}}$) spin matrices back to the $2^{n \cdot l} \times 2^{n \cdot l}$ matrices. The addition of this new matrix $\mathbf{V}_4'$ is important in overcoming the difficulty of dealing with the 3D Ising model, because only its corresponding rotations in a larger dimensional space can remove the topological problem and take into account the non-local property in the

Hamiltonian. It is understood that matrix $\mathbf{V}_4'$ is actually acting as a bridge connecting the routes to solving the 3D Ising problem. $\mathbf{V}_4'$ must vanish if one reduces the dimension of the system to two, since no such topological difficulty occurs in that case. However, the detailed action of matrix $\mathbf{V}_4'$ would lead to a 3D to 2D crossover phenomenon. The additional matrix $\mathbf{V}_4'$ with K''' is attached directly on matrix $\mathbf{V}$ to arrange it in higher dimensional spaces. The eigenvalues before/after such an attachment should be equalized, because the 3D Ising model has to be set up within the $(3+1)$-dimensional framework (as a boundary condition), which could also be due to the fact that we are actually living in four non-compact dimensions. If either K, K' or K'' vanished, the model would immediately return to a 2D model. If two of K, K' or K'' vanished, the model would immediately return to the 1D model. In the next sub-section, we shall try to find the eigenvalues and eigenvectors of the new matrix $\mathbf{V}'$.

3.2. *Eigenvalues and eigenvectors of matrix V'*

Following the finding of Kaufman [17], one could treat the last 'boundary' factor and select the eigenvalues in two subspaces similarly. The complete partition function for the lattice could be written as:

$$\begin{aligned} Z &= (2\sinh 2K)^{mnl/2} \cdot \sum_{i=1}^{2^{nl}} \lambda_i^m \\ &= (2\sinh 2K)^{mnl/2} \cdot \left\{ \sum \exp\left[\frac{m}{2}(\pm\gamma_2 \pm \gamma_4 \pm \cdots)\right] \right. \\ &\quad \left. + \sum \exp\left[\frac{m}{2}(\pm\gamma_1 \pm \gamma_3 \pm \cdots)\right] \right\} \end{aligned} \tag{21}$$

For eigenvalues and eigenvectors of the matrix $\mathbf{V}^-$, we could have:

$$\begin{aligned} V_0^- \equiv \prod_{t=1}^{n\cdot l\cdot o} \exp\left(\frac{i}{2}K^* P_t Q_t\right) \cdot \prod_{t=1}^{n\cdot l\cdot o} \exp(-iK' P_{t+1} Q_t) \cdot \prod_{t=1}^{n\cdot l\cdot o} \exp(-iK'' P_{t+1} Q_t) \\ \cdot \prod_{t=1}^{n\cdot l\cdot o} \exp(-iK''' P_{t+1} Q_t) \cdot \prod_{t=1}^{n\cdot l\cdot o} \exp\left(\frac{i}{2}K^* P_t Q_t\right) \equiv S(R_0^-). \end{aligned} \tag{22}$$

The first (and last) product represents the rotation:

$$\begin{bmatrix} \cosh K^* & i\sinh K^* & & & & \\ -i\sinh K^* & \cosh K^* & & & & \\ & & \cosh K^* & i\sinh K^* & & \\ & & -i\sinh K^* & \cosh K^* & & \\ & & & & \cdot & \\ & & & & & \cdot \\ & & & & & & \cdot \end{bmatrix}. \tag{23}$$

The middle three products have the same form:

$$\begin{bmatrix} \cosh 2K_i & & & & & & & & -i\sinh 2K_i \\ & \cosh 2K_i & i\sinh 2K_i & & & & & & \\ & -i\sinh 2K_i & \cosh 2K_i & & & & & & \\ & & & \cosh 2K_i & i\sinh 2K_i & & & & \\ & & & -i\sinh 2K_i & \cosh 2K_i & & & & \\ & & & & & \ddots & & & \\ & & & & & & \ddots & & \\ & & & & & & & \ddots & \\ i\sinh 2K_i & & & & & & & & \cosh 2K_i \end{bmatrix}, \tag{24}$$

but with different quantities K_i ($i = 1, 2, 3$, for K', K'' and K'''). Compared with those in Kaufman's procedure [17], the only differences in our procedure are the appearances of two additional middle products with K'' (due to the third dimension) and K''' (due to the introduction of the fourth curled-up dimension). However, the dimension of each matrix in the present case becomes $2n \cdot l \cdot o$, instead of $2n$ in the 2D case.

$\mathbf{R_0^-}$ could be written schematically as:

$$R_0^- = \begin{bmatrix} a & b & 0 & 0 & \cdot & \cdot & \cdot & 0 & 0 & b^* \\ b^* & a & b & 0 & 0 & \cdot & \cdot & 0 & 0 & 0 \\ 0 & b^* & a & b & 0 & \cdot & \cdot & \cdot & \cdot & \cdot \\ \cdot & \cdot & \cdot & \cdot & \cdot & \cdot & \cdot & \cdot & \cdot & \cdot \\ b & 0 & \cdot & \cdot & \cdot & \cdot & \cdot & 0 & b^* & a \end{bmatrix}, \tag{25}$$

where

$$a = \begin{pmatrix} \cosh 2(K' + K'' + K''') \cdot \cosh 2K^* & -i\cosh 2(K' + K'' + K''') \cdot \sinh 2K^* \\ i\cosh 2(K' + K'' + K''') \cdot \sinh 2K^* & \cosh 2(K' + K'' + K''') \cdot \cosh 2K^* \end{pmatrix} \tag{26a}$$

$$b = \begin{pmatrix} -\frac{1}{2}\sinh 2(K' + K'' + K''') \cdot \sinh 2K^* & i\sinh 2(K' + K'' + K''') \cdot \sinh^2 K^* \\ -i\sinh 2(K' + K'' + K''') \cdot \cosh^2 K^* & -\frac{1}{2}\sinh 2(K' + K'' + K''') \cdot \sinh 2K^* \end{pmatrix}, \tag{26b}$$

$$b^* = \begin{pmatrix} -\frac{1}{2}\sinh 2(K' + K'' + K''') \cdot \sinh 2K^* & i \sinh 2(K' + K'' + K''') \cdot \cosh^2 K^* \\ -i \sinh 2(K' + K'' + K''') \cdot \sinh^2 K^* & -\frac{1}{2}\sinh 2(K' + K'' + K''') \cdot \sinh 2K^* \end{pmatrix}. \tag{26c}$$

The eigenvectors are:

$$\frac{1}{(2n \cdot l \cdot o)^{1/2}} \begin{bmatrix} \varepsilon^{2t} \cdot W_{2t} \\ \varepsilon^{4t} \cdot W_{2t} \\ \cdot \\ \cdot \\ \cdot \\ \cdot \\ \varepsilon^{2(n \cdot l \cdot o)t} \cdot W_{2t} \end{bmatrix}$$

where W_{2t} is an eigenvector of the 2-dimensional matrix α_{2t}. Therefore, the $2n \cdot l \cdot o$-eigenvalues of $\mathbf{R}_\mathbf{0}^-$ are the eigenvalues of the $n \cdot l \cdot o$ 2-dimensional matrices:

$$\alpha_{2t} = a + \varepsilon^{2t} \cdot b + \varepsilon^{2(nlo-1)t} \cdot b^* = a + \varepsilon^{2t} \cdot b + \varepsilon^{-2t} \cdot b^*. \tag{27}$$

where

$$\varepsilon^{2t} = w_x e^{i(\pi/n)} + w_y e^{i(\pi/l)} + w_z e^{i(\pi/o)}. \tag{28a}$$

and

$$\varepsilon^{2(t_{x,y,z})t} = w_x e^{i(t_x \pi/n)} + w_y e^{i(t_y \pi/l)} + w_z e^{i(t_z \pi/o)}. \tag{28b}$$

At this step, we need to introduce our second conjecture.

Conjecture 2: *The weight factors w_x, w_y and w_z, varying in range of* [-1, 1], *on the eigenvectors represent the contribution of $e^{i(t_x \pi/n)}$, $e^{i(t_y \pi/l)}$ and $e^{i(t_z \pi/o)}$ in the 4D space to the energy spectrum of the system.*

By introducing **Conjecture 1**, the 3D physical system is embedded in the $(3+1)$-dimensional space, with the same maximal eigenvalues as those of the original 3D model. By introducing **Conjecture 2**, the over-estimation of the total free energy of the $(3+1)$-dimensional model is compensated by the weight factors, leaving the total free energy unchanged.

The determinant of this matrix is $+1$. Its eigenvalues could be written as $\exp(\pm\gamma_{2t})$, and γ_{2t} could be determined by:

$$\begin{aligned} \frac{1}{2}\ \text{trace}\ (\alpha_{2t}) &= \frac{1}{2}(e^{\gamma_{2t}} + e^{-\gamma_{2t}}) = \cosh \gamma_{2t} = \cosh \gamma_{2t_x, 2t_y, 2t_z} \\ &= \cosh 2K^* \cdot \cosh 2(K' + K'' + K''') \\ &\quad - \sinh 2K^* \cdot \sinh 2(K' + K'' + K''') \\ &\quad \times \left(w_x \cos\left(\frac{2t_x \pi}{n}\right) + w_y \cos\left(\frac{2t_y \pi}{l}\right) + w_z \cos\left(\frac{2t_z \pi}{o}\right) \right) \end{aligned} \tag{29}$$

Here, t stands for variation of t_x, t_y and t_z. Similar to the 2D Ising case, γ_{2t} is geometrically the third side of a hyperbolic triangle, whose other two sides are $2(K'+K''+K''')$ and $2K^*$. The angle between the two sides $2(K'+K''+K''')$ and $2K^*$ is determined by the combinational effects of three angles $\omega_{2t_x}=(2t_x\pi/n)$, $\omega_{2t_y}=(2t_y\pi/l)$ and $\omega_{2t_z}=(2t_z\pi/o)$. This situation is similar to the band structure of a three-dimensional material, which is determined by three wave-vectors k_x, k_y and k_z along three crystallographic axes. The effects of the three wave-vectors together contribute to the band structure of a 3D crystal. In the present case, all three angles ω_{2t_x}, ω_{2t_y} and ω_{2t_z}contribute to the angle between the two sides $2(K'+K''+K''')$ and $2K^*$; however, with different weights w_x, w_y and w_z. For the 2D Ising model, only one angle ω_{2t} exists, as constructed by the two-dimensional coordinates. The analogy of only one angle ω_{2t} in the 2D Ising system to the energy band of a 1D spin chain is clear. For the 3D Ising model, the three angles ω_{2t_x}, $\omega_{2t_y}$and ω_{2t_z}exist as constructed by the three-dimensional coordinates and the extra-dimensional coordinate. The analogy of the three angles ω_{2t_x}, ω_{2t_y} and ω_{2t_z} in the 3D Ising system to the energy band of a 3D crystal is realized only by introducing the extra-dimensional coordinate. Note that the unit of the dimensions changes due to the introduction of the extra-dimensional coordinate. The effects of $e^{i(t_x\pi/l)}$, $e^{i(t_y\pi/l)}$and $e^{i(t_z\pi/o)}$ with their weights w_x, w_y and w_z will be discussed in details in Appendices A and B.

Introducing the angle δ'_{2t} between $2K^*$ and γ_{2t} simplifies the matrix $\boldsymbol{\alpha_{2t}}$. Since the procedure is similar to the 2D Ising case, we quote other relations:

$$\begin{aligned}\sinh\gamma_{2t}\cdot\cos\delta'_{2t} &= \sinh 2K^*\cdot\cosh 2(K'+K''+K''')\\ &\quad-\cosh 2K^*\cdot\sinh 2(K'+K''+K''')\\ &\quad\times\left(w_x\cos\omega_{2t_x}+w_y\cos\omega_{2t_y}+w_z\cos\omega_{2t_z}\right)\end{aligned}\tag{30}$$

$$\begin{aligned}\sinh\gamma_{2t}\cdot\sin\delta'_{2t} &= \sinh 2((K'+K''+K'''))\\ &\quad\cdot\left(w_x\sin\omega_{2t_x}+w_y\sin\omega_{2t_y}+w_z\sin\omega_{2t_z}\right).\end{aligned}\tag{31}$$

Therefore, the matrix $\boldsymbol{\alpha_{2t}}$ could be reduced to:

$$\begin{aligned}\alpha_{2t} &= \cosh\gamma_{2t}\cdot\begin{pmatrix}1 & 0\\ 0 & 1\end{pmatrix}+\sinh\gamma_{2t}\cdot\begin{pmatrix}0 & \sin\delta'_{2t}-i\cos\delta'_{2t}\\ \sin\delta'_{2t}+i\cos\delta'_{2t} & 0\end{pmatrix}\\ &= \cosh\gamma_{2t}-i\sinh\gamma_{2t}\cdot\begin{pmatrix}0 & e^{i\delta'_{2t}}\\ -e^{-i\delta'_{2t}} & 0\end{pmatrix}.\end{aligned}\tag{32}$$

The normalized eigenvectors of $\boldsymbol{\alpha_{2t}}$ are:

$$\frac{1}{\sqrt{2}}\begin{pmatrix}e^{\frac{i}{2}\delta'_{2t}}\\ ie^{-\frac{i}{2}\delta'_{2t}}\end{pmatrix},\quad \frac{1}{\sqrt{2}}\begin{pmatrix}ie^{\frac{i}{2}\delta'_{2t}}\\ e^{-\frac{i}{2}\delta'_{2t}}\end{pmatrix},$$

corresponding to the eigenvalues $\exp(\gamma_{2t})$, $\exp(-\gamma_{2t})$, respectively. The $2n \cdot l \cdot o$-normalized eigenvectors of $\mathbf{R}_0^-$ would behave as:

$$u_{2t} \equiv \frac{1}{(2n \cdot l \cdot o)^{1/2}} \begin{bmatrix} \left(w_x e^{i\omega_{2t_x}} + w_y e^{i\omega_{2t_y}} + w_z e^{i\omega_{2t_z}}\right) \cdot e^{\frac{i}{2}\delta'_{2t}} \\ i\left(w_x e^{i\omega_{2t_x}} + w_y e^{i\omega_{2t_y}} + w_z e^{i\omega_{2t_z}}\right) \cdot e^{-\frac{i}{2}\delta'_{2t}} \\ \left(w_x e^{i\omega_{4t_x}} + w_y e^{i\omega_{2t_y}} + w_z e^{i\omega_{2t_z}}\right) \cdot e^{\frac{i}{2}\delta'_{2t}} \\ i\left(w_x e^{i\omega_{4t_x}} + w_y e^{i\omega_{2t_y}} + w_z e^{i\omega_{2t_z}}\right) \cdot e^{-\frac{i}{2}\delta'_{2t}} \\ \cdot \\ \cdot \\ \cdot \\ i\left(w_x e^{i\omega_{2nt_x}} + w_y e^{i\omega_{2lt_y}} + w_z e^{i\omega_{2ot_z}}\right) \cdot e^{-\frac{i}{2}\delta'_{2t}} \end{bmatrix}, \tag{33a}$$

and

$$v_{2t} \equiv \frac{1}{(2n \cdot l \cdot o)^{1/2}} \begin{bmatrix} i\left(w_x e^{i\omega_{2t_x}} + w_y e^{i\omega_{2t_y}} + w_z e^{i\omega_{2t_z}}\right) \cdot e^{\frac{i}{2}\delta'_{2t}} \\ \left(w_x e^{i\omega_{2t_x}} + w_y e^{i\omega_{2t_y}} + w_z e^{i\omega_{2t_z}}\right) \cdot e^{-\frac{i}{2}\delta'_{2t}} \\ i\left(w_x e^{i\omega_{4t_x}} + w_y e^{i\omega_{2t_y}} + w_z e^{i\omega_{2t_z}}\right) \cdot e^{\frac{i}{2}\delta'_{2t}} \\ \left(w_x e^{i\omega_{4t_x}} + w_y e^{i\omega_{2t_y}} + w_z e^{i\omega_{2t_z}}\right) \cdot e^{-\frac{i}{2}\delta'_{2t}} \\ \cdot \\ \cdot \\ \cdot \\ \left(w_x e^{i\omega_{2nt_x}} + w_y e^{i\omega_{2lt_y}} + w_z e^{i\omega_{2ot_z}}\right) \cdot e^{-\frac{i}{2}\delta'_{2t}} \end{bmatrix}. \tag{33b}$$

The formation of the $2n \cdot l \cdot o$-normalized eigenvectors above, is in a sense analogous to the construction of a quaternion. As all physicists know, a complex number of the form $z = x + yi$, where $i = \sqrt{-1}$, can be represented by the point (x, y) on a Cartesian plane. Conversely, any point on the plane can be represented by a complex number. A quaternion is a 4D complex number in the form of $q = w + xi + yj + zk$, where i, j and k are all different square roots of -1. The quaternion can be regarded as an object composed of a scalar part, a real number w and a 3D vector part, $xi + yj + \mathrm{zk}$. For the procedure of solving the Ising models, as shown in section 2 for example, wrapping our crystal on a cylinder greatly simplifies the calculations. In the 2D Ising case [17], this process led to eigenvectors in the form of a 1D vector, as the wrapped dimension was treated as the form of a scalar. In the 3D Ising case, as shown in equations (5) and (6), wrapping our crystal on a cylinder again treats one of the three original dimensions as the form of a scalar, which does not contribute to the eigenvectors. Only when the additional fourth curled-up dimension is introduced and taken into account, can the eigenvectors in the form of a 3D vector be constructed successfully.

Similar to Kaufman [17], let the matrix of these eigenvectors be denoted by $\mathbf{t}=\mathbf{t_1}\cdot\mathbf{t_2}\cdot\mathbf{t_3}$, so that

$$t\cdot R^{-}\cdot t^{-1}=\lambda^{-1}, \tag{34}$$

where λ^{-} is the diagonal form of $\mathbf{R_0^-}$. Neither λ^{-} nor $\mathbf{t}$ are orthogonal, which cannot be represented in the spin space. Thus, one needs to apply the transformation $\mathbf{I}$ to both sides of (34):

$$(It)\cdot R^{-}\cdot\left(t^{-1}I^{-1}\right)\equiv T^{1}\cdot R^{-}\cdot T^{-1}=I\cdot\lambda^{-1}\cdot I^{-1}\equiv \mathrm{K}. \tag{35}$$

where $\mathbf{I}$ is chosen as it brings λ^{-} into its canonical form and makes $\mathbf{T}=\mathbf{I}\cdot\mathbf{t}$ orthogonal.

The spin representative of the canonical form $\mathbf{K}$ could be given by:

$$S(\mathrm{K})=\prod_{t=1}^{n\cdot l\cdot o}S(\mathrm{K}_t)=\prod_{t=1}^{n\cdot l\cdot o}\exp\left\{\frac{\theta_t}{2}\cdot\Gamma_{t1}\Gamma_{t2}\right\}, \tag{36}$$

Since **S(T)** is a complicated matrix, we do not know the spin representative of $\mathbf{T}$ explicitly. However, we must ensure that $\mathbf{T}$ is orthogonal and does possess a spin representative. The transformation $\mathbf{T}$ could be given by:

$\mathbf{T}$:

$$P_{a,b,c}\rightarrow\sum_{t_x=1}^{n}\sum_{t_y=1}^{l}\sum_{t_z=1}^{o}\sigma_{t_xa,t_yb,t_zc}P_{t_x,t_y,t_z}+\sum_{t_x=1}^{n}\sum_{t_y=1}^{l}\sum_{t_z=1}^{o}\tau_{t_xa,t_yb,t_zc}Q_{t_x,t_y,t_z}, \tag{37}$$

$$Q_{a,b,c}\rightarrow\sum_{t_x=1}^{n}\sum_{t_y=1}^{l}\sum_{t_z=1}^{o}\sigma'_{t_xa,t_yb,t_zc}P_{t_x,t_y,t_z}+\sum_{t_x=1}^{n}\sum_{t_y=1}^{l}\sum_{t_z=1}^{o}\tau'_{t_xa,t_yb,t_zc}Q_{t_x,t_y,t_z}, \tag{38}$$

where

$$\sigma_{t_xa,t_yb,t_zc}=\frac{1}{(nlo)^{1/2}}\left\{w_x\cos\left[\frac{2t_xa\pi}{n}+\frac{\delta'_{2t}}{2}\right]+w_y\cos\left[\frac{2t_yb\pi}{l}+\frac{\delta'_{2t}}{2}\right]+w_z\cos\left[\frac{2t_zc\pi}{o}+\frac{\delta'_{2t}}{2}\right]\right\} \tag{39a}$$

$$\tau_{t_xa,t_yb,t_zc}=\frac{-1}{(nlo)^{1/2}}\times\left\{w_x\sin\left[\frac{2t_xa\pi}{n}+\frac{\delta'_{2t}}{2}\right]+w_y\sin\left[\frac{2t_yb\pi}{l}+\frac{\delta'_{2t}}{2}\right]+w_z\sin\left[\frac{2t_zc\pi}{o}+\frac{\delta'_{2t}}{2}\right]\right\} \tag{39b}$$

$$\sigma'_{t_xa,t_yb,t_zc}=\frac{1}{(nlo)^{1/2}}\times\left\{w_x\sin\left[\frac{2t_xa\pi}{n}-\frac{\delta'_{2t}}{2}\right]+w_y\sin\left[\frac{2t_yb\pi}{l}-\frac{\delta'_{2t}}{2}\right]+w_z\sin\left[\frac{2t_zc\pi}{o}-\frac{\delta'_{2t}}{2}\right]\right\} \tag{39c}$$

$$\tau'_{t_xa,t_yb,t_zc}=\frac{-1}{(nlo)^{1/2}}\times\left\{w_x\cos\left[\frac{2t_xa\pi}{n}-\frac{\delta'_{2t}}{2}\right]+w_y\cos\left[\frac{2t_yb\pi}{l}-\frac{\delta'_{2t}}{2}\right]+w_z\cos\left[\frac{2t_zc\pi}{o}-\frac{\delta'_{2t}}{2}\right]\right\} \tag{39d}$$

T is now orthogonal and possesses a spin representative, so that the equation:

$$T \cdot (R^{-}) \cdot T^{-1} = \mathrm{K}, \tag{40}$$

yields:

$$S(T) \cdot \left(V_0^{-}\right) \cdot S(T)^{-1} = S(\mathrm{K}) = \prod_{t=1}^{n \cdot l \cdot o} \exp\left[\frac{i}{2}\gamma_t P_t Q_t\right]. \tag{41}$$

But **S(K)** is still not diagonal, because our coordinate system $\mathbf{iP_tQ_t = C_t}$. To diagonalize **S(K)**, we use the transformation

$$g = 2^{nlo/2} \cdot (C+s) \times (C+s) \times \cdots \times (C+s) = g^{-1}, \tag{42}$$

$$gC_t g = s_t, \tag{43}$$

which is not the spin representative of any rotation. Then, we find:

$$g \cdot S(T) \cdot \left(V_0^{-}\right) \cdot S(T)^{-1} \cdot g = g \cdot S(K) \cdot g = \Lambda^{-}. \tag{44}$$

Furthermore, we have:

$$V_0 = V^{-1/2} \cdot V^{-} \cdot V^{1/2} \equiv S(H) \cdot (V^{-}) \cdot S(H)^{-1}. \tag{45}$$

Therefore,

$$g \cdot S(TH) \cdot (V^{-}) \cdot S(TH)^{-1} \cdot g \equiv \Psi_{-} \cdot (V^{-}) \cdot \Psi_{-}^{-1} = \Lambda^{-}, \tag{46}$$

with

$$\Psi_{-} = g \cdot S(TH). \tag{47}$$

Here, **H** stands for the rotation represented by $\mathbf{V_1^{-1/2}}$, i.e. the reciprocal of the rotation in (23):

H:

$$P_t \to \cosh K^* \cdot P_t - i \sinh K^* \cdot Q_t, \tag{48a}$$

$$Q_t \to i \sinh K^* \cdot P_t + \cosh K^* \cdot Q_t. \tag{48b}$$

Again, similar to the 2D case [17], it is not feasible to write down explicitly the components of $\mathbf{\Psi}_{-}$ due to the complexity of **S(T)**. On the other hand, one could easily evaluate the eigenvalues and eigenvectors of $\mathrm{V}^{+} = \mathrm{S}(\mathrm{R}^{+})$ [17].

The partition function of simple orthorhombic lattices could be expressed as

$$\begin{aligned} N^{-1} \ln Z = \ln 2 + \frac{1}{2(2\pi)^4} \int_{-\pi}^{\pi}\int_{-\pi}^{\pi}\int_{-\pi}^{\pi}\int_{-\pi}^{\pi} \ln[&\cosh 2K \cosh 2(K' + K'' + K''') \\ &- \sinh 2K \cos\omega' - \sinh 2(K' + K'' + K''')(w_x \cos\omega_x \\ &+ w_y \cos\omega_y + w_z \cos\omega_z)]\, d\omega' d\omega_x d\omega_y d\omega_z. \end{aligned} \tag{49}$$

In accordance with details of the weights w_y and w_z, revealed in Appendices A and B, the putative exact solution for the partition function of 3D simple orthorhombic

(and simple cubic) Ising lattices could be fitted to the high temperature series expansion at/near infinite temperature [80, 93, 107]. Equation (49) contains yet-to-be determined coefficients, i.e. three weights, which are in the form of a series. However, as shown in the Appendices, all of the series can be represented or curled inside the square form, with very regular laws—all high-order terms are regularly negative for $i \geq 1$.

Because w_y and w_z become zero for finite temperatures, one immediately obtains:

$$\cosh \gamma_0 = \cosh 2(K^* - K' - K'' - K'''), \tag{50}$$

from which the critical point is determined by $\gamma_0 = 0$, i.e.

$$K^* = K' + K'' + K'''. \tag{51}$$

Namely, from equation (18), one has:

$$KK^* = KK' + KK'' + K'K''. \tag{52}$$

The following relations could also derive the critical point of the simple orthorhombic lattice Ising system:

$$\sinh 2K \cdot \sinh 2(K' + K'' + K''') = 1. \tag{53}$$

or

$$\tanh^{-1} e^{-2K} = K' + K'' + K'''. \tag{54}$$

These formulae would be the same as those of 2D rectangular Ising lattices if either K' or K'' equalled zero, the 1D Ising model if both K' and K'' equalled zero, or the simple cubic Ising model if $K = K' = K''$.

The partition function (49) directly yields the free energy F of the crystal, from which the internal energy U and the specific heat C are derived by differentiation with regard to the temperature T. For a crystal of N atoms, we have the expressions:

$$\begin{aligned} F &= U - TS = -Nk_B T \log \lambda, \\ U &= F - T\frac{dF}{dT} = Nk_B T^2 \frac{d(\log \lambda)}{dT}, \\ C &= \frac{dU}{dT}. \end{aligned} \tag{55}$$

For the present 3D system, it is convenient to evaluate the internal energy U and the specific heat C by adopting notations $K = J/\mathrm{k_B}T$ and $\tilde{K} = (J' + J'' + J'J''/J)/k_{\mathrm{B}}T$:

$$U = -NJ\frac{\partial \log \lambda}{\partial K} - N\left(J' + J'' + \frac{J'J''}{J}\right)\frac{\partial \log \lambda}{\partial \tilde{K}} = Nk_B T\left[H\frac{\partial \log \lambda}{\partial K} + \tilde{K}\frac{\partial \log \lambda}{\partial \tilde{K}}\right], \tag{56}$$

$$C = Nk_B\left[K^2\frac{\partial^2 \log \lambda}{\partial K^2} + 2K\tilde{K}\frac{\partial^2 \log \lambda}{\partial K \partial \tilde{K}} + \tilde{K}^2\frac{\partial^2 \log \lambda}{\partial \tilde{K}^2}\right]. \tag{57}$$

The discussion of Onsager [13] for the energy and the specific heat of the rectangular Ising lattice could be easily extended to simple orthorhombic

Ising lattices. However, in the present case, two terms of (56) are not separated since both K and $\tilde{K}$ are related to J. Nevertheless, we could discuss the problem using $\tilde{K} = (J' + J'' + J'J''/J)/k_B T$ in the 3D instead of $K' = J'/k_B T$ in the 2D. The following formulae could be derived:

$$\frac{dK^*}{dK} = -\sinh 2K^* = -\frac{1}{\sinh 2(K' + K'' + K''')}, \tag{58}$$

$$\begin{aligned}
\frac{\partial \gamma}{\partial \tilde{K}} &= 2\cos\delta^*, \\
\frac{\partial \gamma}{\partial K^*} &= 2\cos\delta', \\
\frac{\partial^2 \gamma}{\partial \tilde{K}^2} &= 4\sin^2\delta^* \coth\gamma, \\
\frac{\partial^2 \gamma}{\partial K^{*2}} &= 4\sin^2\delta' \coth\gamma, \\
\frac{\partial^2 \gamma}{\partial \tilde{K}\partial K^*} &= -\frac{4\sin\delta^* \sin\delta'}{\sinh\gamma}.
\end{aligned} \tag{59}$$

We would have:

$$\begin{aligned}
\frac{\partial \log\lambda}{\partial \tilde{K}} &= \int_0^\pi \cos\delta^* \frac{d\omega}{\pi}, \\
\frac{\partial \log\lambda}{\partial K} &= \cosh 2K^* - \sinh 2K^* \int_0^\pi \cos\delta' \frac{d\omega}{\pi},
\end{aligned} \tag{60}$$

and

$$\begin{aligned}
\frac{\partial^2 \log\lambda}{\partial \tilde{K}^2} &= \frac{2}{\pi}\int_0^\pi \sin^2\delta^* \coth\gamma d\omega, \\
\frac{\partial^2 \log\lambda}{\partial K \partial \tilde{K}} &= 2\sinh 2K^* \int_0^\pi \frac{\sin\delta^* \sin\delta'}{\pi \sinh\gamma} d\omega, \\
\frac{\partial^2 \log\lambda}{\partial K^2} &= 2\sinh^2 2K^* \left(-1 + \coth 2K^* \int_0^\pi \cos\delta' \frac{d\omega}{\pi} + \int_0^\pi \sin^2\delta' \coth\gamma \frac{d\omega}{\pi}\right).
\end{aligned} \tag{61}$$

The integrals (60) are continuous functions of $\tilde{K}$ and K (or K^*) for all values of these parameters, even for $\tilde{K} = K^*$ (critical point), whereas the three integrals (61) are infinite at the critical point, otherwise finite. Figure 1 shows the temperature dependence of the specific heat C for 3D simple orthorhombic Ising lattices with $K' = K'' = K$, $0.5K$, $0.1K$ and $0.0001K$. The critical point decreases with decreasing K' and K'', until the singularity disappears, as no ordering occurs in the 1D system. Clearly, if the conjectures were valid, the analytic nature of the singularity of the specific heat for 3D simple orthorhombic Ising lattices would be the same as 2D Ising lattices [13].

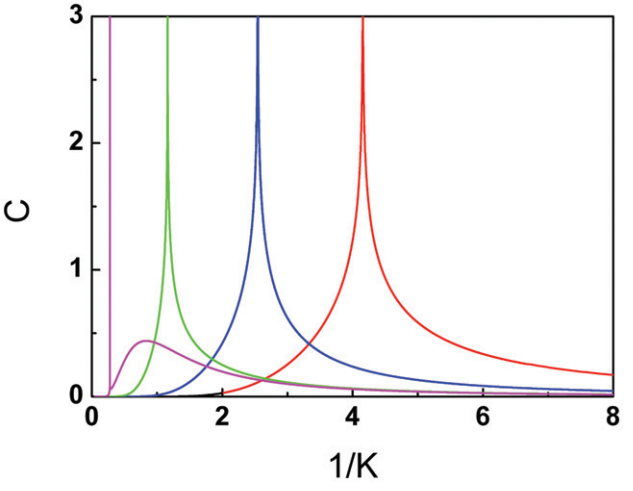

Figure 1. Temperature dependence of the specific heat C for the 3D simple orthorhombic Ising lattices with $K' = K'' = K$, $0.5K$, $0.1K$ and $0.0001K$ (from right to left).

For a simple cubic Ising lattice, $K' = K'' = K$, resulting in $K''' = K$. The eigenvalues of the matrix $\mathbf{V}$ could be represented as:

$$\begin{aligned}\cosh\gamma_{2t} &= \cosh 2K^* \cdot \cosh 6K - \sinh 2K^* \cdot \sinh 6K \\ &\quad \cdot \left(w_x \cos\left(\frac{2t_x\pi}{n}\right) + w_y \cos\left(\frac{2t_y\pi}{l}\right) + w_z \cos\frac{2t_x\pi}{o}\right) \\ &= \cosh 2K^* \cdot \cosh 6K - \sinh 2K^* \cdot \sinh 6K \cdot \left(w_x \cos\omega_{2t_x}\right. \\ &\quad \left. + w_y \cos\omega_{2t_y} + w_z \cos\omega_{2t_z}\right), \end{aligned} \tag{62}$$

and we would have:

$$\begin{aligned}\sinh\gamma_{2t}\cos\delta'_{2t} &= \sinh 2K^* \cosh 6K - \cosh 2K^* \sinh 6K\left(w_x \cos\omega_{2t_x}\right. \\ &\quad \left. + w_y \cos\omega_{2t_y} + w_z \cos\omega_{2t_z}\right) \end{aligned} \tag{63}$$

$$\sinh\gamma_{2t}\sin\delta'_{2t} = \sinh 6K\left(w_x \sin\omega_{2t_x} + w_y \sin\omega_{2t_y} + w_z \sin\omega_{2t_z}\right). \tag{64}$$

Figure 2 gives the $\gamma - K$ plots for different values of $\omega_{2t_x} = \pi$, $3\pi/4$, $\pi/2$, $\pi/4$ and 0, neglecting the effects of ω_{2t_y} and ω_{2t_z}. The minimum of the $\gamma - K$ curve shifts toward small K range (i.e. high temperature range). The minimum of the $\gamma - K$ curve for $\omega_{2t_x} = \pi$ is located at $x_d = e^{-2K_d} = ((\sqrt{10} - 1)/3) = 0.72075922\ldots\ldots$.

However, the behaviour of γ_0 for $\omega_{2t_x} = 0$ dominates most sensitively the behaviour of the physical quantities at the critical point K_c of the phase transition, where $\gamma_0 = 0$. For finite temperatures, it is easy to reduce equation (62) to the following expression:

$$\cosh\gamma_0 = \cosh 2(K^* - 3K), \tag{65}$$

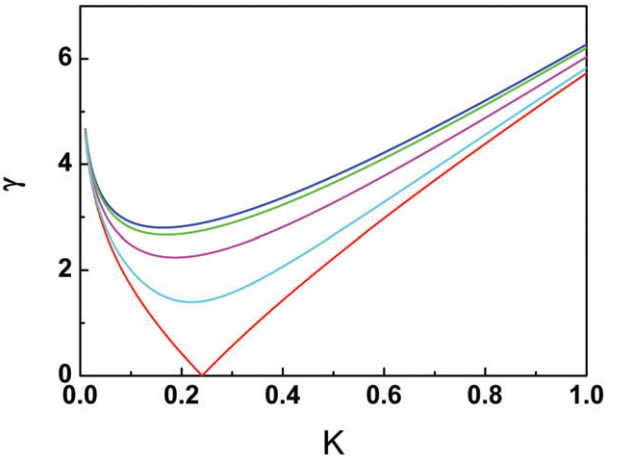

Figure 2. Plots of $\gamma - K$ of the simple cubic Ising lattice for different values of $\omega_{2t_x} = \pi$, $3\pi/4$, $\pi/2$, $\pi/4$ and 0 (from top to bottom), neglecting the effects of ω_{2t_y} and ω_{2t_z}.

from which we could determine the critical point $x_c = e^{-2K_c} = ((\sqrt{5}-1)/2) = 0.61803398874989484820458683436563811\ldots$ by $\gamma_0 = 0$, i.e. $K^* = 3K$. The following formulae also hold for the critical point:

$$\sinh 2K_c = \frac{1}{2}, \tag{66}$$

$$\cosh 2K_c = \frac{\sqrt{5}}{2}, \tag{67}$$

$$K_c = 0.24060591\ldots \tag{68}$$

$$\frac{1}{K_c} = 4.15617384\ldots \tag{69}$$

The putative critical point of the 3D simple cubic Ising system is located at $x_c = e^{-2K_c} = ((\sqrt{5}-1)/2)$, one of the golden solutions of equation $x^2 + x - 1 = 0$. One could compare it with the critical point of the 2D square Ising system, which is located at $x_c = e^{-2K_c} = \sqrt{2} - 1$, one of the silver solutions of the equation $x^2 + 2x - 1 = 0$. One could also compare it with the formulae of $\sinh 2K_c = 1$ and $\cosh 2K_c = \sqrt{2}$ for the critical point of the 2D square Ising system. The similarity between the exact solution for the critical points of the simple cubic and square Ising lattices is seen more clearly when the golden and silver solutions are expressed as the following continued fractions:

$$\frac{\sqrt{5}-1}{2} = \cfrac{1}{1 + \cfrac{1}{1 + \cfrac{1}{1 + \cfrac{1}{1 + \cdots}}}}, \tag{70a}$$

$$\frac{\sqrt{5}+1}{2} = 1 + \cfrac{1}{1+\cfrac{1}{1+\cfrac{1}{1+\cfrac{1}{1+\cdots}}}}, \tag{70b}$$

$$\sqrt{2}-1 = \cfrac{1}{2+\cfrac{1}{2+\cfrac{1}{2+\cfrac{1}{2+\cdots}}}}, \tag{70c}$$

$$\sqrt{2}+1 = 2 + \cfrac{1}{2+\cfrac{1}{2+\cfrac{1}{2+\cfrac{1}{2+\cdots}}}}. \tag{70d}$$

In addition, the golden and silver solutions can also be expressed in the infinite series of square roots:

$$\frac{\sqrt{5}\pm 1}{2} = \sqrt{1\pm\sqrt{1\pm\sqrt{1\pm\sqrt{1\pm\sqrt{1\pm\cdots}}}}}, \tag{71a}$$

$$\sqrt{2}\pm 1 = \sqrt{1\pm 2\sqrt{1\pm 2\sqrt{1\pm 2\sqrt{1\pm 2\sqrt{1\pm\cdots}}}}}, \tag{71b}$$

Equations (70) and (71) could be related to the conceptions of self-similarity and fractals.

The putative critical point of the simple cubic Ising system could be derived by the following relations:

$$\sinh 2K_c \cdot \sinh 6K_c = 1. \tag{72}$$

or

$$\tanh^{-1}\left(e^{-2K_c}\right) = 3K_c. \tag{73}$$

Note that these formulae are the same as those for the 2D asymmetric Ising lattice with $K' = 3K$. Although the solution of the golden ratio also exists in this 2D Ising system, it can be eliminated by setting the larger value between K and K' as the starting standard axis (as discussed in section 8).

The partition function of the simple cubic Ising model reads as

$$\begin{aligned} N^{-1}\ln Z = \ln 2 + \frac{1}{2(2\pi)^4}\int_{-\pi}^{\pi}\int_{-\pi}^{\pi}\int_{-\pi}^{\pi}\int_{-\pi}^{\pi} \ln[\cosh 2K\cosh 6K \\ - \sinh 2K\cos\omega' - \sinh 6K\left(w_x\cos\omega_x + w_y\cos\omega_y \right. \\ \left. + w_z\cos\omega_z\right)]d\omega' d\omega_x d\omega_y d\omega_z \end{aligned} \tag{74}$$

Again, as revealed in Appendix A, at/near infinite temperature, the partition function (74) of 3D simple cubic Ising lattices equals the high-temperature series expansion [80, 93, 107]. This is actually a closed-form solution, as long as *Ansatz* 1 in Appendix A is true. This *Ansatz* is an uncertain section of the whole approach, but from the regular tendency of parameters b_1-b_{10}, it should be true for all of high-order terms b_i ($i>11$). It is believed that the *Ansatz* is true, although it has not been proved rigorously.

3.3. *Critical point*

It is important to compare the putative exact solution for the critical point with the results of previous approximation methods. We shall first compare it with the data obtained over the last six decades and then with those obtained most recently. It is understood that the exact value for $1/K_c$ should be lower than the values obtained by various approximation methods. The mean field theory yields $1/K_c = z$ (where z is the coordination number), which is correct only for $d \geq 4$ [212, 226, 227]. For the 3D Ising model, the mean field value of $1/K_c = 6$ is the highest approximation value, which is not quantitatively correct, since the mean field theory overestimates the critical point in every case of $d<4$. Oguchi [62–64] concluded that the existence of the Curie point for the 3D ferromagnet is in the range $0.21 < K_c < 0.24$, correspondingly, $4.7619 > 1/K_c > 4.16667$. Our putative exact solution $K_c = 0.24060591\ldots$ (i.e. $1/K_c = 4.15617384\ldots$) is exactly located at the upper border of K_c (or the lower border of $1/K_c$) of Oguchi's estimation [62–64], within an error of ~0.25%. A comparison with the lower border of $1/K_c$ is meaningful, since the upper border of $1/K_c$ should be far from the true value and only the lower border of $1/K_c$ could be close to the exact value. The value of K_c for the Bethe [74, 228] first approximation is equal to 0.202 (i.e. $1/K_c = 4.939$). The putative exact solution for $1/K_c$ is much smaller than that of Bethe's first approximation [74, 228]. The putative exact solution is also lower than Kikuchi's estimation $4.2221 < \tau_c < 4.6097$ and $\tau_t \approx 4.5810$ (where τ_c or τ_t is our $1/K_c$) [61]. Actually, this solution is very close to the low limit of $1/K_c$ of Kikuchi's estimation [61], within an error of 1.6%. Meanwhile, the solution $x_c = e^{-2K_c} = (\sqrt{5}-1)/2 = 0.618033988\ldots$ is much lower than the values obtained by various approximation methods, such as Wakefield's method at 0.641 (i.e. $1/K_c = 4.497$) [73, 74], Bethe's first approximation at 0.667 (i.e. $1/K_c = 4.939$) [74, 228], Bethe's second approximation at 0.656 (i.e. $1/K_c = 4.744$) [74, 228], Kirkwood's method at 0.658 (i.e. $1/K_c = 4.778$) [74, 229] and Burley's best known value of 0.642 (i.e. $1/K_c = 4.513$) [209]. Methods with higher order approximations have lower values for the critical temperature and the exact solution must have the lowest value. On the other hand, the corrections of higher order terms are much lower than those of lower order terms, especially the first leading term. The mean field theory can be treated as a zero-order approximation. The correction of Bethe's first approximation on the mean field value is evaluated by $\delta_1(1/K_c) = 1/K_c^{MF} - 1/K_c^{Bethe-1}$, which is ~1.061. The correction of Bethe's second approximation on Bethe's first approximation value is evaluated by $\delta_2(1/K_c) = 1/K_c^{Bethe-1} - 1/K_c^{Bethe-2}$, which is ~0.195. The value of $\delta_2(1/K_c)$ is ~18.38% of $\delta_1(1/K_c)$. It is reasonable that this tendency is

approximately held by all high-order terms, namely, all of $\delta_{i+1}(1/K_c)$ is about one order less than $\delta_i(1/K_c)$. Suppose the ratios between every neighbouring terms in the Bethe's approximations are similar, we obtain the value of $1/K_c = 4.700$ for the upper limit of the critical point of the 3D simple cubic Ising model. However, the ratios may not be the same, but vary over a certain range. The evaluation of the lower limit gives us a criterion that the exact solution $1/K_c$ for the critical point of the 3D simple cubic Ising model must not be smaller than 3.878 ($= 6 - 2\,\delta_1(1/K_c)$), because the sum of all the high-order terms of the corrections must not be larger than the first correction, i.e. $\sum_{i=2}^{\infty} \delta_i(1/K_c) < \delta_1(1/K_c)$.

In 1985, Rosengren [230] conjectured that the critical point of the symmetric, simple cubic Ising model is given by $v_c \equiv \tanh(J/k_B T_c) = \left(\sqrt{5} - 2\right)\cos(\pi/8) = 0.218098372\ldots$, i.e. $K_c = 0.22165863\ldots$, in consideration of a certain circumstance for the 2D case and possible generalizations of the combinatorial solution to three dimensions. One could easily check from $x_c = e^{-2K_c} = (\sqrt{5} - 1)/2$ that our putative solution gives $v_c \equiv \tanh K_c = \sqrt{5} - 2$. Surprisingly, what we obtained for the critical point of the simple cubic Ising model is exactly the same as the first factor $\left(\sqrt{5} - 2\right)$ in Rosengren's conjecture [230]. As noted by Fisher [231], it is fair to say that the basis for the Rosengren guess remains somewhat obscure: Rosengren did sketch an argument suggesting that a relevant class of weighted lattice walks with no backsteps would yield a factor $\left(\sqrt{5} - 2\right)$; but the second factor in the Rosengren conjecture was then selected to match various critical point estimates based on series, renormalization group and Monte Carlo studies published in 1981–1984 [120, 121, 173, 232–234]. The factor $\cos(\pi/8)$ introduced confusion, which certainly misled Fisher's efforts on the critical polynomial, claiming finally that the critical points of true 3D models may not be the root of any polynomial [231]. Although the Rosengren conjecture of $K_c = 0.22165863\ldots$ is still in good agreement with the most recent estimates of the high-temperature series extrapolation [113, 116, 118, 121, 122, 213], Monte Carlo and renormalization group techniques [161–163, 168, 170, 172–175, 177, 180, 181, 186, 213, 235], there are strong theoretical arguments again it as the exact solution [231]. This implies that the most recent estimates of the Monte Carlo and renormalization group techniques are not close to the exact value, although they have been determined with high precision.

Various new approximation methods have been developed for studying critical phenomena in different systems [106, 107, 141–144, 149, 152–160, 192–202, 208–225] since the discovery of the renormalization group theory in 1971. Over recent decades, further estimates of the critical point and critical exponents have become available [107–225], many being precise but of doubtful accuracy. Two review articles by Pelissetto and Vicari [154] and Binder and Luijten [213] summarized recent results from the renormalization group theory and Monte Carlo simulations, respectively, among other methods. As summarized in table 2 of Binder and Luijten's review [213], the critical point [113, 116, 118, 121, 122, 161–163, 168, 170, 172–175, 177, 180, 181, 186, 235] occurs at $K_c = 0.221655(5)$, i.e. $1/K_c = 4.511505(5)$ – in good agreements with the results in various studies [119, 164, 167, 191]. This value of $1/K_c$ is slightly higher than our solution $1/K_c = 4.15617384\ldots$, as the approximation should be. It is well-known that in all the approximation methods, systematic errors are difficult to assess with confidence [106, 107, 141–144, 149, 152–160, 192–202, 208–225], which might be the origin of such deviations. The reasons for the existences

of systematic errors in the approximation methods will be discussed in detail in section 8.

In the following paragraphs, we will compare the results of the critical points of the renormalization group theory and Monte Carlo simulations with the exact solutions of the 2D and 3D Ising models and even some possibly existing analytical solutions.

Before the comparison, it is interesting to examine the mathematical characters of the exact solutions of the 2D square and the 3D simple cubic Ising models. The exact solution of the 2D square Ising model is located exactly at $x_c = e^{-2K_c} = \sqrt{2}-1$, $\sinh 2K_c = 1$ and $\cosh 2K_c = \sqrt{2}$, yielding $K_c = 0.44068679\ldots$, i.e. $1/K_c = 2.26918531\ldots$. The putative exact solution of the 3D simple cubic Ising model is located exactly at $x_c = e^{-2K_c} = ((\sqrt{5}-1)/2) = 0.618033988\ldots$, $\sinh 2K_c = 1/2$ and $\cosh 2K_c = \sqrt{5}/2$, yielding $K_c = 0.24060591\ldots$, i.e. $1/K_c = 4.15617384\ldots$. We also found that the minimum in the $\gamma - K$ curve for $\omega_{2t_x} = \pi$ is located at $x_d = e^{-2K_c} = (\sqrt{10}-1)/3 = 0.72075922\ldots$, $\sinh 2K_d = 1/3$ and $\cosh 2K_d = \sqrt{10}/3$, $K_d = 0.16372507\ldots$ and $1/K_d = 6.10779991\ldots$ Although the minimum of the $\gamma - K$ curve for $\omega_{2t_x} = \pi$ does not correspond to the critical point or any phase transition, nature shows the hidden intrinsic relationship between the 2D square and the 3D simple cubic Ising lattices, as revealed by the values of $\sinh 2K = 1$, $1/2$ and $1/3$. It is also interesting to compare the critical points of the 2D square and the 3D simple cubic Ising lattices together with that of the 2D triangular Ising model: for the 2D square lattice, $\coth K_c = 1+\sqrt{2} = 2.414213562\ldots$; for the 2D triangular lattice, $\coth K_c = 2+\sqrt{3} = 3.732050808\ldots$ [24–31, 93]; for the simple cubic lattice, $\coth K_c = 2+\sqrt{5} = 4.236067977\ldots$. It is worth noting that these values are simply related to the smallest three, subsequent irregular numbers, again showing some hidden intrinsic relationships between the three lattices. The value of $\coth K_c$ for each of these three lattices equals one of the two smallest integers plus one of the smallest three irregular numbers.

The competition between interaction energy and thermal activity is balanced at the critical temperature. Critical point values could be used for the evaluation of the contribution of the interactions to the ordering of the systems. For the 1D Ising model, there is no order, i.e. $1/K_c = 0$, and the value of $1/K_c$ per J equals zero for the existence of one interaction per unit cell. For the 2D square Ising model, the critical point of $1/K_c = 2.26918531\ldots$ and the existence of two interactions J per unit cell gives a value of $1/K_c$ per J equal to $1.13459265\ldots$ For the 3D simple cubic Ising model, the critical point of $1/K_c = 4.15617384\ldots$ and the existence of three interactions J per unit cell results in $1/K_c$ per J being equal to $1.38539128\ldots$ For models with their dimensions $d \geq 4$, the mean field theory yields $1/K_c = z$ (where z is the coordination number) [212, 226, 227]. Namely, the value of $1/K_c$ per J is equal to 2 for the $d \geq 4$ models, in consideration of the existence of $z/2$ interactions J per unit cell. It is reasonable that the value of $1/K_c$ per J increases monotonously from 0 *via* $1.13459265\ldots$ and $1.38539128\ldots$ to 2 when the dimension of the Ising models alters from 1 *via* 2 and 3 to 4 and above. Namely, the value of $1/K_c$ per J varies smoothly with dimensionality. This is because the correlations between spins are strengthened with increasing dimension of the system, which contribute more action to the ordering of the system.

The putative exact critical point of $1/K_c = 4.15617384\ldots$ for the 3D simple cubic Ising model is derived by the introduction of the extra dimension, in accordance with the topologic problem of three dimensions. One might assume that the procedure put extra energy in the final result. Now, let us treat the third interaction of the 3D simple cubic Ising model as for the 2D Ising model. Simply taking the sum of the two interactions into the expressions of the eigenvalues as well as the partition function, one derives the values of $x_c = e^{-2K_c} = \sqrt[3]{(17/27) + \sqrt{(11/27)}} + \sqrt[3]{(17/27) - \sqrt{(11/27)}} - (1/3) = 0.543689012\ldots$ and $K_c = 0.30468893\ldots$, i.e. $1/K_c = 3.28203585\ldots$ by $\cosh \gamma_0 = \cosh 2(K^* - 2K)$ or $\sinh 2K \cdot \sinh 4K = 1$. However, this value of $1/K_c = 3.28203585\ldots$ is clearly lower than the real value, since it does not take the topological effects of the three dimensions into account. Actually, this value is even smaller than the exact solution of the 2D triangular Ising model, which is located exactly at $x_c = e^{-2K_c} = 1/\sqrt{3} = 0.577350269\ldots$, i.e. $1/K_c = 3.6409569\ldots$ [24–31, 93]. It is known that the 2D triangular Ising model is equalized to the 2D square Ising model with only one next nearest neighbouring interaction [31, 83, 93]. The critical point of these two models must be lower than the 2D Ising model with two next nearest neighbouring interactions and the 3D simple cubic Ising model, because the latter two models have topologic problems with crosses/knots. It is a criterion that the critical point of the 3D simple cubic Ising model must be much higher than that of the 2D triangular Ising model. This criterion can be verified by the following consideration: the mean field theory is not sensitively dependent on the lattice geometry, which predicts better results in higher dimensions. The mean field theory predicts the same critical point for the simple cubic lattice in three dimensions and the triangular lattice in two dimensions, since both have the coordination number $z = 6$. The difference between the exact and mean field value in the simple cubic lattice should be smaller than that in the triangular lattice, indicating clearly that the critical point of the former must be higher than that of the latter. The solution of $1/K_c = 4.15617384\ldots$ was found to satisfy this criterion for the 3D simple cubic Ising model. It is thought that the difference between the critical points of the simple cubic lattice and the triangular lattice can be treated as a pure contribution of the 3D lattice, which originates not only from the third dimension and but also the curled-up fourth dimension.

Finally, we would like to compare, in more detail, the putative exact critical points with the results of the mean field theory. The mean field theory predicts that the critical point should depend on the geometry of the model only through the coordination number z, namely, $1/K_c$ is equal to the coordination number, and it is non-zero for all $z \neq 0$. The mean field theory gives the correct predictions only for $d \geq 4$ and it overestimates the critical point in every case of $d < 4$. Especially, the mean field theory is obviously wrong for the 1D Ising model because it predicts $1/K_c = 2$, in contradiction with the fact that the exact calculation proves no order exists at finite temperatures. For the 2D square Ising model, the mean field theory suggests $1/K_c = 4$, which is much higher than the Onsager exact solution of $1/K_c = 2.26918531\ldots$ For the 3D simple cubic Ising model, the mean field theory gives $1/K_c = 6$, which is also higher than our exact solution of $1/K_c = 4.15617384\ldots$ The feature of the mean field theory is that it identifies the order

parameter of the system and tries to describe it as simply as possible [212]. It assumes that one only takes account of configurations in which the order parameter is uniform and, therefore, that every spin, bond, etc. behaves in an average manner, regardless of its neighbours. This means that it neglects all fluctuations in the order parameter in which nearby parts of the system, while remaining interrelated, do something different from the average. In other words, all Fourier components with $q \neq 0$ are suppressed [236]. This neglect is responsible for the consistent overestimation of the critical point in 2D and 3D and the incorrect prediction of the existence of the order in 1D. It is evident that such neglect is more serious in lower dimensions, because the correlations more dramatically affect the physical properties. To compare the effects of this neglect in models of different dimensions, we define a parameter, $\Delta(1/K_c) = (((1/K_c^{MF}) - (1/K_c^{Exact}))/(1/K_c^{MF}))$ to evaluate the difference between the critical points of the mean field theory and the exact solution. Immediately, we find that $\Delta(1/Kc)$ equals 100, ~ 43.27, ~ 30.73 and 0% for 1D, 2D, 3D and 4D, respectively. Clearly, the error due to this neglect decreases monotonously with increasing dimension of the system. It is relevant that the mean field theory predicts better results in higher dimensions.

Other factors concerning the critical point are: (a) The critical point predicted by high-temperature expansions is even higher than the exact value obtained by introducing an additional dimension, rotation and, thus, energy. (b) The approximation value obtained by series expansions is usually higher than the exact value, whereas that obtained by removing one interaction should be lower than the exact value. If the golden ratio were not for the 3D model (but, say, for a $(3+1)$-dimensional model), then the value obtained by high-temperature expansions would correspond to a model with even higher dimensionality, since the higher dimensionality, the higher critical point. The question is how to construct the function of the free energy to obtain such high values predicted by high-temperature expansions? A reasonable situation might be that the golden ratio is exact for the 3D model, while the value of the critical point obtained by the high-temperature expansions is inexact, but as high as an approximate should be.

The 3D Ising model has been judged by several criteria: (1) At/near infinite temperature, the putative exact solution for the partition function of 3D simple orthorhombic (and simple cubic) Ising lattices equals the high-temperature series expansion [80, 93, 107]. (2) The formulae for the eigenvalues, eigenvectors, the partition function and the critical point of 3D simple orthorhombic lattices can return to those of 2D rectangular Ising lattices if either K' or K'' vanishes, the 1D Ising lattice if both K' and K'' vanish, and the simple cubic Ising lattice if $K = K' = K''$. (3) Our putative exact solution coincides with the first factor of the Rosengren conjecture for the critical point of the 3D simple cubic Ising model [230], while the second factor of the Rosengren conjecture certainly has to be omitted [231]. (4) The putative exact solution of the 3D simple cubic Ising model is lower than the approximation values obtained by various series expansion methods, such as Kikuchi's estimation (note: the exact solution is very close to the low limit of Kikuchi's estimation, within an error of 1.6%) [61], Wakefield's method [73, 74], Bethe's first and second approximations [74, 228], Kirkwood's method [74, 229], etc.

(5) The putative exact solution of the 3D simple cubic Ising model is in good agreement with the range of $4.16667 < 1/K_c < 4.7619$, as Oguchi estimated, and is exactly located at the lowest boundary of Oguchi's estimations within an error of ~0.25% [62–64]. (6) The exact solution for the critical point $1/K_c$ of the 3D simple cubic Ising model must be not smaller than 3.878, because the corrections of all terms of the Bethe high-order approximations on the mean field theory must not be larger than twice the correction of the Bethe first approximation. (7) The critical point $1/K_c$ of the 3D simple cubic Ising model must be higher than that (3.6409569 . . .) of the 2D triangular Ising model. (8) The putative exact solution is close to and lower than the value of $1/K_c = 4.511505(5)$ in the Binder and Luijten review [213], which has been well established from the results of high-temperature series extrapolation, Monte Carlo renormalization group, Monte Carlo and finite-size scaling in recent years. (9) The value of $1/K_c$ per J increases monotonously with increasing dimension of the Ising model because the correlations between spins are strengthened, contributing more efficiently to the ordering of the system in higher dimensions. (10) The parameter, $\Delta(1/K_c)$, as the evaluation of the difference between the exact solution and the mean field value, decreases monotonously with increasing dimension of the system, and, as a consequence, the mean field theory predicts better results in higher dimensions because the errors due to the neglects of fluctuations in the order parameter become smaller. (11) The exact solutions of the 3D simple cubic and 2D square Ising models are closely correlated with similar mathematical structures, such as the golden and the silver ratios as the solutions of the equations $x^2 + x - 1 = 0$ and $x^2 + 2x - 1 = 0$, the two simplest continued fractions, the critical point formulae of $\sinh 2K_c = 1/2$ and $\sinh 2K_c = 1$, etc. (12) The exact solution satisfies the principles of simple symmetry and beauty with aesthetic appeal, which are the most important principles for judging the validity and correctness of a theory where the answer is unknown. The principles of simple symmetry and beauty have been employed widely for establishing the elegance theories, such as Einstein's theory of general relativity, Dirac's equation, Feynman's path integrals or Onsager's solution, etc.

4. Spontaneous magnetization

4.1. *Perturbation procedure*

The spontaneous magnetization of the square Ising magnet was calculated exactly by Yang using a perturbation procedure [20]. Chang [21] and Potts [22] derived the spontaneous magnetization of the rectangular Ising lattice and Potts also dealt with the triangular Ising lattice. Schultz *et al.* [237] investigated the two-spin correlation function in an infinite 2D lattice, in terms of many fermions and reconciled the different approaches of previous authors, and discussed the definitions of spontaneous magnetization. Although the definition of spontaneous magnetization was argued by Schultz *et al.* [237], in this section, we shall follow Yang's method to calculate the spontaneous magnetization of the 3D Ising model, based on the two conjectures introduced previously. We shall focus on the

spontaneous magnetization of simple orthorhombic lattices and then on the simple cubic lattice.

As a weak magnetic field $\aleph$ is introduced, the partition function of the 3D simple orthorhombic Ising magnet becomes:

$$Z_{\mathrm{K}} = (2\sinh 2K)^{mnl/2}\mathrm{trace}\ (V_5V_4V_3V_2V_1)^m, \tag{75}$$

where

$$V_5 = \exp\left\{\aleph\sum_1^{n\cdot l} s_t\right\}. \tag{76}$$

For a large crystal, as discussed above, only the eigenvector of $\mathbf{V} = \mathbf{V_5V_4V_3V_2V_1}$ with the largest eigenvalue is important. The limiting form of this eigenvector as $\aleph \to 0$ is the one of interest. The largest eigenvalue of $\mathbf{V_4V_3V_2V_1}$ is doubly degenerate below the critical temperature. This is also true of the symmetrical matrix $\mathbf{V_1^{1/2}V_4V_3V_2V_1^{1/2}}$. Let $\boldsymbol{\psi}_+$ and $\boldsymbol{\psi}_-$ be the even and odd eigenvectors corresponding to the largest eigenvalue λ. Introducing the operator

$$U = C_1C_2\cdots C_{nl}, \tag{77}$$

that reverses the spins of all atoms, we have

$$U\psi_+ = \psi_+, \quad U\psi_- = -\psi_-, \tag{78}$$

for the even and odd eigenvectors, respectively.

When the magnetic field $\aleph$ is applied, the degeneracy is removed. Analogous to Yang's consideration [20], we perform a perturbation calculation, since we are only interested in the limit of $\aleph \to 0$. We consider only the largest eigenvalue of

$$\begin{aligned} V_1^{1/2}VV_1^{-1/2} &= V_1^{1/2}V_5V_4V_3V_2V_1^{1/2} \\ &= V_1^{1/2}V_4V_3V_2V_1^{1/2} + \aleph V_1^{1/2}\left(\sum_1^{nl} s_t\right)V_4V_3V_2V_1^{1/2}. \end{aligned} \tag{79}$$

The last term is a real symmetrical matrix anticommuting with $\mathbf{U}$, which has no diagonal matrix element with respect to either $\boldsymbol{\psi}_+$ or $\boldsymbol{\psi}_-$. Ordinary perturbation theory shows that as $\aleph \to 0$, the eigenvector of (79) with the largest eigenvalue approaches

$$\psi_{\max} = \frac{1}{\sqrt{2}}(\psi_+ + \psi_-), \tag{80}$$

if the phases of $\boldsymbol{\Psi}_+$ and $\boldsymbol{\Psi}_-$ are chosen that they are real and that:

$$\psi_+'V_1^{1/2}\left(\sum_1^{nl} s_t\right)V_4V_3V_2V_1^{1/2}\psi_- \geq 0. \tag{81}$$

From the general definition of the matrix method, the average magnetization per atom reads as:

$$I = \frac{1}{mnl}\frac{m \cdot \operatorname{trace}(V_5V_4V_3V_2V_1)^m \sum_1^{nl} s_t}{\operatorname{trace}(V_5V_4V_3V_2V_1)^m}$$

$$= \frac{1}{nl}\frac{\operatorname{trace}\left(V_1^{1/2}V_5V_4V_3V_2V_1^{1/2}\right)^m \left(V_1^{1/2}\sum_1^{nl} s_t V_1^{-1/2}\right)}{\operatorname{trace}\left(V_1^{1/2}V_5V_4V_3V_2V_1^{1/2}\right)^m}$$

$$= \frac{1}{nl}\psi'_{\max} V_1^{1/2} \sum_1^{nl} s_t V_1^{-1/2}\psi_{\max}, \tag{82}$$

As $\aleph \to 0$, (82) becomes by (80)

$$I = \frac{1}{2nl}\left(\psi'_+ + \psi'_-\right) V_1^{1/2} \sum_1^{nl} s_t V_1^{-1/2}(\psi_+ + \psi_-). \tag{83}$$

Similar to the discussion in Yang's study [20], the spontaneous magnetization is

$$I = \frac{1}{nl}\psi'_- V_1^{1/2} \sum_1^{nl} s_t V_1^{-1/2}\psi_+. \tag{84}$$

By replacing the summation $\sum s_t$, it can be written as:

$$I = \psi'_- V_1^{1/2} s_1 V_1^{1/2}\psi_+. \tag{85a}$$

The relation would be expressed as:

$$I^{1/3} = \varphi'_- V_1^{1/2} s_1 V_1^{1/2}\varphi_+. \tag{85b}$$

where φ'_- and φ_+ are the reduced normalized eigenvectors in consideration of weights at finite temperature. The 2n-reduced normalized eigenvectors is represented as:

$$u_{2t} \equiv \frac{1}{(2n)^{1/2}}\begin{bmatrix} e^{i\omega_{2t_x}} \cdot e^{(i/2)\delta'_{2t}} \\ ie^{i\omega_{2t_x}} \cdot e^{(-i/2)\delta'_{2t}} \\ e^{i\omega_{4t_x}} \cdot e^{(i/2)\delta'_{2t}} \\ ie^{i\omega_{4t_x}} \cdot e^{(-i/2)\delta'_{2t}} \\ . \\ . \\ . \\ ie^{i\omega_{2nt_x}} \cdot e^{(-i/2)\delta'_{2t}} \end{bmatrix},$$

and

$$v_{2t} \equiv \frac{1}{(2n)^{1/2}} \begin{bmatrix} ie^{i\omega_{2t_x}} \cdot e^{(i/2)\delta'_{2t}} \\ e^{i\omega_{2t_x}} \cdot e^{(-i/2)\delta'_{2t}} \\ ie^{i\omega_{4t_x}} \cdot e^{(i/2)\delta'_{2t}} \\ e^{i\omega_{4t_x}} \cdot e^{(-i/2)\delta'_{2t}} \\ . \\ . \\ . \\ e^{i\omega_{2nt_x}} \cdot e^{(-i/2)\delta'_{2t}} \end{bmatrix}.$$

The power 1/3 for spontaneous magnetization I comes automatically from the dimensional unit of the 3D system as one uses the reduced eigenvectors. The physical significance of I is the same as that defined for the 2D Ising magnet. Following Yang's study [20], we introduce an artificial limiting process and reduce the problem to an eigenvalue problem of an $n \times n$ matrix. One arrives after some algebra at:

$$I^{1/3} = \lim_{a \to i\infty} (2\cos a)^{-n} \operatorname{trace} V_1^{1/2} s_1 V_1^{-1/2} S\left(T_+^{-1} M T_-\right). \tag{86}$$

The next step is to follow the procedure of subsections B, C, D and E of section II in Yang's paper [20].

The procedure for an infinite crystal could be simplified greatly. Considering the weights $w_x \equiv 1$, $w_y = w_z = 0$ for finite temperatures, the relationship between δ' and ω shown in equation (29) could be reduced explicitly, in term of $z = e^{i\omega_x}$ ($\omega_x = t_x\pi/n$, $t_x = 1, 2, \ldots, n$), to:

$$e^{2i\delta'} = \frac{\tanh^2 K^*(z - \coth(K' + K'' + K''')\coth K^*)(z - \tanh(K' + K'' + K''')\coth K^*)}{(z - \coth(K' + K'' + K''')\tanh K^*)(z - \tanh(K' + K'' + K''')\tanh K^*)}. \tag{87}$$

Then, $e^{i\delta'}$ behaves as

$$\Theta(z) = e^{i\delta'} = \frac{1}{(AB)^{1/2}} \left[\frac{(z - A)(z - B)}{(z - A^{-1})(z - B^{-1})}\right]^{1/2}, \tag{88}$$

where

$$A = \coth(K' + K'' + K''')\coth K^* = \frac{1 + x_2x_3x_4}{x_1(1 - x_2x_3x_4)}, \tag{89a}$$

$$B = \tanh(K' + K'' + K''')\coth K^* = \frac{1 - x_2x_3x_4}{x_1(1 + x_2x_3x_4)}, \tag{89b}$$

with

$$x_1 = e^{-2K};\ x_2 = e^{-2K'};\ x_3 = e^{-2K''};\ x_4 = e^{-2K'''}.$$

For $T < T_c$, $A > B > 1$. $\Theta(z)$ is analytic everywhere except at the points $z = A$, B, $1/A$, or $1/B$, where it has branch points. The square root in equation (88) is defined as that branch of the function taking the value -1 at $z = 1$ [20]. Similar to Yang's procedure [20], one has:

$$F^{-2} = \frac{4}{\pi}\frac{1}{A-B}k_{-1}^{1/2}K(k_{-1}), \tag{90}$$

where

$$k_{-1} = \left[\frac{(A^2-1)^{1/2} - (B^2-1)^{1/2}}{A(B^2-1)^{1/2} + B(A^2-1)^{1/2}}\right]^2, \tag{91}$$

and $K(k_{-1})$ is the complete elliptic integral of the first kind. It is convenient to change the modulus:

$$k = \frac{2k_{-1}^{1/2}}{1+k_{-1}} = \frac{4x_1x_2x_3x_4}{(1-x_1^2)(1-x_2^2x_3^2x_4^2)} = \sinh^{-1} 2K \sinh^{-1} 2(K' + K'' + K'''). \tag{92}$$

Then

$$F^{-2} = \frac{2kK(k)}{\pi(A-B)}. \tag{93}$$

and

$$I^{4/3} = \left[\prod_2^{nl}\left(\frac{l_\alpha^2}{4}\right)\right]F^4A^{-2}B^{-2}\cosh^4 K^*, \tag{94}$$

which can be further simplified to

$$I^{4/3} = \left(\prod_2^{nl}\frac{l_\alpha^2}{4}\right)\frac{\pi^2}{4}\left[\frac{1}{K(k)}\right]^2. \tag{95}$$

Similar to Chang [21], the elliptic transformation (81) in Yang's paper [20] is replaced by:

$$z = -\frac{(cnu - i(1+k_1)^{1/2}snu)(dnu - i(k_1+k_1k_2)^{1/2}snu)}{1+k_1sn^2u}, \tag{96}$$

where the modulus is given by equation (92). It is easy to verify that:

$$\frac{1}{z}\frac{dz}{du} = -i\frac{1-k^2}{(1+k_1)^{1/2}}\frac{1}{dnu - [k_1(1+k_2)/(1+k_1)]^{1/2}cnu}. \tag{97}$$

where $k_1 = \sinh^{-2} 2K$ and $k_2 = \sinh^{-2} 2(K' + K'' + K''')$. The essential properties of the variable z as a function of u remain the same as in the 2D lattices. There are still two singularities per unit cell ($4K \times 4iK'$) (note: only here the denotions K and K' are

the same as Yang's K and K' in u-plane [20, 21]), although their positions are changed. Finally, we quote:

$$\prod_{2}^{\infty}\frac{l_\alpha^2}{4}=\frac{4}{\pi^2}[K(k)]^2(1-k^2)^{1/2}=\frac{4}{\pi^2}K^2\frac{1}{(1-x_1^2)(1-x_2^2x_3^2x_4^2)}\times\left[(1-x_1^2+4x_1x_2x_3x_4-x_2^2x_3^2x_4^2+x_1^2x_2^2x_3^2x_4^2)\times(1-x_1^2-4x_1x_2x_3x_4-x_2^2x_3^2x_4^2+x_1^2x_2^2x_3^2x_4^2)\right]^{1/2}\tag{98}$$

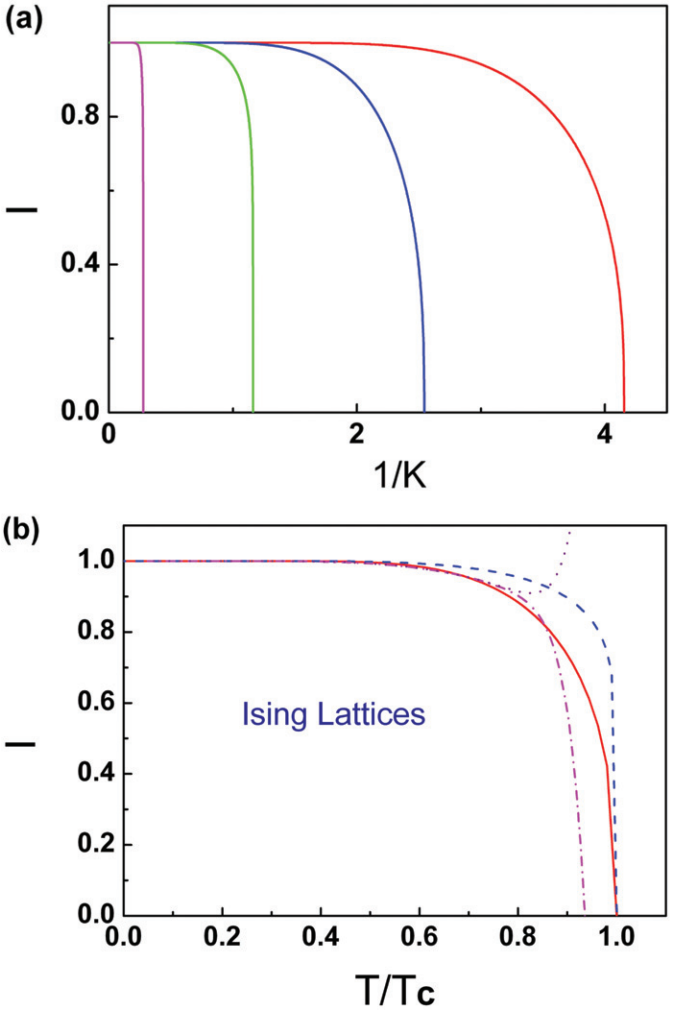

Figure 3. Temperature dependence of the spontaneous magnetization I for (a) several simple orthorhombic lattices with $K'=K''=K$, $0.5K$, $0.1K$ and $0.0001K$ (from right to left) and (b) simple cubic Ising lattice (solid curve) in comparison with that (dashed curve) obtained by Yang for the square Ising model [20] and the result of the low-temperature series expansion (the dotted curve with terms up to the 52nd order [111, 238]; the dash/dot curve with terms up to the 54th order [238] of the simple cubic Ising lattice).

The spontaneous magnetization I for the simple orthorhombic lattices is obtained from equations (95) and (98) as:

$$I = \left\{ \frac{\left[\begin{array}{c} \left(1 - x_1^2 + 4x_1x_2x_3x_4 - x_2^2x_3^2x_4^2 + x_1^2x_2^2x_3^2x_4^2\right) \\ \times\left(1 - x_1^2 - 4x_1x_2x_3x_4 - x_2^2x_3^2x_4^2 + x_1^2x_2^2x_3^2x_4^2\right) \end{array} \right]^{1/2}}{\left(1 - x_1^2\right)\left(1 - x_2^2x_3^2x_4^2\right)} \right\}^{3/4} \tag{99}$$

The temperature dependence of the spontaneous magnetization I for several simple orthorhombic lattices with $K' = K'' = K$, $0.5K$, $0.1K$ and $0.0001K$ is represented in figure 3a. The spontaneous magnetization decreases with increasing temperature to zero at the critical point. The critical point decreases with decreasing K' and K'', until disappearing as $K' = K'' = 0$ as a 1D system. For a simple cubic lattice, because $x_1 = x_2 = x_3 = x_4 = x$, k is reduced to:

$$k = \frac{2k_{-1}^{1/2}}{1 + k_{-1}} = \frac{4x^4}{(1 - x^2)(1 - x^6)} = \sinh^{-1} 2K \sinh^{-1} 6K. \tag{100}$$

Then, the spontaneous magnetization I for the simple cubic lattices could be:

$$I = \left\{ \frac{1}{(1 - x^2)(1 - x^6)} \left[\left(1 - x^2 + 4x^4 - x^6 + x^8\right)\left(1 - x^2 - 4x^4 - x^6 + x^8\right) \right]^{1/2} \right\}^{3/4}. \tag{101}$$

or

$$I = \left[1 - \frac{16x^8}{(1 - x^2)^2(1 - x^6)^2} \right]^{3/8}. \tag{102}$$

At low temperatures, this gives the expansion in power of x as:

$$\begin{aligned} I = 1 &- 6x^8 - 12x^{10} - 18x^{12} - 36x^{14} - 84x^{16} - 192x^{18} - 408x^{20} - 864x^{22} - 1970x^{24} \\ &- 4680x^{26} - 10980x^{28} - 25480x^{30} - 59970x^{32} - 143940x^{34} - 347730x^{36} \\ &- 838956x^{38} - 2028870x^{40} - 7790088x^{42} \ldots \end{aligned} \tag{103}$$

This series is convergent up to the critical point, where $x = x_c = ((\sqrt{5} - 1)/2)$. Near the critical point, I has a branch point:

$$I \cong \left[\left(\frac{5\sqrt{5}(\sqrt{5} + 1)}{2} \right)(x_c - x) \right]^{3/8}. \tag{104}$$

In figure 3b, the spontaneous magnetization I of the simple cubic Ising lattice is plotted against the temperature, in comparison with the spontaneous magnetization obtained by Yang for the square Ising model [20], and the result of the series expansion [111, 238] of the simple cubic Ising model. It is interesting to note that two golden solutions, $((\sqrt{5} - 1)/2)$ and $((\sqrt{5} + 1)/2)$ of the equation $x^2 + x - 1 = 0$ appear as x_c and the constant in the formula for the critical behaviour of the spontaneous magnetization of the 3D simple cubic Ising model, while two silver solutions of the equation $x^2 + 2x - 1 = 0$ show up in the Yang's formula for the 2D square

Ising model [20]. Being plotted as a function of T/T_c, the different critical behaviour of the spontaneous magnetization of the 3D and 2D Ising lattices are clearly seen, which originate from their different powers of 3/8 and 1/8. We believe that the low-temperature series expansion is not exact and the appearance of a plus sign is clearly incorrect [59], which is to compensate the incorrectness of the x^6 term (this issue will be discussed in detail in section 8). Nevertheless, the series expansion of the simple cubic Ising model numerically fits well with the putative exact model, and oscillates around it, up to $T \approx 0.9T_c$, and then deviates from it. The spontaneous magnetization obtained by the low-temperature series expansion depends sensitively on how many terms are taken into account. It is seen from figure 3b that the curve with terms up to the 52nd order (with a positive coefficient) rises above $\sim 0.9T_c$ [111, 238], while the curve with terms with the 54th order (with a negative coefficient) as its last term drops monotonously [238]. This indicates clearly that the low-temperature series diverges. Moreover, the curve with more terms is closer to the putative exact solution. It is expected that if more terms were taken into account, the curves of the low-temperature series would numerically fit better with the putative solution in a broader temperature range (however, the curves of the low-temperature series are still divergent, depending sensitively on the sign of the last term). This implies that our putative exact solution might be correct.

4.2. *3D-to-2D crossover phenomenon*

It is interesting to see how the exponent $\beta = 3/8$ for 3D becomes the well-known $\beta = 1/8$ for 2D and whether the 3D-to-2D crossover phenomenon is similar to the 2D-to-1D crossover phenomenon. There was no evident indication in Yang's formula [20] to show how the $\beta = 1/8$ disappears when either x_1 or x_2 equals 1, as it was not represented directly as a function of x_1 and x_2. The 2D-to-1D crossover phenomenon embodied in the expression in the brackets of their formula cannot be directly understood from the power 1/8 itself. One can understand the 2D-to-1D crossover phenomenon more easily by Chang's general formula for a rectangular lattice [21], compared with a square lattice [20]. As Chang discovered [21], the exponent 1/8 does not change with varying ratios of the vertical and horizontal interactions. It is tempting to conclude that the exponent is dependent only on the dimensionality of the lattice and not on the number of nearest neighbours [21].

For the 3D-to-2D crossover phenomenon, one might expect a similar situation. From first impressions, as $x_3 = x_4 \equiv 1$ (i.e. $K'' = K''' \equiv 0$), the spontaneous magnetization (equation (99)) for the simple orthorhombic lattices should automatically return Onsager's original 2D Ising model and, hence, the critical exponent β automatically becomes 1/8. This could be realized, since one does not need the additional rotation in the 2D limit. However, another mechanism is uncovered on the 3D-to-2D crossover phenomenon based on the validity of our solution. Namely, there should be a gradual crossover between the 3D and 2D behaviour when $x_3 = x_4 \to 1$ as $K'' = K''' \to 0$. The criterion for illustrating the existence of this crossover is described as follows: at the same temperature, the spontaneous magnetization of a 3D Ising system with $x_3 = x_4 \neq 1$ must always be higher than that of a 2D Ising system with the same values of x_1 and x_2 as the 3D Ising system.

This criterion is not based on a hypothesis, but a fact with physical significances. The spontaneous magnetization (i.e. the order parameter) of the system depends on competition between the order energy (controlled by the Hamiltonian) and the disorder energy (i.e. the thermal activity). How the order parameter decreases with increasing temperature reveals this competition. To compare the spontaneous magnetization of different systems at the same temperature involves comparing their order energy only because at a fixed temperature, the thermal activity is maintained for these systems. From the Hamiltonian, it is clear that the order energy of a 3D Ising system with $K'' \neq 0$ is always larger than that of a 2D Ising system with the same values of K and K', no matter how small the K'' is. In other words, this criterion can also apply in the regime where one of the coupling interactions of the 3D ferromagnet approaches zero, namely, when $T_{c,3D}$ is close to $T_{c,2D}$. The 3D Ising system can be constructed by connecting the l planes of the 2D Ising systems by the third interaction K''. With the help of the third interaction K'' to defy the thermal activity, the order parameter of the 3D Ising system is always higher than that of the 2D Ising system at the same temperature. Clearly, this criterion is always true, whether one or both of the systems are in the critical region.

The exponent $\beta = 3/8$ gives a curve lower than that of the exponent $\beta = 1/8$ for 2D if plotting the spontaneous magnetization as a function of T/T_c. When K'' and K''' are sufficiently large to have a Curie point that keeps the spontaneous magnetization for 3D always higher than 2D plots, the system behaves as a real 3D system with $\beta = 3/8$. Otherwise, the system behaves as a crossover with an exponent β in the range 1/8 – 3/8, though the small values of K'' and K''' do not yet vanish. The range of this crossover could be determined numerically to be from $K'' = K''' \approx 0.195K$ (in case of $K = K'$) to zero. One could derive the area of the 3D-to-2D crossover in the parametric diagram of the whole system (see figure 4). The dashed curve of $(K'/K) + (K''/K) + (K'K''/K^2) = 1$ in figure 4 corresponds to the points with the critical temperature of the silver solution. The 3D-to-2D crossover phenomenon appears in the area between the dashed and the dash-dot curve of $(K'/K) + (K''/K) + (K'K''/K^2) \approx 1.39$. All the points with a critical temperature below the silver solution would have the 2D critical exponent, while all the points in the area above the dash-dot curve would behave as a real 3D system. It is difficult to illustrate mathematically in detail how the exponent $\beta = 3/8$ for 3D changes to be the well-known $\beta = 1/8$ for 2D in this crossover.

In the following, the occurrence of this crossover is proved briefly. As shown in figure 3b, when plotted as a function of T/T_c, the spontaneous magnetization of the 3D Ising model is always lower than that of the 2D Ising model at every normalized temperature. This is always true, whether we choose the exponent of 3/8 or 5/16 (as high-temperature series expansions suggested). Supposed we have a function $m_{3D}(x_1, x_2, x_3)$ for the expression in the brackets for the spontaneous magnetization of the 3D Ising model, and a function $m_{2D}(x_1, x_2)$ for 2D. From the two functions, one can determine directly the critical point, without considering how large the exponent is. With the third interaction value being small enough (say, $K'' \to 0^+$ in case of $K = K'$), the difference between the critical points of the 3D and 2D Ising models can also be small enough ($T_{c,3D} \to T_{c,2D}{}^+$). Then, the large difference between the exponents of the two systems results in most of the spontaneous magnetization of the 3D Ising model at temperatures below $T_{c,2D}$ being lower than

that of the 2D system. The spontaneous magnetization of the 3D Ising model at temperatures above $T_{c,2D}$ is higher than that of the 2D system. There is a cross point between the two curves for the spontaneous magnetization of the two systems. In principle, this situation must occur, irrespective of the functions m_{3D} and m_{2D} or whether the exponent β for the 3D Ising model is 3/8 or 5/16. It is unreasonable to believe that the spontaneous magnetization of the 3D Ising model is smaller than that of the 2D Ising model, as the existence of the third interaction should increase the order energy and, hence, enhance the spontaneous magnetization. A rational mechanism is that the exponent β in this limit is not 3/8 (or 5/16), but slightly larger than that of the 2D Ising model (i.e. $\beta \to (1/8)^{+}$). Similar analysis reveals that as K'' decreases to less than $\sim$0.195K, the exponent β should be slightly less than 3/8 (i.e. $\beta \to (3/8)^{-}$). This indicates clearly that there is a crossover of exponent β from the 3D value of 3/8 to the 2D value of 1/8, as K'' decreases to zero. This does not depend on the detail expression of the solution. This kind of the 3D-to-2D crossover phenomenon implies that the action of the additional rotation becomes gradually weaker as K'' decreases to zero. Similar proof can be obtained for the cases with both K' and K'' decreasing. One easily derives the condition of $(K'/K)+(K''/K)+(K'K''/K^2) \approx 1.39$ for the boundary between the areas for real 3D behaviour and the 3D-to-2D crossover. The present work shows that the 3D-to-2D crossover phenomenon differs with the 2D-to-1D crossover phenomenon. This is because from 3D to 2D, the crossover is between two different ordering systems, whereas from 2D to 1D, the crossover is between ordering and disordering systems. Also in 3D to 2D, the crossover is between two systems with and without topologic problems, respectively, whereas from 2D to 1D, the crossover occurs between two systems, both without a topologic problem.

It is widely accepted (mainly based on numerical calculations) that the 3D system always shows 3D critical behaviour, no matter what the relative ratios between the strengths of interactions along three crystallographic axes. It is known from numerical results that even with a small enough interlayer interaction, the system shows 3D critical behaviour for a narrow range near the critical temperature. This range becomes narrower when the interlayer interaction becomes smaller. However, to fit the 3D critical exponent well within a narrower range near the critical temperature means that 3D critical behaviour becomes weaker, while other terms (such as the subleading order in expansions) of different critical behaviour become comparatively stronger. If one insisted on fitting the 3D critical exponents as the interlayer interaction becomes extremely smaller, the critical region would be extremely narrow (zero or infinitesimal, with no physical meaning). This raises the problem: how does the 3D system with a very narrow critical region and the 3D critical exponents suddenly jump to the 2D system with a much wider critical region and the 2D critical exponents as the infinitesimal interaction K'' vanishes? Such a sudden jump should not occur, because the 3D system with the infinitesimal interaction K'' should have 2D-like behaviour. The infinitesimal interaction K'' make the l planes of the 2D Ising systems almost independent of each other. The 3D system, in this case, is close to many, separate 2D Ising systems. The critical behaviour of the 3D system with the infinitesimal interaction K'' should be close to the 2D critical behaviour. It is emphasized that any numerical results, obtained by fitting the data points of the calculations, cannot serve as a standard for discussion

on the present topic, due to the limited accuracy of the numerical calculation (though it might be highly precise), such as systematic errors originating from approximation disadvantages and computer power (in dealing with the cooperative phenomena of infinite spins in the system).

To discuss the situation in detail, one could assume that the 3D magnetization is of the typical form in the expansion: $M_{3D}(T) \sim A(T_c)\,|T-T_c|^{\beta} + B(T_c)\,|T-T_c|^{\beta'} +$ higher order terms ($\beta \neq \beta'$). Then, one could argue that, to satisfy the criterion above, there is no need of a crossover, specifically, by taking into account the next leading order term in the 3D magnetization expansion close to T_c. $\beta < \beta'$ is not the case here, since it may correspond to the 3D to 4D crossover. For $\beta > \beta'$ ($\beta \sim 3/8$ (or 5/16) and $\beta' = 1/8$ for the 3D-to-2D crossover), it could happen, that in the limit $T_{c,3D}$ to $T_{c,2D}$, the subleading order could take over with a divergent amplitude B, such that $B(T_c)\,|T - T_c|^{\beta'}$ to $C(T_c)\,|\,T - T_c|^{1/8}$. However, the action of the subleading order depends sensitively on the relative ratio r_{AB} ($=A/B$) between amplitudes A and B. In the limited case of a pure 3D system, the subleading order is negligible since amplitude A is dominant ($r_{AB} \to \infty$), whereas in the pure 2D case, the subleading order takes over as the amplitude B becomes dominant ($r_{AB} \to 0$). Regarding continuity, there should exist a region in the parametric plane where amplitudes A and B are comparable ($r_{AB} \sim 1$). In this region, the contributions from the leading and the subleading orders in the expansion above are comparably in the same order and one cannot neglect the effects of both terms. In this region, the 3D magnetization expansion above fails to derive a unique critical exponent and the actual critical exponent of the system is neither β nor β'. The only possibility is to describe the critical behaviour by $D(T_c)\,|T - T_c|^{\beta''}$ with $\beta > \beta'' > \beta'$ for $r_{AB} \sim 1$. Finally, note that β' should not be smaller than 1/8; otherwise, it would create another difficulty in interpreting how the critical behaviour of the system changes from β' to the 2D value 1/8.

It is clear that during the 3D-to-2D crossover, as one of the coupling interactions of the 3D ferromagnet approaches zero (e.g. $K_3 \to 0$, $x_3 \to 1$), the difference between the functions $m_{3D}(x_1, x_2, x_3)$ and $m_{2D}(x_1, x_2)$ in the brackets of the expression for the spontaneous magnetization of the 3D and 2D Ising models can be negligible. On the other hand, if the system still had a 3D critical exponent, the existence of the large difference between the 3D and 2D critical exponents would violate the criterion that, at the same temperature, the spontaneous magnetization of a 3D Ising system with $K'' \neq 0$ (i.e. $x_3 \neq 1$) must always be higher than that of a 2D Ising system with the same values of x_1 and x_2. The only possibility to satisfy this criterion is that the critical exponent of the system approaches the 2D system during a crossover.

5. Spin correlation function

The spin–spin correlations in the 2D Ising model were studied first by Kaufman and Onsager [18], then by various authors [239–251]. The combinatorial method was used by Potts and Ward to calculate the partition function of a finite rectangular Ising lattice and the correlation functions of an infinite lattice [60, 239].

The proof necessary to make this solution rigorous was supplied by Sherman [240, 241] and Burgoyne [242]. Kadanoff [243] phrased the Onsager solution of the 2D Ising model in the language of thermodynamic Green's functions and discussed the spin correlation functions for temperatures smaller/greater than the critical point. The Pfaffians was first introduced by Hurst and Green [244] to derive the solution of the Ising problem for a rectangular lattice. The number of ways in which a finite quadratic lattice (with edges or periodic boundary conditions) can be fully covered with given numbers of 'horizontal' and 'vertical' dimers was rigorously calculated by a combinatorial method involving Pfaffians [245]. The Ising problem was shown to be equivalent to a generalized dimer problem and the Onsager expression for the Ising partition function of a rectangular lattice graph was derived on the basis of this equivalence [246–248]. As revealed by Kasteleyn [245, 246] neither the (C) nor (D) theorem in his paper is true if a nonplanar graph is represented in a plane (with intersecting lines). The Onsager–Kaufman formulae for the correlations and the Onsager formula for the spontaneous magnetization of the rectangular 2D Ising lattice were revived by Montroll *et al.* [249]. The Pfaffian approach was used to derive the correlation in terms of Pfaffians and, for the correlations in a row, a single Toepltiz determinant was obtained, which was proved equivalent to the Onsager–Kaufman result. The Pfaffian representation of the partition function of the 2D triangular lattice was also applied to derive the expressions for various two, four, and six spin correlations in terms of Pfaffians [250]. It is clear that one cannot simply apply the technique of Pfaffians to deal with the problem of the 3D Ising model. In addition, the short-range order parameters were evaluated for the triangular and honeycomb Ising nets in ferro- and antiferromagnetic cases by the method of Kaufman and Onsager [251].

In this section, we shall investigate the spin correlation function for the 3D simple orthorhombic Ising lattices, also based on the introduction of the two conjectures. We first give the general formula for the spin correlation function of the simple orthorhombic Ising system. Then, we discuss the spin correlation function separately, in its different features. The initial approach is to follow the Montroll *et al.* [249] procedure to evaluate the spin correlation function, which is related to the spontaneous magnetization in its long-range order. The second is to follow the Wu [252] procedure to study the short-range order. The third is to follow the Fisher [247] procedure to discuss the true range of the spin correlation function, which is related to the correlation length. The fourth is to extend the discussion of Kaufman and Onsager [18] on the short-range order to the three-dimensional binary Ising lattice.

5.1. *General formula*

Each site in the lattice could be indexed by (i, j, k) for its location in the coordinate system (rows, column, plane). In general, the spin in the jth site in the ith row of the kth plane, when the crystal is in configuration $\{\nu_1, \nu_1, \ldots \nu_m\}$, is $(s_{jk})_{vivi}$.

The average value of this spin is [18]:

$$\begin{aligned}\overline{s}_{jk} &= \frac{1}{Z}\sum_{\nu_1,\nu_2,\ldots\nu_m}\left(s_{jk}\right)_{\nu_k\nu_k}V_{\nu_1\nu_2}V_{\nu_2\nu_3}\cdots V_{\nu_{i-1}\nu_i}V_{\nu_i\nu_{i+1}}\cdots V_{\nu_m\nu_1}\\ &= \frac{1}{Z}\sum_{\nu_1,\nu_2,\ldots\nu_m}V_{\nu_1\nu_2}V_{\nu_2\nu_3}\cdots V_{\nu_{i-1}\nu_i}\left(s_{jk}\right)_{\nu_i\nu_i}V_{\nu_i\nu_{i+1}}\cdots V_{\nu_m\nu_1}\\ &= \frac{1}{Z}\cdot\text{trace}\left\{V^{i-1}s_{ij}V^{m-i+1}\right\} = \left(\frac{1}{Z}\right)\text{trace}\left(s_{jk}V^{m}\right).\end{aligned} \tag{105}$$

This result is independent of i, and $\overline{s}_{jk}$ vanishes identically for every (j, k).

The correlation function between the spins of the site j in row i and the site b in row a within plane k, i.e. (i, j, k) and (a, b, k), is written as:

$$\begin{aligned}< s_{ijk}s_{abk} >_{Av} &= \frac{1}{Z}\sum_{\nu_1,\nu_2,\ldots\nu_m}V_{\nu_1\nu_2}\cdots V_{\nu_{i-1}\nu_i}\left(s_{jk}\right)_{\nu_i\nu_i}V_{\nu_i\nu_{i+1}}\cdots V_{\nu_{a-1}\nu_a}\left(s_{bk}\right)_{\nu_a\nu_a}V_{\nu_a\nu_{a+1}}\cdots\\ &= \frac{1}{Z}\cdot\text{trace}\left\{V^{i-1}s_{jk}V^{a-i}s_{bk}V^{m-a+1}\right\} = \left(\frac{1}{Z}\right)\text{trace}\left(s_{jk}V^{a-i}s_{bk}V^{m-a+i}\right)\end{aligned} \tag{106}$$

For the correlation function between the spins of the site located in plane k and row i and that located in plane χ and row α within column j, i.e. (i, j, k) and (α, j, χ), we have:

$$\begin{aligned}< s_{ijk}s_{\alpha j\chi} >_{Av} &= \frac{1}{Z}\sum_{\nu_1,\nu_2,\ldots\nu_m}V_{\nu_1\nu_2}\ldots V_{\nu_{i-1}\nu_i}\left(s_{jk}\right)_{\nu_i\nu_i}V_{\nu_i\nu_{i+1}}\ldots V_{\nu_{\alpha-1}\nu_\alpha}\left(s_{j\chi}\right)_{\nu_\alpha\nu_\alpha}V_{\nu_\alpha\nu_{\alpha+1}}\ldots\\ &= \frac{1}{Z}\cdot\text{trace}\left\{V^{i-1}s_{jk}V^{\alpha-i}s_{j\chi}V^{m-\alpha+1}\right\} = \left(\frac{1}{Z}\right)\text{trace}\left(s_{jk}V^{\alpha-i}s_{j\chi}V^{m-\alpha+i}\right)\end{aligned} \tag{107}$$

The correlation function between the spins of site b in row a in plane k and site j in row α in plane χ, i.e. (a, b, k) and (α, j, χ), could be calculated by multiplication of the two correlation functions (106) and (107):

$$\begin{aligned}< s_{abk}s_{\alpha j\chi} >_{Av} &= < s_{abk}s_{ijk} >_{Av}\cdot < s_{ijk}s_{\alpha j\chi} >_{Av}\\ &= \left(\frac{1}{Z}\right)\text{trace}\left(s_{jk}V^{a-i}s_{bk}V^{m-a+i}\right)\cdot\left(\frac{1}{Z}\right)\text{trace}\left(s_{jk}V^{\alpha-i}s_{j\chi}V^{m-\alpha+i}\right)\end{aligned} \tag{108}$$

At zero temperature, all spins are aligned and, as a result, we have:

$$< s_{abk}s_{ijk} >_{Av} = +1, \tag{109a}$$

$$< s_{ijk}s_{\alpha j\chi} >_{Av} = +1, \tag{109b}$$

and

$$< s_{abk}s_{\alpha j\chi} >_{Av} = +1. \tag{109c}$$

for all pairs of sites. At higher temperatures, the correlation functions decrease and tend to zero for very high temperatures. The correlation function $<s_{abk}s_{\alpha j\chi}>_{Av}$ between the spins of two sites in different planes in the lattice will be known,

as soon as we know the correlation function $<s_{abk}s_{ijk}>_{Av}$ between spins of two sites within one plane and the correlation function $<s_{ijk}s_{\alpha j\chi}>_{Av}$ between spins of two sites within one column. The procedures for evaluating the correlation functions $<s_{abk}s_{ijk}>_{Av}$ and $<s_{ijk}s_{\alpha j\chi}>_{Av}$ are the same due to the symmetry of the lattice.

5.2. *Correlation functions*

The partition function for the 3D simple orthorhombic Ising lattices could be written as:

$$\begin{aligned} Z &= \sum_{\sigma=\pm1}\prod_{n.n.n}\exp\left(K\sigma_{\alpha,\beta,\gamma}\sigma_{\alpha,\beta+1,\gamma}+K'\sigma_{\alpha,\beta,\gamma}\sigma_{\alpha+1,\beta,\gamma}+K''\sigma_{\alpha,\beta,\gamma}\sigma_{\alpha,\beta,\gamma+1}\right) \\ &= (\cosh K\cosh K'\cosh K'')^N \\ &\quad\times\sum_{\sigma=\pm1}\prod_{n.n.n}\left(1+z_1\sigma_{\alpha,\beta,\gamma}\sigma_{\alpha,\beta+1,\gamma}\right)\left(1+z_2\sigma_{\alpha,\beta,\gamma}\sigma_{\alpha+1,\beta,\gamma}\right)\left(1+z_3\sigma_{\alpha,\beta,\gamma}\sigma_{\alpha,\beta,\gamma+1}\right) \end{aligned} \tag{110}$$

where $z_1=\tanh K$, $z_2=\tanh K'$ and $z_3=\tanh K''$. The square of the Pfaffian is the determinant of a skew-symmetric matrix A so that:

$$Z^2=(2\cosh K\cosh K'\cosh K'')^{2N}|A|. \tag{111}$$

The correlation between two spins at the sites $(1,1,1)$ and $(1+m,1+n,1+l)$ could be defined as:

$$\begin{aligned} <\sigma_{1,1,1}\sigma_{1+m,1+n,1+l}> &= \frac{1}{Z}(\cosh K\cosh K'\cosh K'')^N\sum_{\sigma=\pm1}\sigma_{1,1,1}\sigma_{1+m,1+n,1+l} \\ &\quad\times\prod_{n.n.n}\left(1+z_1\sigma_{\alpha,\beta,\gamma}\sigma_{\alpha,\beta+1,\gamma}\right)\left(1+z_2\sigma_{\alpha,\beta,\gamma}\sigma_{\alpha+1,\beta,\gamma}\right) \\ &\quad\times\left(1+z_3\sigma_{\alpha,\beta,\gamma}\sigma_{\alpha,\beta,\gamma+1}\right). \end{aligned} \tag{112}$$

Similar to the 2D Ising case, the determinant of a skew-symmetric matrix A is equal to the square of the Pfaffian. However, the skew-symmetric matrix A for the 3D simple orthorhombic Ising lattices is actually a three-dimensional matrix and the laws of its operations are unknown. It is difficulty to evaluate the spin correlation function of 3D Ising lattices, simply following the Montroll *et al.* method [249]. Fortunately, we have found the putative solution (49) for 3D simple orthorhombic Ising lattices for finite temperatures, based on the two conjectures. We could immediately find out the similarity between the formulae for the 3D and 2D Ising lattices. Therefore, following the Montroll *et al.* procedure for the 2D Ising lattice [249], we could define an effective skew-symmetric matrix $A_{\rm eff}$ as.

$$A_{eff}=\begin{bmatrix} 0 & 1+z_1e^{i\omega'} & -1 & 1 \\ -1-z_1e^{-i\omega'} & 0 & 1 & -1 \\ 1 & -1 & 0 & 1+z_{2,eff}e^{i\omega} \\ 1 & 1 & -1-z_{2,eff}e^{-i\omega} & 0 \end{bmatrix}, \tag{113}$$

with $z_{2,\rm eff}=\tanh(K'+K''+K''')=z_2\,z_3\,z_4$ and $z_4=\tanh K'''$.

The spin correlation function at finite temperatures of the 3D simple orthorhombic Ising lattices could be expressed effectively as:

$$
\begin{aligned}
&Z z_1^{-n} z_{2,eff}^{-l} < \boldsymbol{\sigma}_{1,1} \boldsymbol{\sigma}_{1+n.1+l}^{eff} > \\
&= (\cosh K \cosh(K' + K'' + K'''))^N \sum_{\sigma=\pm 1} \prod_{n'=1}^{n} \left(1 + z_1^{-1} \sigma_{1,n'} \sigma_{1,1+n'}\right) \\
&\times \prod_{l'=1}^{l} \left(1 + z_{2,eff}^{-1} \sigma_{l',1+n} \sigma_{1+l',1+n}\right) \prod_{n.n}{}' \left(1 + z_1 \sigma_{\alpha,\beta} \sigma_{\alpha,\beta+1}\right)\left(1 + z_{2,eff} \sigma_{\alpha,\beta} \sigma_{\alpha+1,\beta}\right). \qquad (114)
\end{aligned}
$$

The formula (114) has a form similar to that used by Montroll *et al.* [249] Following the same procedure same as equations (18) – (40) of the Montroll *et al.* paper [249], one gets:

$$
< \sigma_{1,1} \sigma_{1,2}^{eff} > = \frac{1}{2\pi} \int_{-\pi}^{\pi} e^{i\delta^*(\omega)} d\omega. \qquad (115)
$$

Here $\delta^*(\omega)$ is the function, as expressed by:

$$
e^{2i\delta^*} = \frac{\left(z_1 z_{2,eff}^* e^{i\omega} - 1\right)\left(z_1 e^{i\omega} - z_{2,eff}^*\right)}{\left(e^{i\omega} - z_1 z_{2,eff}^*\right)\left(z_{2,eff}^* e^{i\omega} - z_1\right)}, \qquad (116)
$$

with

$$
z_{2,eff}^* = \frac{1 - z_{2,eff}}{1 + z_{2,eff}} = e^{-2(K' + K'' + K''')}. \qquad (117)
$$

Finally, the correlation could be written as the Toeplitz determinant [249, 253, 254]:

$$
< \sigma_{1,1} \sigma_{1,1+l}^{eff} > = \begin{vmatrix}
a_0 & a_1 & a_2 & . & . & . & a_{l-1} \\
a_{-1} & a_0 & a_1 & . & . & . & a_{l-2} \\
a_{-2} & a_{-1} & a_0 & . & . & . & a_{l-3} \\
. & . & . & . & . & . & . \\
. & . & . & . & . & . & . \\
. & . & . & . & . & . & . \\
a_{-l+1} & a_{-l+2} & a_{-l+3} & . & . & . & a_0
\end{vmatrix}, \qquad (118)
$$

where

$$
a_r = \frac{1}{2\pi} \int_{-\pi}^{\pi} e^{-ir\omega} e^{i\delta^*(\omega)} d\omega, \qquad (119)
$$

are the coefficients in a series expansion of $e^{i\delta^*}$.

According to the dimension units for the expressions of the correlation functions, the following relations could be realized:

$$
< \sigma_{1,1,1} \sigma_{1,1,1+l} > = < \sigma_{1,1} \sigma_{1,1+l}^{eff} >^3, \qquad (120)
$$

and it yields:

$$I^{2/3} = \lim_{l\to\infty} < \sigma_{1,1,1}\sigma_{1,1,1+l} >^{1/3} = \lim_{l\to\infty} < \sigma_{1,1}\sigma^{eff}_{1,1+l} > . \tag{121}$$

Following the procedure of Montroll *et al.* [249], it is known from the Szego theorem that, if $D_{\mathrm{m}}(f)$ is the determinant of a Toepltiz matrix whose elements are the coefficients in the Laurent expansion of a function $f(\omega)$, then [249, 253, 254]:

$$\lim_{m\to\infty} \frac{D_m(f)}{G(f)^{m+1}} = \exp\left(\sum_1^\infty nk_nk_n\right), \tag{122}$$

where

$$G(f) = \exp\left[\frac{1}{2\pi}\int_{-\pi}^{\pi} \ln f(\omega)d\omega\right], \tag{123}$$

and

$$\ln f(\omega) = \sum_{n=-\infty}^{\infty} k_n e^{in\omega}. \tag{124}$$

To obtain k_n, we require the Fourier expansion of:

$$\ln f(\omega) = i\delta^*(\omega) = \frac{1}{2}\ln\frac{\left(z_1z^*_{2,eff}e^{i\omega}-1\right)\left(z_1e^{i\omega}-z^*_{2,eff}\right)}{\left(e^{i\omega}-z_1z^*_{2,eff}\right)\left(z^*_{2,eff}e^{i\omega}-z_1\right)}. \tag{125}$$

in two different temperature ranges, for $T<T_{\mathrm{c}}$, $z^*_{2,eff}<z_1<1$; for $\infty>T>T_{\mathrm{c}}$, $z_1<z^*_{2,eff}<1$. The spontaneous magnetization below the critical temperature could be derived as:

$$\begin{aligned} I &= \left[1-\frac{\left(1-z_1^2\right)^2 z^{*2}_{2,eff}}{z_1^2\left(1-z^{*2}_{2,eff}\right)^2}\right]^{3/8} = \left[1-\frac{\left(1-z_1^2\right)^2\left(1-z_2^2z_3^2z_4^2\right)^2}{16z_1^2z_2^2z_3^2z_4^2}\right]^{3/8} \\ &= \left[1-\frac{16x_1^2x_2^2x_3^2x_4^2}{\left(1-x_1^2\right)^2\left(1-x_2^2x_3^2x_4^2\right)^2}\right]^{3/8} \\ &= \left[1-\sinh^{-2}2K\sinh^{-2}2(K'+K''+K''')\right]^{3/8} \end{aligned} \tag{126}$$

The spontaneous magnetization I derived in this method is inconsistent with that obtained in section 4. Similarly, we could prove that, for $\infty>T>T_{\mathrm{c}}$, $I=0$, since $\sum_1^\infty nk_nk_{-n} = -\infty$, as $\sum(1/n)$ is divergent.

5.3. *Short-range order*

The above results for the correlation and spontaneous magnetization could be summarized as follows. The form of the formula for the correlation or the spontaneous magnetization of the 3D simple orthorhombic Ising model should be

the same as the cubic power of that for the 2D rectangular Ising model, where transformations of $z_2 \to z_{2,eff} = z_2 z_3 z_4$, $z_2^* \to z_{2,eff}^*$, $x_2 \to x_2 x_3 x_4$, and $K' \to K' + K'' + K'''$ are performed. Furthermore, from the point of view of the dimensions of units, one could expect the transformation of $N \to N^{3/2}$.

Following Wu's study [252], the correlation function S_N of the 3D simple orthorhombic Ising lattices is re-written as:

$$S_N^{1/3} = \begin{vmatrix} a_0 & a_{-1} & a_{-2} & . & . & . & a_{-N+1} \\ a_1 & a_0 & a_{-1} & . & . & . & a_{-N+2} \\ a_2 & a_1 & a_0 & . & . & . & a_{-N+3} \\ . & . & . & . & . & . & . \\ . & . & . & . & . & . & . \\ . & . & . & . & . & . & . \\ a_{N-1} & a_{N-2} & a_{N-3} & . & . & . & a_0 \end{vmatrix}, \tag{127}$$

where

$$a_n = \frac{1}{2\pi} \int_0^{2\pi} \varphi(\theta) e^{-in\theta} d\theta, \tag{128}$$

with

$$\varphi(\theta) = e^{i\delta^*} = \left[\frac{(1 - \alpha_1 e^{i\theta})(1 - \alpha_2 e^{-i\theta})}{(1 - \alpha_1 e^{-i\theta})(1 - \alpha_2 e^{i\theta})} \right]^{1/2}. \tag{129}$$

Here

$$\alpha_1 = z_1 z_{2,eff}^* = z_1 z_2^* z_3^* z_4^*, \tag{130a}$$

$$\alpha_2 = \frac{z_{2,eff}^*}{z_1} = \frac{z_2^* z_3^* z_4^*}{z_1}. \tag{130b}$$

For a temperature above the critical point, $\infty > T > T_c$, similar to the Wu procedure [252] and according to the Szego theorem [253,254], the $N \times N$ Toeplitz determinant R_N is given by:

$$\lim_{N \to \infty} (-1)^N R_N = \left[(1 - \alpha_1^2)(1 - \alpha_2^{-2}) \left(1 - \frac{\alpha_1}{\alpha_2} \right)^2 \right]^{3/4}. \tag{131}$$

S_N reads as:

$$S_N = (-1)^N R_{N+1} x_N. \tag{132}$$

The Wiener–Hopf procedure is employed for solving x_N [252]. For $\infty > T > T_c$, the desired x_N is found to be:

$$\begin{aligned} x_N^{1/3} &\doteq \frac{1}{2\pi i} \oint d\xi \cdot \xi^{N-1} P(\xi^{-1}) Q(\xi)^{-1} \\ &= \frac{1}{2\pi i} \oint d\xi \cdot \xi^{N-1} \left[(1 - \alpha_1 \xi)(1 - \alpha_1 \xi^{-1})(1 - \alpha_2^{-1} \xi)(1 - \alpha_2^{-1} \xi^{-1}) \right]^{-1/2} \end{aligned} \tag{133}$$

Then

$$S_N^{1/3} = \left[(-1)^N R_{N+1}\right]^{1/3} x_N^{1/3} = \left[\left(1-\alpha_1^2\right)\left(1-\alpha_2^{-2}\right)\left(1-\frac{\alpha_1}{\alpha_2}\right)^2\right]^{1/4} \cdot x_N^{1/3}. \tag{134}$$

Expanding the integrand of the equation and integrating term by term lead to S_N and, finally, performing the transformation of $N \to N^{3/2}$ results in:

$$\begin{aligned} S_N \doteq & \pi^{-3/2} N^{-9/4} \alpha_2^{-3N^{3/2}} \left(1-\alpha_1^2\right)^{3/4} \left(1-\alpha_2^{-2}\right)^{-3/4} (1-\alpha_1\alpha_2)^{-3/2} \\ & \times \left[1+\frac{1}{4}N^{-3/2}A_{1>}+\frac{3}{16}N^{-3}\left(A_{2>}-\frac{5}{6}\right)+\frac{15}{64}N^{-9/2}\left(A_{3>}-\frac{7}{6}A_{1>}\right)+\cdots\right]^3 \end{aligned} \tag{135}$$

The functions and parameters in equations (132)–(135) were defined in section II of Wu's paper [252].

For temperatures below T_c, the spontaneous magnetization of the 3D simple orthorhombic Ising magnet would behave as:

$$S_\infty = \left(1-\alpha_1^2\right)^{3/4}\left(1-\alpha_2^2\right)^{3/4}(1-\alpha_1\alpha_2)^{-3/2}, \tag{136}$$

so that,

$$S_\infty^{1/3} = \left(1-\alpha_1^2\right)^{1/4}\left(1-\alpha_2^2\right)^{1/4}(1-\alpha_1\alpha_2)^{-1/2}\prod_{n=N}^{\infty} x_{0n}^{1/3}. \tag{137}$$

Then, one would obtain:

$$\begin{aligned} S_N = & \left(1-\alpha_1^2\right)^{3/4}\left(1-\alpha_2^2\right)^{3/4}(1-\alpha_1\alpha_2)^{-3/2}\left\{1+\frac{1}{2\pi N^3}\alpha_2^{2N^{3/2}}\left(\alpha_2^{-1}-\alpha_2\right)^{-2}\right. \\ & \left.\times\left[1+\frac{1}{2N^{3/2}}(-A_{1<}+4x_3')+\frac{3}{4N^3}\left(-A_{2<}+A_{1<}^2-2x_3'A_{1<}+6x_3'^2-\frac{13}{6}\right)+\cdots\right]\right\}^3 \end{aligned} \tag{138}$$

after performing the transformation of$N \to N^{3/2}$. The parameters in equation (138) are the same as those in section III of Wu's paper [252].

At the critical point, $T = T_c$, one would derive:

$$\left(S_N^{(0)}\right)^{1/3} = e^{1/4}2^{1/12}A^{-3}N^{-1/4}\left(1-\frac{1}{64}N^{-2}+\cdots\right). \tag{139}$$

Namely,

$$S_N^{(0)} = e^{3/4}2^{1/4}A^{-9}N^{-3/4}\left(1-\frac{1}{64}N^{-2}+\cdots\right)^3. \tag{140}$$

Performing the transformation of $N \to N^{3/2}$ leads to:

$$S_N^{(0)} = e^{3/4} 2^{1/4} A^{-9} N^{-9/8} \left(1 - \frac{1}{64} N^{-3} + \cdots\right)^3$$
$$= e^{3/4} 2^{1/4} A^{-9} N^{-9/8} \left(1 - \frac{3}{64} N^{-3} + \cdots\right). \tag{141}$$

Similar to the 2D Ising case [252], the following relationship is valid

$$S_N \sim \left(1 - \alpha_1^2\right)^{3/4} (1 - \alpha_1 \alpha_2)^{-3/2} S_N^{(0)}, \tag{142}$$

for the whole temperature range of $\infty > T > 0$. More explicitly, at the critical point:

$$S_N \sim (1 + \alpha_1)^{3/4} (1 - \alpha_1)^{-3/4} S_N^{(0)}, \tag{143}$$

as $N \to \infty$. Thus, the correlation at the critical point would behave as:

$$S_N \sim e^{3/4} 2^{1/4} A^{-9} (1 + \alpha_1)^{3/4} (1 - \alpha_1)^{-3/4} N^{-9/8} \left(1 - \frac{3}{64} N^{-3} + \cdots\right), \tag{144}$$

approximately for large N.

Therefore, for the 3D Ising lattice, the correlation at the critical point could be written as:

$$\Gamma_c(r) \approx D \left(\frac{a}{r}\right)^{9/8} = D \left(\frac{a}{r}\right)^{d-2+\eta}. \tag{145}$$

The critical exponent η is found to be 1/8 for $d = 3$. The Fourier transformation yields:

$$\hat{\chi}(k, v_c) \approx 4\pi \int_0^{1/ka} D \left(\frac{a}{r}\right)^{9/8} e^{ik \cdot r} r^2 dr \approx \frac{\hat{D}}{|ka|^{15/8}} = \frac{\hat{D}}{|ka|^{2-\eta}}. \tag{146}$$

From equation (146), again, the critical exponent η is 1/8.

5.4. *True range of the correlation*

The true range κ_x of the correlation of the 3D simple orthorhombic Ising system could be determined by a procedure similar to that used for the 2D Ising system [103,247].

$$[\kappa_x a]^{3/2} = -\lim_{n \to \infty} \ln \frac{\lambda_{\max}^-}{\lambda_{\max}^+} = 2(K^* - K' - K'' - K''') = \ln \coth K - 2(K' + K'' + K''')$$
$$= \ln \frac{(1 - z_2)(1 - z_3)(1 - z_4)}{z_1(1 + z_2)(1 + z_3)(1 + z_4)} = \ln \frac{x_2 x_3 x_4 (1 + x_1)}{(1 - x_1)} \tag{147}$$

with $\kappa_x = 1/\xi$, ξ is the correlation length. The power 3/2 for $\kappa_x a$ is added, in accordance with the scale dimension. At the Curie temperature, $\kappa_x \to 0$ or

$\xi \to \infty$, namely,

$$\frac{(1-z_2)(1-z_3)(1-z_4)}{z_1(1+z_2)(1+z_3)(1+z_4)} = \frac{x_2x_3x_4(1+x_1)}{(1-x_1)} = 1. \tag{148}$$

For the simple cubic lattice, the relation is reduced to:

$$\begin{aligned}[\kappa_x a]^{3/2} &= -\lim_{n\to\infty} \ln \frac{\lambda^-_{\max}}{\lambda^+_{\max}} = 2(K^* - 3K) = \ln\coth K - 6K \\ &= \ln \frac{(1-z)^3}{z(1+z)^3} = \ln \frac{x^3(1+x)}{(1-x)}\end{aligned} \tag{149}$$

At the Curie temperature, $\kappa_x \to 0$ or $\xi \to \infty$, we would have,

$$\frac{(1-z)^3}{z(1+z)^3} = \frac{x^3(1+x)}{(1-x)} = 1. \tag{150}$$

It is:

$$z^4 + 4z^3 + 4z - 1 = 0, \tag{151}$$

or

$$x^4 + x^3 + x - 1 = 0. \tag{152}$$

One of the solutions of the equations above leads to the critical point of the simple cubic Ising lattice: $z_c = \sqrt{5} - 2$ or $x_c = ((\sqrt{5}-1)/2)$. Notice that the values of z_c and x_c for the 3D simple cubic Ising lattice differ, whereas those for the 2D square Ising lattice are the same [103, 247]. For the 2D square Ising lattice [103, 247], $z_c = x_c = \sqrt{2} - 1$ is derived from $((1-z)/(z(1+z))) = (x(1+x)/(1-x)) = 1$, i.e. $z^2 + 2z - 1 = 0$ and $x^2 + 2x - 1 = 0$. It is worthwhile noting that only the 2D square Ising lattice satisfies the existence of the same values for z_c and x_c, since $z = (1-x)/(1+x)$ (or $x = (1-z)/(1+z)$) is always valid for $z = \tanh K$ and $x = e^{-2K}$ and, if one set $z = x$, one would immediately obtain $x^2 + 2x - 1 = 0$ (or $z^2 + 2z - 1 = 0$).

Near the critical point, the critical behaviour of the true range κ_x of the correlation of the simple cubic Ising lattice could be described by:

$$[\kappa_x a]^{3/2} = 5\ln\frac{\sqrt{5}+1}{2}\left(\frac{T-T_c}{T_c}\right)\left\{1 + \left[\frac{\sqrt{5}}{5}\ln\frac{\sqrt{5}+1}{2} - 1\right]\left(\frac{T-T_c}{T_c}\right) + o\left[\left(\frac{T-T_c}{T_c}\right)^2\right]\right\} \tag{153}$$

Thus, the leading term of the true range κ_x of the correlation is taken to be:

$$\kappa_x a \propto \left[\frac{T-T_c}{T}\right]^{2/3}. \tag{154}$$

The critical exponent ν is found to equal to 2/3. Noticed again that the two golden solutions, $((\sqrt{5}-1)/2)$ and $((\sqrt{5}+1)/2)$ of the equation $x^2 + x - 1 = 0$ appear in the formula for the critical behaviour of the true range κ_x of the correlation of the

3D simple cubic Ising model, while the two silver solutions of the equation $x^2+2x-1=0$ show up in the Fisher formula for the 2D square Ising model [103, 247]. It is interesting to note that, if the coordinates of a point in the golden spiral are written as $[r=\varphi^{2\theta/\pi}, \theta]$ as graphed on a polar axis, the golden ratio is related with the golden spiral by $\ln\varphi = \ln\big((\sqrt{5}+1)/2\big) = (\pi/2\theta)\ln r$.

The combination of the critical behaviours of the spin correlation functions results in:

$$\Gamma(r,T) \approx D\Big(\frac{a}{r}\Big)^{9/8} e^{-\kappa r}[1+Q(\kappa,r)] = D\Big(\frac{a}{r}\Big)^{9/8} e^{-\kappa r}\Big(1-\frac{3}{64}r^{-3}+\cdots\Big). \tag{155}$$

In the following sub-section, we shall focus on evaluating the correlation function $<s_{ijk}s_{abk}>_{Av}$ between spins of two sites within one plane.

5.5. *Procedure for evaluating averages*

Following the previous work of Kaufman and Onsager [18], we shall first evaluate the correlation function $<s_{ijk}s_{abk}>_{Av}$ between spins of two sites within one plane. We shall employ the approximation that all eigenvalues of $\mathbf{V}$ are negligible compared with the largest value, when the power of the eigenvalues is sufficiently high. To make use of this approximation, we transform (106) by $\mathbf{\Psi}$, which brings $\mathbf{V}$ to its diagonal form:

$$< s_{1,1,k}s_{1+a,b,k} >_{Av} = \left\{\sum_{i=1}^{2^{nl}} \lambda_i^m\right\}^{-1} \cdot \left\{\sum_{i=1}^{2^{nl}} \lambda_i^{m-a} \cdot \big(\Psi s_{1,k} V^a s_{b,k} \Psi^{-1}\big)_{ii}\right\}. \tag{156}$$

Similar to Kaufman and Onsager's work [18], for simplicity of notation, we will no longer differentiate between odd- and even-indexed angles for $\mathbf{\Psi}_+$ and $\mathbf{\Psi}_-$ and use the following at all temperatures:

$$< s_{1,1,k}s_{1+a,b,k} >_{Av} \cong \lambda^{-a} \cdot \big(\Psi_+ s_{1,k} V^a s_{b,k} \Psi_+^{-1}\big)_{11}. \tag{47'}$$

The quantity $\mathbf{\Psi}$ has been shown in section 3, in terms of the rotation it reduces in the spinor base $\mathbf{P_1}$, $\mathbf{Q_1}$, $\mathbf{P_2}$, $\mathbf{Q_2}$, ..., $\mathbf{P_{nl}}$, $\mathbf{Q_{nl}}$. In section 3, we had:

$$\Psi = g \cdot S(TH), \tag{157}$$

where the transformations $\mathbf{g}$, $\mathbf{T}$ and $\mathbf{H}$ are represented by equations (42), (38) and (48), respectively. The simplest correction function is found to be [18]:

$$< s_1 s_2 >_{AV}^{1/3} = \frac{1}{(nl)^{3/2}} \sum_t \cos\delta_t^* = -\cosh^2 K^* \cdot \Sigma_1 + \sinh^2 K^* \cdot \Sigma_{-1}, \tag{158}$$

with

$$\Sigma_{k-l} = \frac{1}{n\cdot l\cdot o} \times \sum_{t_x,t_y,t_z} \left\{ w_x \cos\left[(k-l)\frac{t_x\pi}{n} + \delta_t'\right] + w_y \cos\left[(k-l)\frac{t_y\pi}{l} + \delta_t'\right] + w_z \cos\left[(k-l)\frac{t_z\pi}{o} + \delta_t'\right]\right\} \tag{159}$$

and the general form for the correction function along a row in the 3D lattice is derived as:

$$< s_1 s_{1+k} >_{AV}^{1/3} = (-1)^k \left[\cosh^2 K^* \cdot \Delta_k - \sinh^2 K^* \cdot \Delta_{-k}\right], \tag{160}$$

with

$$\Delta_k = \begin{vmatrix} \Sigma_1 & \Sigma_2 & \Sigma_3 & \Sigma_4 & \cdot & \cdot & \cdot & \Sigma_k \\ \Sigma_0 & \Sigma_1 & \Sigma_2 & \Sigma_3 & \cdot & \cdot & \cdot & \Sigma_{k-1} \\ \Sigma_{-1} & \Sigma_0 & \Sigma_1 & \Sigma_2 & \cdot & \cdot & \cdot & \Sigma_{k-2} \\ \cdot & \cdot & \cdot & \cdot & \cdot & \cdot & \cdot & \cdot \\ \Sigma_{-k+2} & \Sigma_{-k+3} & \Sigma_{-k+4} & \Sigma_{-k+5} & \cdot & \cdot & \cdot & \Sigma_1 \end{vmatrix}, \tag{161}$$

and

$$\Delta_{-k} = \begin{vmatrix} \Sigma_{-1} & \Sigma_{-2} & \Sigma_{-3} & \Sigma_{-4} & \cdot & \cdot & \cdot & \Sigma_{-k} \\ \Sigma_0 & \Sigma_{-1} & \Sigma_{-2} & \Sigma_{-3} & \cdot & \cdot & \cdot & \Sigma_{-k+1} \\ \Sigma_1 & \Sigma_0 & \Sigma_{-1} & \Sigma_{-2} & \cdot & \cdot & \cdot & \Sigma_{-k+2} \\ \cdot & \cdot & \cdot & \cdot & \cdot & \cdot & \cdot & \cdot \\ \Sigma_{k-2} & \Sigma_{k-3} & \Sigma_{k-4} & \Sigma_{k-5} & \cdot & \cdot & \cdot & \Sigma_{-1} \end{vmatrix}, \tag{162}$$

Montroll *et al*. [249] proved that the correlations in a row in the form of a single Toeplitz determinant are equivalent to the Onsager–Kaufman results in the form of two Toeplitz determinants. Therefore, for the present 3D system, the results obtained following the Onsager–Kaufman process are also equivalent to those obtained following the Montroll *et al*.

6. Susceptibility

The susceptibility of the 3D simple orthorhombic Ising system could be derived by a procedure similar to that developed by Fisher [98, 99]. The susceptibility could be evaluated by:

$$\chi_0(T) = \frac{N\mu^2}{k_B T} \sum\nolimits_{l,m,n} v_{lmn} \omega_{lmn}(T). \tag{163}$$

For 3D simple orthorhombic Ising lattices, from the correlation at the critical point one has:

$$\omega_{0mn}(T_c) = < s_{1,1,1} s_{1,1+m,1} > \approx \frac{A}{m^{9/8}} (m \to \infty) \tag{164}$$

where A is a constant. The relation above could be extended as:

$$\omega_{lmn}(T_c) \approx \frac{A(\theta, \varphi)}{k^{9/8}} (k \to \infty) \tag{165}$$

where $k^2 = l^2 + m^2 + n^2$, $A(\theta, \varphi)$ is similar to A. Similar to the 2D case, one would arrive at:

$$\omega_{lmn}(T) \approx A(\theta, \varphi) k^{-9/8} \exp\left[-kb\left(1 - \frac{T_c}{T}\right)^{2/3}\right]. \tag{166}$$

Thus, one could derive the susceptibility:

$$\chi_F(T) \approx \frac{N\mu^2}{k_B T} \int_0^\infty \int_0^{2\pi} \int_0^\pi A(\theta, \varphi) k^{-9/8} \exp\left[-kb\left(1 - \frac{T_c}{T}\right)^{2/3}\right] k^2 \sin\theta d\theta d\varphi dk. \tag{167}$$

Finally,

$$\chi_F(T) \approx \frac{N\mu^2}{k_B T} \frac{4\pi b^{-15/8} \Gamma(15/8)}{(1 - T_c/T)^{5/4}} \propto \frac{1}{(1 - T_c/T)^{5/4}}. \tag{168}$$

Therefore, the critical exponent γ is equal to 5/4 for the 3D Ising model.

7. Critical exponents

The critical exponents of various physical systems have been investigated intensively, since they are the most important factors in understanding the critical behaviour of continuous phase transitions. The 2D Ising model is an example solved explicitly, which provides the exact values of the critical exponents [13]. Due to the lack of an exact solution for the 3D Ising model, the most reliable information on its critical behaviour is provided by renormalization group theory near the critical point [126–191, 208–225]. To date, the region near the critical point has been explored by various methods of approximation with high precision [59–225], but the exact mathematical solution for the 3D Ising model is the key for deriving the exact values of the critical exponents.

Fisher and Chen [255] evaluated the validity of hyperscaling in three dimensions for scalar spin systems. By applying a real space version of the Ginzburg criterion, the role of fluctuations and, hence, the self-consistency of the mean field theory were assessed in a simple fashion for a variety of phase transitions [256]. Based on the concept of the marginal dimensionality d^*, critical behaviour was discussed [257]. When the dimensionality d for a system is larger than the corresponding d^*, the mean field theory describes the correct critical behaviour [142], where $d^* = 4$ for the short-range interactions and $d^* = 3$ for uniaxial dipolar ferromagnets or ferroelectrics and for tricritical behaviour. When $d = d^*$, the renormalization group equations are exact and the Landau behaviour is modified by additional 'weak' singular behaviour, such as logarithmic corrections. One then makes the so-called ε expansion, $\varepsilon = d^* - d$, to estimate the critical behaviour for $d < d^*$.

Various physical quantities diverge to infinity or converge to zero as the temperature or other variables approach its critical point. The exponents near the critical temperature are defined as follows. In the region just below the

critical point, the spontaneous magnetization is well approximated by a power law [142–144, 152, 153]:

$$M \propto (T_c - T)^{\beta}. \tag{169}$$

The magnetization at T_c has a critical behaviour as:

$$M \sim |h|^{1/\delta}. \tag{170}$$

The correlation function has property that, if $T > T_c$, it falls off with r, with asymptotic behaviour for large r:

$$\Gamma(r) \sim \exp\left[-\frac{r}{\xi(T)}\right], \tag{171}$$

where $\xi(T)$ is the correlation length, which approaches infinity as $T \to T_c$.

$$\xi(T) \sim (T - T_c)^{-\upsilon}. \tag{172}$$

The correlation function at T_c falls as a power of r in the form:

$$\Gamma_c(r) \sim \frac{1}{r^{d-2+\eta}}. \tag{173}$$

The critical behaviour of the magnetic susceptibility is described as:

$$\chi \sim (T - T_c)^{-\gamma}. \tag{174}$$

Similarly, the critical exponent α controls the critical behaviour of the specific heat near the critical temperature:

$$C_h \sim (T - T_c)^{-\alpha}. \tag{175}$$

The zero-angle ($k \to 0$) scattering intensity apparently diverges at the critical point as:

$$I_c(k) \sim \frac{1}{k^{2-\eta}}, \quad (k \to 0). \tag{176}$$

An inverse range parameter $\kappa_1(T)$ is defined to measure the slope of $1/I(k, T)$ against k^2 as $k \to 0$. This again vanishes at the critical point and in zero field it has:

$$\kappa_1(T) \sim (T - T_c)^{\nu}. \tag{177}$$

Actually, there are six critical exponents α, β, γ, δ, η and ν, which are related by the following four scaling laws [142–144, 152, 153, 258, 259]:

$$\alpha + 2\beta + \gamma = 2 \text{ (Rushbrooke's law)}; \tag{178a}$$

$$\gamma = \beta(\delta - 1) \text{ (Wisdom's law)}; \tag{178b}$$

$$\gamma = \nu(2 - \eta) \text{ (Fisher's law)}; \tag{178c}$$

$$\nu d = 2 - \alpha \text{ (Josephson's law)}. \tag{178d}$$

There are several other expressions between the critical exponents, but not independent of these four equations [255, 260, 261]. Therefore, only two independent parameters exist among these critical exponents.

The value for the critical exponent ν can be evaluated in a simpler manner. The scale dimension $[\kappa_x]$ for the true range of the correlation is 1, while the scale dimension $[f]$ for the free energy equals d. From

$$\xi = \frac{1}{\kappa_x} \propto |T - T_c|^{-\nu} = \tau^{-\nu}. \tag{179}$$

Here $\tau = T - T_c$. We have

$$f \sim \kappa_x^d \sim |T - T_c|^{\nu d} = \tau^{\nu d}. \tag{180}$$

On the other hand, the specific heat C_B is determined by:

$$C_B = -T\frac{\partial^2 f}{\partial T^2} \sim \tau^{\nu d-2} \sim \tau^{-\alpha}. \tag{181}$$

One has the relation of $\nu d = 2-\alpha$, which could be introduced to equation (180) to have:

$$\kappa_x \sim \tau^{\nu} = \tau^{(2-\alpha)/d}. \tag{182}$$

Therefore, we have $\nu = 2/3$ for $d = 3$ and $\alpha = 0$, in comparison to $\nu = 1$ for $d = 2$ and $\alpha = 0$.

According to Ryazanov [262], three temperature regions: (1) $\tau < -r^{-3/2}$, (2) $-r^{-3/2} < \tau < r^{-3/2}$, (3) $\tau > r^{-3/2}$, exist with different behaviours of the correlation. r represents the distance (p in Ryazanov's paper). Compared with Ryazanov's description for the 2D Ising system [262], the transformation of $r \to r^{3/2}$ has been performed for the present 3D Ising system. In the second region (in the vicinity of the critical point), the distance to the phase transition point is smaller than the temperature fluctuations ($\sim 1/\sqrt{N}$; N is the number of particles) in regions with dimensions of order $r^{3/2}$. The temperature fluctuations are defined as $\tau_f = r^{3/2}$ for $d = 3$. It is expected that the correlation functions depend only on the ratio $\tau/\tau_f = r^{3/2}\tau$. In the region with large values of $r^{3/2}\tau$, the correlation decays as $\exp(-r\tau^{2/3})$, also in agreement with $\nu = 2/3$. Near the critical point of the 3D Ising magnet, the spontaneous magnetization behaves as $I \sim \tau^{3/8}$, while the long-range order correlation behaves like $S_\infty \sim \tau^{3/4}$. The relationship between the average temperature and the distance is $\tau \approx 1/r^{3/2}$ and the correlation function is in the order of $\tau^{3/4} = 1/r^{9/8}$. The correlation function near the critical point is:

$$\Gamma_c(r) \sim \frac{1}{r^{9/8}}. \tag{183}$$

and

$$\hat{\chi}(k, \nu_c) \sim \frac{1}{|ka|^{2-\eta}}, \tag{184}$$

in good agreement with the results in the section 5. The critical exponent η is found to be 1/8. It is expected that, as in the 2D case, the correlations for the 3D Ising lattice along the rows and along the diagonals is different only in the region greatly above the transition point, where the correlation radius is small and is close to the distance between the nearest neighbours [262].

The critical exponents $\alpha = 0$, $\beta = 3/8$, $\gamma = 5/4$, $\delta = 13/3$, $\eta = 1/8$ and $\nu = 2/3$ are derived from the two conjectures for 3D simple orthorhombic Ising lattices satisfying the scaling laws, showing universality behaviour. These putative exact critical exponents are tabulated in table 1, together with exact values for 1D and 2D Ising lattices, approximate values obtained by the renormalization group and the high-temperature series expansion for the 3D Ising lattice, and those of the mean field theory. As for the critical point, we will roughly compare data for the last 60 years and then recent data more carefully. It is clear from table 1 that the values of the critical exponents for temperatures below T_c, taken from Fisher [103], are not very reliable due to the appearance of the negative critical exponent η. Thus, we do not include this group of the critical exponents in the discussion below. As stated above, the specific heat of the 3D Ising lattice has the same singularity of logarithm as the 2D one, whereas the specific heat of the 4D system, as predicted by the mean field theory, shows a discontinuity at the critical point. The exact values for the critical exponent α are all equal to zero for the 2D, 3D and 4D (mean field) systems. The small values, but non-zero, of the critical exponent α, range from 0.0625 to 0.125, obtained by the renormalization group and the high-temperature series expansion, are attributed to uncertainties of these approximation methods due to the existence of systematic errors. It is understood that the behaviour of curves with a power law of $\alpha < 0.2$ are very close to that of logarithms so that the approximation approaches cannot resolve it. The exact values for the critical exponent β are 1/8, 3/8 and 1/2 for 2D, 3D and (mean field) 4D systems, respectively. The putative exact critical exponent β of $3/8 = 0.375$ is slightly higher than the approximation values of

Table 1. Putative exact critical exponents for the 3D Ising lattice, together with the exact values for the 2D Ising lattice, the approximate values obtained by the Monte Carlo renormalization group (PV-MC) [154], the renormalization group (RG) with the ε expansion to order ε^2, the high-temperature series expansion (SE) for the 3D lattice [103, 142] and those of the mean field (MF) theory. PV taken from Pelissetto and Vicari's review [154], WK from Wilson and Kogut's review [142], F from Fisher's series expansion [103]. Note that Domb's values in [107] are the same as Fisher's ($T > T_c$) [103].

Ising	α	β	γ	δ	η	ν
1D Exact	–	–	2	∞	1	2
2D Exact	0	1/8	7/4	15	1/4	1
3D Exact	0	3/8	5/4	13/3	1/8	2/3
4D MF	0	1/2	1	3	0	1/2
3D WK-RG	0.077	0.340	1.244	4.46	0.037	0.626
3D PV-MC	0.110	0.3265	1.2372	4.789	0.0364	0.6301
3D WK-SE	0.125	0.312	1.250	5.150	0.055	0.642
	$\pm$0.015	$\pm$0.003	$\pm$0.003	$\pm$0.02	$\pm$0.010	$\pm$0.003
3D F($T < T_c$)	1/16	5/16	21/16	26/5	$-1/31$	31/48
3D F($T > T_c$)	1/8	5/16	5/4	5	0	5/8

0.312–0.340. The exact values for the critical exponent γ are 2, 7/4, 5/4 and 1 for 1D, 2D, 3D and (mean field) 4D systems, respectively. The putative exact critical exponent γ of $5/4 = 1.25$ is exactly the same as the approximation values ranging from 1.244 to 1.25, within errors of 0.48%. Series for the initial susceptibility at high temperatures provided the smoothest and most regular patterns of behaviour of coefficients, which were all found to be positive in sign, and used to estimate the Curie temperatures and critical exponents [107]. One was tempted to conjecture that the exact value for the critical exponent γ of the 3D Ising lattice is simply $\gamma = 5/4$ [95, 103]. Even if it is not exact, it appears to be accurate to within 1/2% and certainly provides an excellent representation of the susceptibility coefficients [83, 95, 103, 107]. We are confident that the exact critical exponent γ equals 5/4 for the 3D Ising model. The putative exact critical exponent δ of $13/3 = 4.333\ldots$ for the 3D Ising lattice is between 15 and 3 for the 2D and 4D (mean field) Ising lattices, which is slightly lower than the approximation values of 4.46–5.15. The putative exact critical exponent η of $1/8 = 0.125$ for the 3D Ising lattice is half that for the 2D Ising lattice, which is slightly larger than the approximation values of 0–0.055. The putative exact critical exponent ν of 2/3 for the 3D Ising lattice is reasonable since it is between 1 and 1/2 for the 2D and 4D (mean field) Ising lattices and is very close to the approximation values of 0.625–0.642. It could be concluded that all the putative exact critical exponents for the 3D Ising lattice are located between those for the 2D and 4D (mean field) values, which are close to those obtained by various approximation methods, if compared roughly.

The critical exponents $\alpha = 1/8$, $\beta = 5/16$, $\gamma = 5/4$, $\delta = 5$, $\eta = 0$ and $\nu = 5/8$, suggested by Fisher [103] and Domb [107], which were established by conjectures from the results of series expansions, have been well-accepted by the community for almost 40 years. However, as remarked by Domb [107], there are significant discrepancies in numerical values. These are well illustrated by the formula for η, $2 - \eta = d(\delta - 1)/(\delta + 1)$, if one takes $\delta = 5$ as has been estimated for the Ising model of spin 1/2 in 3D, one finds that $\eta = 0$. But direct numerical analysis gives $\eta \approx 1/18$, and this is consistent with the result of renormalization group expansions. If one substitutes $\eta \approx 1/18$ into this equation, one will obtain $\delta \approx 4.7$, which is outside the confidence limits in the analysis of series expansions. This must be regarded as a serious inconsistency [107, 263]. Furthermore, the value of $\eta = 0$ in the group of critical exponents, suggested by Fisher [103] and Domb [107], gives the same result as predicted by the main field theory, which is not relevant. η denotes the deviation from the Ornstein–Zernike behaviour, which cannot be zero [236].

Regarding the actual values of critical exponents, one knows that in 2D they are all simple integers and fractions. Numerical data suggest a similar result in 3D. It would be difficult to support any such conclusions from a renormalization group treatment. Nevertheless, as stated by Domb [107], the possibility is appealing and hints that there may be simplifying features of the 3D Ising model which remain to be discovered. Our putative exact critical exponents $\alpha = 0$, $\beta = 3/8$, $\gamma = 5/4$, $\delta = 13/3$, $\eta = 1/8$ and $\nu = 2/3$ for the 3D Ising lattices are all simple integers and fractions, which are much simpler than those suggested by Fisher and Domb [103, 107]. It is interesting to compare our putative critical exponents further with those for the 1D Ising model. It is impossible to derive the critical exponents α and β directly for the 1D Ising model, since there is no spontaneous magnetization at finite temperature.

Assuming that the scaling laws still hold for the 1D case, however, one would have $\alpha = 0$ and $\beta = 0$ as derived from $\gamma = 2$, $\delta = \infty$, $\eta = 1$ and $\nu = 2$ (as shown in table 1) [264]. The difference between the critical exponents β for the 1D and 2D Ising lattices is 1/8, which is the same as the difference between the critical exponents β for the 3D and 4D Ising lattices. The difference between the critical exponents β for the 2D and 3D Ising lattices is twice this value. Similarly, the difference between the critical exponents γ for the 2D and 3D Ising lattices is twice the difference between the critical exponents γ for the 1D and 2D Ising lattices. The latter is the same as the difference between the critical exponents γ for the 3D and 4D Ising lattices, which equal 1/4. Indeed, the feature is very simple, symmetric and beautiful.

Recent advances in Monte Carlo and renormalization group techniques have improved the precision of calculations of critical exponents. If compared precisely, our putative exact values $\alpha = 0$, $\beta = 3/8$, $\gamma = 5/4$, $\delta = 13/3$, $\eta = 1/8$ and $\nu = 2/3$ differ with the values of $\alpha = 0.110(1)$, $\beta = 0.3265(3)$, $\gamma = 1.2372(5)$, $\delta = 4.789(2)$, $\eta = 0.0364(5)$ and $\nu = 0.6301(4)$, well-established in the Pelissetto and Vicari review [154], in consideration of the high–precision of simulations. Nowadays, these Pelissetto and Vicari values are widely accepted. We could evaluate the difference between the putative exact solution and the approximations by errors of $\Delta\alpha = |\alpha^{EX} - \alpha^{PV}|/\alpha^{EX}$, $\Delta\beta = |\beta^{EX} - \beta^{PV}|/\beta^{EX}, \ldots$ for all the critical exponents, where the subscripts of EX and PV denote the exact solutions and the Pelissetto and Vicari values. We find that $\Delta\alpha = \infty$, $\Delta\beta = 12.93\%$, $\Delta\gamma = 1.02\%$, $\Delta\delta = 10.51\%$, $\Delta\eta = 70.88\%$ and $\Delta\nu = 5.48\%$ for these critical exponents. It is evident that our putative exact solution for the critical exponent γ is very close to the approximation value, within an error of 1.02%. The differences in the estimates of other critical exponents actually arise from the determination of the critical exponent α, since there are only two independent parameters among all the six critical exponents. As discussed in detail in section 8, such differences between the putative exact solutions and the approximations are attributed to the existence of systematical errors of the Monte Carlo and the renormalization group techniques. In the Binder and Luijten review [213], the values of $y_t = 1/\nu = 1.588(2)$ and $y_h = 3 - \beta/\nu = 2.482(2)$ are established, in accordance with data in various references published between 1980 and 1999. Our putative exact solutions yield $y_t = 1/\nu = 1.5$ and $y_h = 3 - \beta/\nu = 2.4375$, which are very close with the Binder and Luijten values within the errors of 5.87 and 1.83%, respectively. The origins of these errors will be discussed in detail in section 8.

Note that the only exception is Kaupuzs' study [167], which predicted $\gamma = 5/4$ and $\nu = 2/3$, exactly the same as we found for the exact solutions. Kaupuzs [167] discussed different perturbation theory treatments of the Ginzburg–Landau phase transition model. The usual perturbation theory was reorganized by an appropriate grouping of Feynman diagrams of φ^4 model with O(n) symmetry [167]. As a result, equations for calculation of the two-point correlation function were obtained, which allowed the prediction of possible exact values of critical exponents in two- and three-dimensions by proving relevant scaling properties of the asymptotic solution at (and near) the criticality [219, 265–267].

It is emphasized that our putative exact critical exponents would represent the behaviour of the system exactly at the critical region, as the critical point could be fixed exactly, which would have physical significances correlated directly with the

existence of the fourth curled-up dimension. From the analysis above, it is clear that the estimate of the critical exponent α plays a key role in deviations between the exact solutions and the approximations. For a deeper understanding, the prediction of a zero critical exponent α reveals that the physical significance completely differs with the non-zero critical exponent α. As the dimension of the systems alters from 1D to 4D, the critical behaviour should change as a consequence of continued logic. Namely, all critical indices should vary smoothly with dimensionality [264]. The 1D Ising model shows no ordering at finite temperature. The specific heat of the 2D Ising model behaves logarithmically near the critical point, with a zero critical exponent α. The 4D Ising model has a zero critical exponent α also, but with discontinuous specific heat at the critical point. It is hard to understand why the 3D Ising lattice has a power law with a non-zero critical exponent α, where both the 2D and 4D Ising lattices have the zero critical exponent α. To date, nobody has succeeded in constructing explicitly a closed form of the eigenvalues as well as the partition function, leading to a power law with a non-zero critical exponent α for the 3D Ising lattice and which can be reduced to a logarithmic singularity with a zero critical exponent α for the 2D Ising lattice. From a logical viewpoint of the evolution of physical properties with dimensionality, it would not be unreasonable to believe that the specific heat of the 3D Ising model has a logarithmic singularity at the critical point. On the other hand, the temperature dependence of the specific heat of the 2D and 3D Ising models, as revealed by various approximation methods [13, 59], have the same trend and the same behaviour near the critical point. The more accurate the method, the more the specific heat is like logarithmic singularity. As shown in the Newell and Montroll review [59], Wakefield's method gave the lowest value for the critical point $1/K_c = 4.497$ [73, 74], which is known to be accurate except near the critical point [59]. The temperature dependence of the specific heat obtained by the extrapolation of high- and low-temperature expansions of the Wakefield method looks more like logarithmic singularity than the others [59]. It is relevant that the exact solution for the specific heat of the 3D Ising model behaves as logarithmic singularity at the exact critical point, which is lower than the Wakefield value. The critical exponent α has proved considerably harder to determine by various theoretical and experimental techniques. Furthermore, it is very hard for the approximation approaches and the experimental data fittings to distinguish the critical behaviour of the logarithmic singularity and the small non-zero critical exponent $\alpha < 0.2$. If one ignored the existence of the non-zero critical exponent α in the 3D Ising model and accepted the logarithmic singularity, then it would become much easier. According to the Fisher conjecture of high-temperature series expansion, the exact value for the critical exponent γ of the 3D Ising lattice is simply $\gamma = 5/4$ [103], being accurate to within 1/2%, which is the only parameter that can be accurately determined by high-temperature series expansion theories [103]. Considering the large differences between the critical points of the high-temperature series expansion and the exact solution, we may conjecture that the determination of the critical exponent γ is insensitive to the exact location of the critical point. Starting from these two critical exponents $\alpha = 0$ and $\gamma = 5/4$, one could immediately solve $\beta = 3/8$, $\delta = 13/3$, $\eta = 1/8$ and $\nu = 2/3$. Considering the insensitive dependence of the critical exponent γ to the exact location of the critical point, we suggest here that the critical exponent γ is the most reliable determined by the renormalization group

theory and Monte Carlo simulations. As other critical exponents depend sensitively on the location of the critical point and because the critical point located by these approximation techniques is far from the exact value, these critical exponents also deviate from the exact exponents. Nevertheless, starting from the two critical exponents of $\alpha = 0$ and $\gamma = 1.2372$, one easily finds that $\beta = 0.3814$, $\delta = 4.2438$, $\eta = 0.1442$ and $\nu = 2/3$. Then, comparing this group of critical exponents with the putative exact values, one finds that the critical exponents α and ν are the same as the putative exact values, while the critical exponents β, γ, δ and η appear to be accurate within 1.7, 1.0, 2.1 and 15%, respectively. This means that the renormalization group theory and Monte Carlo simulations are suitable for investigating the critical phenomena; however, it is better to focus only on the high-accurate determination of the critical exponent γ, since the determination of the critical point and other critical exponents with high accuracy appears unsuccessful.

It is important to compare the putative exact solution of the critical exponents with experimental data. In this paragraph, we compare the putative exact critical exponents with early data collected by Kadanoff *et al.* [105], Fisher [103], and Wilson [149]. The critical exponents α of ferromagnetic iron, $CuK_2Cl_4 \cdot 2H_2O$, is not larger than 0.17, while the specific heat of nickel is fitted by a logarithmic singularity [105]. Actually, it is very difficult to distinguish the fitting of a power law with $\alpha < 0.2$ with that of logarithms. As indicated by Kadanoff *et al.* [105], a set of data for the specific heat of $CoCl_2 \cdot 6H_2O$ can be fitted either by a logarithmic singularity or by $\alpha \lesssim 0.19$. The critical exponents β of ferromagnetic iron, nickel, EuS, $YFeO_3$ and $CrBr_2$, determined experimentally, are 0.34 ± 0.02 (or 0.36 ± 0.08), 0.51 ± 0.04 (or 0.33 ± 0.03), 0.33 ± 0.015, 0.55 ± 0.04 (or 0.354 ± 0.005) and 0.365 ± 0.015, respectively [103, 105]. The values of the critical exponents β varies in range of 0.33–0.55, depending sensitively on the method of determination and also on the data range for fitting. The putative exact value for β is $3/8 = 0.375$, which is very close to the experimental values 0.36 ± 0.08 for iron, 0.365 ± 0.015 for $CrBr_2$, and is not out of the range of 0.33–0.51 for nickel and 0.354–0.55 for $YFeO_3$. The experimental data for the critical exponents γ of iron, nickel, cobalt, gadolinium are 1.33 ± 0.03, 1.29 ± 0.03 (1.35 ± 0.02), 1.21 ± 0.04, 1.33 (1.16 ± 0.02), respectively [103,105]. The putative exact value for γ is $5/4 = 1.25$, which is very close to the experimental values 1.29 ± 0.03 for nickel and 1.21 ± 0.04 for cobalt. The critical exponents δ of nickel, gadolinium, $YFeO_3$ and CrO_2 are found experimentally to be 4.2 ± 0.1, 4.0 ± 0.1, 2.8 ± 0.3 and 5.75, respectively [103,105]. The putative exact value for δ is 13/3, very close to the experimental data for nickel and gadolinium. The experimental evidence, notably on iron, indicated $0.2 > \eta \gtrsim 0$ [103,105], which is not inconsistence with the putative exact critical exponent $\eta = 1/8$. However, experimental uncertainty for a narrow temperature range around the critical temperature precluded drawing any conclusion about the value of η [105]. The critical exponents ν of ferromagnetic iron, antiferromagnetic Cr_2O_3, α-Fe_2O_3 and $KMnF_2$ are 0.64 ± 0.02, 0.67 ± 0.03, 0.63 ± 0.04 and 0.67 ± 0.04, respectively [105], which are very close to the putative exact value 2/3. Furthermore, the putative critical exponents ν is exactly the same as accepted by Wilson in his review article [149].

Many factors reduce experimental accuracy, which will be discussed in details in section 8. For instance, impurities in the magnet sample may affect the value of the

critical temperature and, in a polycrystal, T_c may range in a band of the order of 10^{-4}. Good measurements then require the use of single crystals of extreme purity and well-defined geometry. From bulk measurements, the determination of critical exponents involves extrapolations to zero internal field values. As stated by Vicentini-Missoni [268], up to the early 1970s, good data in the critical region are available only on a few substances, i.e. the nickel data of Weiss and Forrer [269], and those of Kouvel and Comly [270], the gadolinium data of Graham [271] and the $CrBr_3$ data of Ho and Litster [272, 273]. In this paragraph, we compare the exact critical exponents with the data collected in Vicentini-Missoni's review. The data (a) shown in table III of Vicentini-Missoni's paper [268] were determined by least-squares fit of the function $h_{MSG}(x) = E_1((x+x_0)/x_0)[1+E_2((x+x_0)/x_0)^{2\beta}]^{(\gamma-1)/2\beta}$ to the experimental data [274–276]; in this case β and δ were assumed as independent exponents and γ was derived using the scaling relation $\gamma=\beta(\delta-1)$. The critical exponents obtained by the analysis of Kouvel and Comly's data are as follows: $CrBr_3$: $\beta=0.364\pm0.005$, $\delta=4.32\pm0.10$, $\gamma=1.21$; Gd: $\beta=0.370\pm0.010$, $\delta=4.39\pm0.10$, $\gamma=1.25$; Ni: $\beta=0.373\pm0.016$, $\delta=4.44\pm0.18$, $\gamma=1.28$ [268, 270]. The critical exponents obtained by the analysis of Weiss and Forrer's data for Ni are: $\beta=0.375\pm0.013$, $\delta=4.48\pm0.14$, $\gamma=1.31$ [268, 269]. The critical exponents derived from several fluids are: CO_2: $\beta=0.352\pm0.008$, $\delta=4.47\pm0.12$, $\gamma=1.22$; Xe: $\beta=0.35\pm0.07$, $\delta=4.6\pm0.1$, $\gamma=1.26$; He^4: $\beta=0.355\pm0.009$, $\delta=4.44\pm0.01$, $\gamma=1.24$. All the data collected in Vicentini-Missoni's review [268] are in very good agreements with our putative exact solutions. The putative exact critical exponent $\beta=3/8$ is exactly the same as the experimental value for Ni and Gd within error bars. The difference between the putative exact critical exponent β and the experimental value is 2.9% for $CrBr_3$, 6.1% for CO_2, 6.7% for Xe and 5.3% for He^4. In consideration of experimental error bars, such difference would reduce to 1.6% for $CrBr_3$, 4.0% for CO_2, 0% for Xe and 2.9% for He^4. The putative exact value of $\delta=13/3$ is exactly the same as the experimental values for $CrBr_3$, Gd and Ni within error bars. The difference between the putative exact critical exponent δ and the experimental value is 3.1% for CO_2, 6.2% for Xe and 2.5% for He^4. If the experimental error bars are taken into account, such difference would reduce to 0.4% for CO_2, 3.8% for Xe and 2.2% for He^4.

As shown in table 1.3 of Kadanoff [264], the real fluids show indices close to, but not exactly equal to, the indices of the 3D Ising model obtained by various approximations. However, the critical indices $\gamma=1.22\pm0.05$, $\delta=4.4\pm0.2$, $\eta=0.123$ and $\nu=0.65\pm0.05$ of real fluids are in good agreements with our putative exact values. The differences between them are 2.4% for γ, 1.5% for δ, 1.6% for η and 2.5% for ν, which can be further reduced by taking into account experimental errors. It can be concluded that the critical indices γ, δ, η and ν of real fluids are almost exactly equal to the putative exact values.

As temperature T, at which two fluid phases are in equilibrium, approaches the critical temperature T_c, the interfacial tension σ is found experimentally to vanish proportionally to a powder of $T-T_c$: $\sigma\sim(T_c-T)^{\mu}$ [277]. The exponent μ is an important and characteristic critical-point index, with a value that is believed to be universal and is, in any event, almost certainly in the range $\mu=1.28\pm0.06$. We obtain the putative exact exponent $\mu=4/3=1.3333\ldots$ from the scaling law of $\mu+\nu=2-\alpha$ and our exact exponents $\nu=2/3$ and $\alpha=0$. Our putative exact exponent

μ and the experimental value coincide, within experimental error bars. In fact, the experimental data for the exponent μ are in range 1.23–1.34 for various systems, such as argon, xenon, nitrogen, carbon dioxide, chlorotrifluoromethane, hydrogen, cyclohexane–aniline, cyclohexane–methanol, 3-methylpentane–nitroethane [277]. However, it was emphasized by Buff and Lovett [278] and Wims *et al*. [279] that, in the measurement of surface tension by capillary rise and equivalent methods, it is not μ but $\mu - \beta$ that is measured directly, so some of the variability in the value of μ quoted in table I of Widom [277] is a reflection of a discrepancy in the assumed β. The only direct measurement of interface thickness near the critical point is for the cyclohexane–methanol system by Huang and Webb [280], who obtained $\nu = 0.67 \pm 0.02$. This value fits exactly with our putative exact exponent $\nu = 2/3$.

Little data have been reported for the critical exponents of ferromagnetic transition metals, such as Fe, Co and Ni, over the last decade [281, 282]. Shirane *et al*. [281] reported the critical exponent $\gamma = 1.333$ for nickel. Seeger *et al*. [282] obtained values of $\beta = 0.395(10)$, $\gamma = 1.345(10)$ and $\delta = 4.35(6)$ for the asymptotic critical exponents of nickel, which are close to our putative exact values within errors of 5.3, 7.6 and 0.4%, respectively. Some experimental results for the critical exponents, most of them published after 1990, were tabulated in table 7 of the Pelissetto and Vicari [154]. It is seen from the most recent data that the critical exponents α, β, γ, η and ν vary in the range 0.077 – 0.12, 0.315 – 0.341, 1.09 – 1.26, 0.03 – 0.058 and 0.60 – 0.70, respectively, determined by experiments in liquid–vapour transition in simple fluids, the mixing transition in multicomponent fluid mixtures and in complex fluids, the transition in a uniaxial magnetic system, the transition in a micellar system and the mixing transition in Coulombic systems [154, 283–293]. Again, we emphasize that the difference between the logarithmic behaviour and the character of the non-zero critical exponent α in the range 0.077 – 0.12 cannot be distinguished by experiments, especially, in the case of presetting the existence of the non-zero critical exponent α. The putative exact critical exponent γ is in very good agreement with the experimental data [154, 284–286, 288, 290, 291, 294–296], especially, which is exactly the same as determined in [283, 287, 292, 293]. Most of the experimental data for β, η and ν have somewhat larger deviations with the exact values, remaindering us of the fact that only γ is the most reliable critical exponent for highly accurate determination of the critical exponents since it depends most insensitively on the accurate location of the critical point. Nevertheless, it is a common fact that experimental data are less accurate than the theoretical data, which cannot serve as the only standard for judging the correctness of the exact solutions [154, 213].

What follows is a checklist of what we found for the putative critical exponents of the 3D Ising models by several criteria. (1) The putative exact critical exponents satisfy the scaling laws and show universality behaviour. (2) The putative exact critical exponents represent the behaviour of the system exactly at the critical region, as the critical point is fixed exactly. (3) The putative exact critical exponents have physical significances, which are correlated directly with the existence of the fourth curled-up dimension. (4) The putative critical exponent γ is exactly the same as the conjecture of $\gamma = 5/4$ [83, 95, 103, 107]. (5) Our putative exact solutions are in very good agreements with the critical exponents β and δ collected by Vicentini-Missoni [268], which were derived by analysis of the good data in the critical region, believed

to be available only for a few substances. (6) The putative exact critical exponents are almost exactly equal to the critical indices γ, δ, η and ν of real fluids. (7) The putative exact critical exponents μ and ν coincide with experimental values for the interfacial tension in the two phase fluids, within experimental error bars. (8) The putative exact critical exponents satisfy the criterion that the critical behaviour should change as a consequence of continued logic: the critical indices should vary smoothly with dimensionality. All the putative exact critical exponents for the 3D Ising lattice are located between those for the 2D and 4D (mean field) exact critical exponents. The logarithmic behaviour of the specific heat in 3D verifies that all the systems have the zero critical exponent α, regardless of their dimensions. (9) The putative exact critical exponents are comparable to the approximation values and the experimental data, if compared roughly. (10) The putative exact critical exponents would be very close to the approximations and the experimental data if one agreed with the existence of the zero critical exponent α and chose the critical exponent γ as the most reliable for a high-accurate determination of the critical exponents. (11) The putative exact critical exponents satisfy the principles of simple, symmetry and beauty with aesthetic appeal, which are all simple integers and fractions. They are much simpler than those suggested by Fisher and Domb [103, 107]. Finally, we emphasize that the results of the approximation methods and experiments cannot serve as the only standard for judging the correctness of the putative exact solutions, but the exact solution can serve for the evaluation of systematical errors in the approximations and experiments.

8. Discussion

8.1. *Scenario of the (3 + 1)-dimensional space framework*

It is important to justify the correctness of the present procedure for deriving the exact solution of the 3D simple orthorhombic Ising lattices. To do so, we need to justify the validity of the two conjectures introduced in section 3. The main points of the two conjectures are: the topologic problem of the 3D Ising system could be solved by introducing an additional rotation in a $(3+1)$-dimensional space with a curled-up dimension attached on the 3D space. The weight factors w_x, w_y and w_z on the eigenvectors represent the contributions of $e^{i(t_x\pi/n)}$, $e^{i(t_y\pi/l)}$and $e^{i(t_z\pi/o)}$ in the 4D space to the energy spectrum of the system. By introducing the two conjectures, we succeeded in finding the maximum eigenvalues and the free energy, which are the same as those of the original 3D Ising model. There should be a natural mechanism for realizing this scenario.

Actually, introducing additional dimensions to our 3D physical system is not a new concept [297–300]. The aim of the early model of Kaluza and Klein in considering a five-dimensional space-time with one spatial extra dimension was to unify electromagnetism and gravity [301, 302]. Evidence exists that convinces us that we live in four noncompact space-dimensions [303]. Due to experimental constraints, the standard model fields cannot propagate into bulk and are forced to lie on a wall or 3-dimensional brane in higher dimensions [304–307]. Living in $4+n$ noncompact

dimensions is perfectly compatible with experimental gravity [303]. An effective dimensional reduction occurs without the need to compact the fifth dimension, since Kaluza–Klein excitations which have nonvanishing momentum in the fifth direction, are suppressed near the brane. Thus, even though the Kaluza–Klein modes are light, they almost decouple from matter fields, which are constrained to live on the wall [303, 308]. On the other hand, there exist five anomaly-free supersymmetric perturbative string theories, known as type-I, type-IIA, type-IIB, SO(32) heterotic and $E_8 \times E_8$ heterotic theories [297, 309]. In all these string theories, in addition to the four noncompact space-dimensions, more compact dimensions, for instance, a compacted six-dimensional Calabi–Yau space, are needed. The four-dimensional couplings are related to the string mass scale, to the dilation and to the structure of the extra dimensions, mainly in the example of hetereotic theories. These five perturbative string theories are all related to each other by various string dualities (such as T-duality and S-duality) and the $(10+1)$-dimensional M superstring theory could describe these five string theories together with 11-dimensional supergravity [297,298,309]. Nevertheless, even though the compact dimensions may be too small to detect directly, they still can have profound physical implications. In the present case, introducing our two conjectures reveals profound physical significance for the 3D Ising system, which emerges automatically from the requirement of solving the topological problem of the 3D Ising lattice. The putative exact results obtained by our procedure are consistent with high-temperature expansions at/near infinite temperature for the 3D Ising model. However, only the 4D space is sufficient for solving our problem, while the radius of the additional curled-up 4th dimension is presumed to be infinitesimal in the original 3D Ising lattice. Our 4D world remains free for contacting with the $(10+1)$-dimensional world in a 6-dimensional compact Calabi–Yau manifold plus 1-dimensional time.

Introducing the additional curled-up dimension indirectly supports that we might live in four noncompact space-dimensions [303]. This conjecture is not inconsistent with Kaluza and Klein's five-dimensional spacetime and even the super-spring theories [297, 298, 309]. The evidence for possible existence of dark matter or dark energy in the cosmos is still a mystery to scientists [310, 311]. The additional term K''' of the energies is included in the expressions (29) and (49) for the eigenvalues and the partition function of the simple orthorhombic Ising lattices. This extra energy term seems to be related directly to the introduction of the additional curled-up dimension, rather than interactions along the three crystallographic axes themselves. Furthermore, the existence of four noncompact space-dimensions provides sufficient space for the dark matter or dark energy, although we cannot see the fourth curled-up dimension, which are communicating with or acting on the 3D physical world.

The scenario of the 3D Ising model at different temperatures is illustrated as follows. (1) At infinite temperature, $\kappa = 0$, $w_x = 1$, and $w_y = w_z = \pm\sqrt{7/18}$. There is actually a state without any interactions, because any *finite* interactions lost their actions in comparison with *infinite* temperature. The configurations are completely random and extremely chaotic. One cannot distinguish any configurations from this completely random phase. This phase could be defined as Phase 1, which is a formless phase of complete randomness, representing a special state of non-being (non-interaction). (2) As temperature infinitesimal deviates from infinite, the system starts to experience extremely weak interactions. Deviations from complete

randomness occur, which can be systematically taken into account by means of a series expansion in K or $\kappa = \tanh K$. κ becomes non-zero but infinitesimal and then $w_x = 1$, $w_y \to 0$ and $w_z \to 0$; all the configurations of the high-temperature series emerge instantaneously and spontaneously from the complete randomness. The system is still quite random, with strong quantum fluctuations, but less random than at infinite temperature. This phase could be defined as Phase 2, which is a forming phase of randomness with detailed structure, representing a special state of being. (3) As temperature is lowered further, at finite temperatures above T_c (κ becomes finite, i.e. $\kappa \neq 0$; $w_x = 1$, $w_y = w_z = 0$), a disordering phase emerges from the randomness, which could be defined as Phase 3. (4) Exactly at the critical point, a disordering–ordering transition occurs with infinite correlation length, with singularity of the free energy, the specific heat, etc. This phase can be defined as Phase 4 or the critical phase, which is the origin of singularities occurring at/near the critical point. (5) Below the critical point, Phase 5 or the ordering phase emerges from the critical phase. (6) At zero temperature, the system becomes completely ordered, which can be defined as Phase 6. From the scenario above for 3D, there actually are five detailed transformations between six phases, evolving from infinite to zero temperature. The putative exact solution reveals the nature of nature in the disorder and/or random states: The disordering and/or randomness may have different levels and structures! The existence of Phase 2 is an intrinsic characteristic of our 3D world, which does not exist in any models of other dimensions. For instance, in 2D, Phases 2 and 3 coincide with each other from temperature near infinite down to the critical point T_c because the radius of the convergence of high-temperature expansions is the critical point T_c. It is hard to understand the intricate difference between Phases 1 and 2. The basic difference between Phases 1 and 2 is whether the interactions are experienced. Phase 1, without any clear configurations but more random/chaotic, includes everything of Phase 2 and other low-temperature phases. Phase 2, with infinite configurations as described by the high-temperature expansions and strong quantum fluctuations but less random/chaotic than Phase 1, emerges from Phase 1. These two phases are strange twin: Phase 1 is empty since nothing can be distinguished from it, while Phase 2 is filled with all the high-temperature configurations. Phase 3 emerges from the strong quantum fluctuations of Phase 2. However, at the pregnant period of Phase 3, Phases 1 and 2 can transform each other to be like a whole, to form a quantum vacuum-like state, on the infinitesimal fluctuation of temperature at the infinite temperature. As long as temperature approaches finite, Phase 3 with completely different configurations emerges spontaneously, on the break-down of the symmetry and the annihilation of all high-temperature configurations. It is understood that at/near infinite temperature the Phases 1 and 2, representing empty (non-being) and full (being) are actually two-fold degeneracy states if one neglects the infinitesimal deviation from infinite. Spontaneous breaking down of the symmetry at/near infinite temperature is that a new disorder phase emerges from the two-fold degeneracy of states, which differs from the nature of spontaneous breaking down of the symmetry at the critical point where one of two-fold degeneracy of order state emerges from the disorder phase. Then, Phases 1 and 2 cannot return because no body can receive infinite thermal energy to be back at infinite temperature. What happens at/near infinite temperature of the 3D Ising model is analogous to the Big Bang at the origin and successive

evolutions of our Universe. In the present case, we do not require a singularity point as the origin of the Universe, but only interacting spins in the thermodynamic limit at infinite temperature.

The states of Phases 1 and 2 are analogous to what Lao Zi described in his famous book *Dao De Jing* [312]. Lao Zi was a great Chinese philosopher and thinker who lived in c. 585–500 BC and once was the librarian and archivist of the royal court of the Zhou Dynasty. Lao Zi's thoughts have survived for more than two thousand years and, recently, have become popular in the West. The philosophy of Lao Zi is first about the universe, human life and politics. Without any models or knowledge in modern physics, Lao Zi tried to understand the origin of our world and describe the evolution of the world. His most famous rumination is 'Non-being is the beginning of the myriad things; Being, the mother of them'. Simply speaking, 'Being was born out of Non-being; Everything was born out of Being'. Namely, Phase 2, as temperature infinitesimal deviates from infinite, is born out of Phase 1 at infinite temperature; all the phases (including disordering and ordering phases) at finite temperature are born out of Phase 2. However, one might argue that these ruminations seem to have parted from the domain of the Ising model in 3D, 4D, or anything else. Our point of view is: On the top level, philosophies, sciences, arts and even religions are all correlated, since all of us face a unique world. We should respect the wisdom of the great philosopher and thinker Lao Zi. Interestingly, the success in deriving the putative exact solution of the 3D Ising model for a purpose of understanding the critical properties at the critical point helps in having a clear image of the scenario of the physic world at/near infinite temperature.

One may argue that the 4-fold for $\ln Z$ is not, in principle, mathematically impossible, but it may be physically impossible for ferromagnetic Ising models because the Yang–Lee theorem proved rigorously the absence of zeroes for the partition function, except on the imaginary magnetic field axis and together with the existence of a gap in the zero distribution at high enough T ($>T_c$). This implies that the high-temperature expansions of the Ising model converge and fully define $N^{-1}\ln Z$ in the thermodynamic limit, $N\to\infty$, for all $T>T_c$, as demonstrated for the 1D and 2D models. However, this judgment based on the Yang–Lee Theorem is not correct, because the Yang–Lee Theorem disregarded the special case of $T=\infty$. It is clearly seen after Theorem 3 in [9] that 'The lattice gas cannot undergo more than one phase transition, which must occur, if at all, at a value of the fugacity equal to σ, which according to equation (24), corresponds to $z=1$. The isotherms in the $I-H$ diagram of the corresponding Ising model problem is smooth everywhere except possibly at zero magnetic field (which occurs at $z=1$). This is usually believed to be true but was not proved.' The most important issue here is that $z=1$ corresponds to the possibility of the phase transition. Due to this fact, the Yang–Lee Theorem excluded the occurrence of the phase transition in the presence of magnetic fields H, since $H=0$ leads to $z=1$ in accordance with their equation (23) of $z=\exp(-2H/k_BT)$. However, it is clear that Yang and Lee did not discuss the case of infinite temperature. If $T=\infty$, z will also equal 1, providing the possibility of the occurrence of a phase transition at infinite temperature. Since there is no phase transition at infinite temperature in other dimensions, it is believed here that it should occur in a 3D system. Furthermore, the zero distribution as $T\to\infty$ can be quite different with that at finite temperature, as in the case where the zero

distribution in the thermodynamic limit (volume $V \to \infty$) differs from finite volume. It could be true that the behaviour of the phase transition at/near infinite temperature differs from that at the critical point. Therefore, the mathematical structure of the free energy equation (49) is not only mathematically possible, but also physically possible. Nevertheless, all of the above facts suggest that for the 3D Ising lattices, the high-temperature series expansion may not be a standard for judging the validity and correctness of the putative exact solution at finite temperatures. This would imply that the explicit form of the solutions of any 3D lattice theories may have less direct relation with series expansion of perturbation theories.

It should be emphasized here that for a real 3D system, the 4-fold for $\ln Z$ should hold for the whole temperature range, while the weight factors can vary in the range $[-1, 1]$. Considering symmetry, for the simple cubic lattice (and also the simple orthorhombic lattices close to it), the roles of the weight factors w_x, w_y and w_z can be interchanged without altering the eigenvalues (equation (29)) and the partition function (equation (49)). The roles can interchange (and values) at any time from the point of view of symmetry. In this way, the system is within the $(3+1)$-dimensional space framework, even where any of the weights occasionally equal zero. These lattices, as marked by 3D in figure 4, show the critical behaviours of a real 3D system. With a further decrease in one or two of the three interactions K, K' and K'', the symmetry of the simple orthorhombic lattices decreases and, consequently, the mechanism of role interchange of the weight factors w_x, w_y and w_z is gradually weakened so as to be prohibited in the 2D or 1D limit. Namely, $w_x = 1$, $w_y \equiv 0$ and $w_z \equiv 0$ revert the system to the Onsager 2D Ising model, which also corresponds to all the simple orthorhombic lattices with their critical points lower than the silver solution (as marked by 2D in figure 4). The variation in interchange with the symmetry of the system is the origin for the 3D-to-2D crossover phenomenon, i.e. a gradual crossover between the 3D and 2D behaviour, the 2D behaviour of some simple orthorhombic lattices with less symmetry.

The $(3+1)$-dimensional scenario described above for the 3D Ising model might be an intrinsic character of the 3D many-body interacting systems. The physics beyond the $(3+1)$-dimensional scenario might be understood in depth as follows. For a nonconservative system, the time-dependent Schrödinger equation is explicitly expressed by $i\hbar(\partial/\partial t)\Psi(r,t) = H(r, t, -i\hbar(\partial/\partial r))\Psi(r,t)$. For the special case of a conservation system, where H does not depend explicitly on t, a particular solution is $\Psi_n(r,t) = \psi_n(r)\exp(-iE_n t/\hbar)$, where E_n is an eigenvalue and $\psi_n(r)$ is the corresponding eigenfunction of the ordinary Schrödinger equation $H(r,q)\psi(r) = E\psi(r)$. However, according to the relativity theory, any system should be described within the spacetime framework, and spacetime is closely associated by the Lorentz transformation. We might need to rethink the role of the time on the non-relativistic quantum mechanism. Time should have two roles: one to evaluate the movements of a particle within the framework of d-dimensional space; the other to represent the whole system within the $(d+1)$-dimensional spacetime. The first role of time is accounted for by the first-order derivative $\partial/\partial t$, but the second role (the second-order derivative $-\partial^2/\partial t^2$, in accordance with ∇^2 in kinetic energies) is totally neglected in the non-relativistic quantum mechanism. This term of $-\partial^2/\partial t^2$ is eliminated in the famous Schrödinger's equation that plays the role of Newton's law and conservation of energy in classical mechanics. In other

words, the time-dependent Schrödinger equation is of the first order in time but of the second order with respect to the co-ordinates; hence, it is not consistent with relativity. Actually, the Hamiltonian of the whole system (even in the case of non-relativistic) in the $(d+1)$-dimensional spacetime is always associated with time, and any spacetime system is always a nonconservative system taking into account the time evolution. Whether the system is non-relativistic or relativistic, the equation for the dynamic of the system should be consistent with relativity. It is our understanding now that when we deal with a Hamiltonian of a non-relativistic system, which does not depend explicitly on t, the second role of the time is actually hidden. Although this role of the time could be neglected in other non-relativistic systems, it should be taken into account for the 3D many-body interacting system where the Hamiltonian of this non-relativistic system describes the interactions of the spins only in 3D space (like accounting only for ∇^2 in kinetic energies). The introduction of the extra dimension in the present 3D Ising case might correspond to the second role of time (like accounting for the effect of $-\partial^2/\partial t^2$), although its appearance is required instantaneously by solving the topologic problem in the 3D Ising system. This implies that the topologic problem in the 3D many-body interacting system might automatically result in the conception of spacetime. The introduction of the weights might correspond to a mechanism which make the nonconservative system in spacetime conservative during the evolution of time. This work may reveal how the second role of time could be associated physically with the 3D world (Alternatively, however, one could treat the additional dimension as a pure mathematic structure or a boundary condition).

Furthermore, it is understood that a satisfactory quantum general relativistic theory should take into account simultaneously and properly both the two roles ($\partial/\partial t$ and $-\partial^2/\partial t^2$) of time. However, it has been a challenge to properly consider the second role of time, since it certainly causes the nonconservation (at the instant of the evolution of the system, it should be held to be conservative). This might be the origin of one of the difficulties in establishing a satisfactory quantum general relativistic theory. In recent developments on the quantum gravity theory and to study the background-independent formulation of the M theory, bulk dynamics were described in terms of a causal histories framework, in which time evolution was specified by giving amplitudes to certain local changes of states [313, 314]. In this theory, a new kind of fusion between quantum theory and spacetime was achieved in which states were identified with quantum geometries that represent space-like surface and histories were both sequences of states in a Hilbert space and discrete analogues of the causal structures of classical spacetimes. That is to say, to address the issue of time evolution, one may attach a Hilbert space to each node of the causal set graph in a theory of the causal evolution of the Penrose spin networks [313, 314]. In loop quantum gravity, the spin networks are the basic states for the spatial quantum geometry states [313, 314]. On the other hand, it is known that the Ising model can be employed to describe the Penrose spin networks used for the quantum theory of gravity, since one could treat, exactly and equally, triangulations and their dual spin networks. The two conjectures in the present work may shed light on a satisfactory quantum theory of gravity by illustrating the topologic and causal structures of spacetime. The four noncompact space-dimensions mentioned above might be thought of as four spacetime dimensions. Namely, the fourth dimension of

the four noncompact space-dimensions might behave as the time-like space-dimension, representing the causal evolution of spin networks. This implies the possibility that the five-dimensional spacetime with four noncompact space-dimensions, mentioned above, may be mathematically treated as a $(3+2)$-dimensional spacetime (i.e. three space-like space-dimensions, one time-like space-dimension and one time dimension). The two time-related dimensions may correspond, respectively, to the two roles of time: $\partial/\partial t$ and $-\partial^2/\partial t^2$. The second action of the time is hidden in the Hamiltonian of a 3D conservative system and this additional time-like space-dimension is curled-up in the spacetime.

8.2. *Approximation techniques*

8.2.1. General arguments. Next, we need to discuss possible reasons for the differences between the putative exact solution and the approximate values obtained by various, widely accepted standard methods, and the differences between the putative exact solution and experimental data. From the first glance, it seems very difficult to imagine that, over years of experimentation by numerous independent scientists using completely different techniques (Monte Carlo simulations, high- and low-temperature expansions, renormalization group field theory and experiments), the multitude of separate determinations of these critical exponents are wrong and all yield (wrong) results that coincide. However, it is not a question of which results are wrong or correct, but which are inexact or exact. Clearly, approximation results can not be equal to exact results – there is no equalization between them. Strictly speaking, it is of no significance to compare the putative exact solution with approximation values and it makes no sense to contradict the putative exact solution by well-accepted approximation values. The purpose of presenting the putative exact solution here is not to criticize either the approximation or experimental techniques, but to reveal the truth of nature. The results obtained by these techniques can be used as valuable references if carefully considered, but not applied as the only standard for judging the correctness of the putative exact solution. It is difficult to gain any physical insight from approximation values, whereas the exact solution would be physically significant. All of the putative exact critical exponents are derived analytically by simply introducing our first conjecture, namely, the existence of the extra dimension. The putative exact values emerge spontaneously as long as this conjecture is introduced and they would be corrected if the conjecture were valid. The putative critical exponent of $\alpha = 0$ illustrates the logarithmic singularity of the specific heat at the critical point of the phase transition. The factor of three (or one over three) in the putative critical exponent of $\beta = 3/8$ (or $\nu = 2/3$) emerges automatically from this conjecture, which extends the dimensions in the wave-vector space. The putative critical exponents of $\alpha = 0$, $\beta = 3/8$, $\gamma = 5/4$, $\delta = 13/3$, $\eta = 1/8$ and $\nu = 2/3$, show the universality behaviour and satisfy the scaling laws. One would find that these values even have some hidden intrinsic correlations with the critical exponents of $\alpha = 0$, $\beta = 1/8$, $\gamma = 7/4$, $\delta = 15$, $\eta = 1/4$ and $\nu = 1$ of the 2D Ising model. For instance, both the 2D and 3D Ising models have the critical exponent $\alpha = 0$, with the same logarithmic singularity of the specific heat at the critical point; the critical exponent β of the 3D Ising model is exactly three times that of the 2D

model; the critical exponent η of the 3D Ising model is exactly half that of the 2D model. The difference between the critical exponents γ for the 2D and 3D Ising lattices is twice that for the 1D and 2D (or 3D and 4D) Ising lattices (the same is true for β). Most important, the putative critical point of the 3D simple cubic Ising model is located exactly at the golden ratio $x_c = e^{-2K_c} = (\sqrt{5}-1)/2$, while the critical point of the 2D square Ising model is located exactly at the silver ratio $x_c = e^{-2K_c} = \sqrt{2}-1$. Realizing the fact that the golden and silver ratios are the two most beautiful numbers in the mathematical world and that intrinsic similarities and correlations exist between them, as revealed by the continued fractions and the equations of $x^2+x-1=0$ and $x^2+2x-1=0$, one would believe that no other numbers are more reliable and suitable than the golden ratio for the critical point of the 3D simple cubic Ising model. The continued efforts of scientists worldwide for more than 60 years, since Onsager's discovery of the exact solution of the 2D Ising model in 1944, especially the advances in the renormalization group and Monte Carlo simulations since Wilson's discovery of the renormalization group in 1971, contribute greatly to our understanding on the physical behaviour, in particular, the critical behaviour of the 3D Ising model. Previous results of approximation and experimental techniques provide significant information, which is quite helpful in deriving the exact solution of the 3D Ising model. We would like to believe that the finding of the putative exact solution would improve the development of these techniques. In the following paragraphs, we shall explain why the renormalization group theory and Monte Carlo simulations plus other approximation methods cannot yield the exact solution or a solution close enough to the exact one.

Perturbation expansions have been used widely in astronomy and physics to evaluate the effect of small changes in problems for which exact solutions are available. However, for physical phenomena in which an interaction completely changes the character of the solution, it is necessary to derive substantial numbers of terms of such perturbation expansions and, if possible, to estimate the asymptotic behaviour of the coefficients. As remarked by Domb [107], caution must be exercised in using the method of series expansions if wrong conclusions are to be avoided; physical insight into the nature of the expected solution should be invoked wherever possible, which also provides consistency checks. Also methods of series analyses should be tested wherever possible on exact closed form solutions.

The quantity $F(z)$, whose critical behaviour as a function of z is to be studied, must have a power series expansion about the origin $z=0$, $F(z)=\sum_{n=0}^{\infty} a_n z^n$, with a finite radius of convergence [315,316]. There are two criteria for the radius of convergence for series expansions [315–317]. (1) If $\lim_{n\to\infty} |a_n/a_{n+1}| = z_0$, or (2) if $\lim_{n\to\infty} |a_n|^{-1/n} = z_0$, then the series converges for $|z|<z_0$ and diverges for $|z|>z_0$. Correspondingly, there must be at least one singularity (non-analytic point) on the circle of convergence $|z|=z_0$. Unfortunately, the sequence $|a_n|^{-1/n}$ often slowly converges, so that its practical value in estimating z_0 from the leading coefficients is rather limited. If all the coefficients a_n are known exactly, in principle, one can analytically continue the function across the z-plane as far as a natural boundary of the function, beyond which it remains undefined. The nature of the coefficients is determined by the singularities of $F(z)$. The singularities nearest the origin will dominate the behaviour for large n. If the dominant singularity is on the positive real axis, the coefficients will eventually all have the same sign. Conversely, if the

dominant singularity is on the negative real axis, the coefficients will eventually alternate the sign. More irregular behaviour of the sign for large n indicates that the dominant singularities are in the complex plane. Since the coefficients are assumed real, the singularities must then occur in complex conjugate pairs [316].

One difficulty with series expansions is principal: if we are lucky, as with the 2D Ising model, the critical point as a physical singularity point will be located exactly on the circle of convergence. However, the most common case is that the existence of a non-physical singularity point with $z<0$ reduces the circle of convergence so that one cannot reach the critical point that is a physical singularity point outside the circle of convergence. It is believed that the 3D Ising model belongs to this category. The Padé approximant method has been applied to overcome the difficulty of getting more information outside the circle of convergence. Nevertheless, the radius of the circle of convergence for high temperature expansions has not yet been proved rigorously.

The other difficulty with series expansions is technical: usually, a finite number of the coefficients a_n can be determined, $a_0, a_1, \ldots, a_{n\,\max}$. Typically, the calculation is, in principle, straightforward; however, the increased labour necessary for calculating each succeeding coefficient is large. Obviously, the computation of a_{n+1} involves at least as much labour as the cumulative calculation of $a_0, a_1, \ldots, a_n$. While there is, in principle, no limit to the number of calculable coefficients; there is, in practice, a rather sharp upper bound $a_{n\,\max}$ determined by such practical considerations as time, patience and even computer capacity and funding [315]. At present, the upper bound $a_{n\,\max}$ of terms in various approximations for the Ising model is around $n=26$ (too far from infinite). This is the main reason why almost all the approximation techniques provide the (almost) same inexact results in the 3D Ising case.

All systematic methods for the determination of series coefficients are, at some level, graphical or diagrammatic. A set of graphs of some given topological type is associated with each coefficient. A numerical contribution corresponds to each graph according to a well-defined rule. To calculate the required coefficient, one simply sums all contributions. As a rule, the restrictive embeddings are best in low dimensionality and for rather open lattice structure. For close-packed and in higher dimensionality, the renormalization method seems preferable. In any given study, there may be additional considerations favouring one method or another [315]. The early expansions for magnetic systems, especially the Ising and Heisenberg models, which have been important in the study of critical phenomena, were all of the weak (high-temperature) and strong (low-temperature) embedding types. This may partially explain why the high- and low-temperature expansions can give the exact terms for the 2D Ising model, but not for the 3D Ising model. This may also explain why the results of the high-temperature expansions are better and more regular than those of the low-temperature expansions, but worse than those of the renormalization group techniques.

The renormalization group concepts are concerned with the basic physics of a critical point, namely, the long-wavelength fluctuations that are the cause of critical singularities. The starting point in the renormalization group approach is to realize that the most important fluctuations at the critical point do not have a characteristic length. Instead, the important fluctuations have *all* wavelengths ranging from the atomic spacing up to the correlation length; close to the critical

point, the correlation length is much larger than the atomic spacing. Thus, the important wavelengths near the critical point cover many decades [318]. However, the renormalization group techniques are, in a certain sense, similar to the series expansions because, during the renormalization group procedures, various approximations, such as expansions, perturbations, linearizations, normalizations, etc., are performed. In every procedure, the disadvantages, similar to those of low- and high-temperature expansions, have not been removed completely. The starting point for the ε expansion is Landau's mean field theory, which is exact apart from logarithms in four dimension ($\varepsilon = 0$). For the simplest (Ising-like) case, the critical exponents move in the direction of the 2D values obtained by Onsager and, in three dimensions, agree well with high-temperature calculations.

In principle, we can focus our attention only on those methods for which the progressive inclusion of more coefficients leads to successive approximation schemes, which appear to converge with reasonable regularity and speed. Extrapolation, in principle, enables one to draw conclusions about the critical point behaviour and to estimate the 'errors' involved. However, we have to stress that the estimated errors are, unfortunately, in no sense rigorous and only represent a subjective assessment of the rate of convergence of available numerical data. In principle, one could easily be misled by the initial coefficients, for there is no mathematical reason why the apparent asymptotic behaviour of the first 10–20 terms, say, should continue to infinity [316]. Indeed, the position is less satisfactory for 3D lattices for which the series converge more slowly; further information is needed to provide direct estimates of critical exponents and amplitudes which can be considered as adequate [107]. We would like to emphasize that, to serve as a standard of judging the correctness of a putative exact solution, the necessary conditions for any approximation results are as follows. (1) The approximation expansions must be exact and convergent and (2) the variable for such expansions (even exact and convergent ones) must be kept small. The accidental success of low- and high-temperature expansions in 1D and/or 2D cannot be the basis for over-optimism of their validity in 3D. It should be borne in mind that, when using approximation techniques, the final state, determined by choosing an initiate state plus high-order (perturbation or non-perturbation) corrections, can deviate far from the real state, no matter how many correction terms used or how precision the techniques.

8.2.2. Low temperature expansions. For low-temperature expansions, the appropriate choice is to define the partition function such that the fully aligned spin-up state is taken as having zero energy, since the low-temperature series is a perturbation expansion about this state. It has been widely accepted that the exact solution of the 3D Ising model must be equal to the exact low-temperature expansions. Unfortunately, the low-temperature expansions in 3D are divergent. It is our opinion that nobody can find an exact solution with the close form, which diverges at/near critical point. It is also our opinion that the requirement, where the exact expression for spontaneous magnetization must be equal, term by term, to the so-called *exact* low-temperature expansions, has, for a long time, reflected a pious hope.

Compared with high-temperature expansions, the situation at low temperatures is far less satisfactory [107, 111]. As remarked by Domb [107], the low-temperature

series in 3D alternated in sign so that spurious non-physical singularities were masking the true critical behaviour. Note that in the low-temperature series, the leading term is $-2x^6$, while the coefficient for x^8 term is zero. The first term with positive coefficient is $14x^{12}$, which follows the term of $-12x^{10}$ (with the same coefficient with the present exact solution). The appearance of a plus sign in the low-temperature series expansion appears incorrect [59] and appears to compensate the incorrectness of other terms (especially the leading term). Since there is a masking unphysical singularity, the conjecture of $\beta = 5/16$, based on the low-temperature series expansion, is also questionable. Furthermore, the low-temperature expansions, evaluated by systematically overturning spins from the ground state with all spins 'up', give the same fundamental leading term for the 2D triangular Ising lattice and the 3D simple cubic lattice because it relates directly with the Ising model lattice of coordination number q, regardless of the dimension. It is our belief that the fundamental leading term of $-2x^6$ (correct for the 2D triangular Ising lattice) has to disappear for the 3D simple cubic Ising model. The leading term of our putative exact series of the spontaneous magnetization, $-6x^8$, reminds us that we live in four noncompact space-dimensions (as discussion above), which are required intrinsically for dealing with the topologic problem and the non-local behaviour of the 3D Ising model [303]. The introduction of the fourth curled-up dimension realizes its contribution to spontaneous magnetization, while removing, instantaneously, the problem of the dominant singularity on the negative real axis. This contribution is the real effect of the interacting many-body spins in the 3D lattice, which spontaneously leads to the additional contribution of the free energy due to the 3D topologic problem. What the putative exact solution reveals is that the dominant singularity is located on the positive real axis for both 2D and 3D. Furthermore, the variable $x = e^{-2K}$ used for the low- temperature series expansion is small only at extremely low temperatures, so that it fits well with the exact solution only in the low-temperature range. As shown in figure 3b, the low-temperature series expansion, with terms up to the 54th order of the simple cubic Ising model, fits numerically well with the putative exact solution and oscillates around it up to $T \approx 0.9T_c$ and then deviates from it. If more terms are taken into account, the low-temperature expansions would fit better with the putative exact solution. The putative exact solution is actually the centre of the oscillation of the low-temperature expansions. This could prove indirectly that the present putative exact solution for spontaneous magnetization (and also free energy) might be correct and, furthermore, that the low-temperature series expansion could not provide valuable information on the critical region.

Next, one needs to ask why the low-temperature expansions give the same sign in 2D but the alternate sign in 3D. Why and how does the dominant singularity located on the positive real axis for 2D change to the negative real axis for 3D? It is our opinion that, in the correct answer, all the terms should have the same sign, as in 2D, and in the wrong series they alternate in sign. Guttmann used the method of N-point fits to locate unphysical singularities for various lattices [107, 319]. For the simple cubic lattice, he found that there is one singularity on the negative real axis. These singularities lie closer to the origin than the physical singularity, thus masking the critical behaviour. Domb [107] and Guttmann [320] initiated a configurational analysis of terms in the low temperature series, which showed how the spurious

singularities arise. Starting from the empirical observation that Carley-tree embeddings are far more numerous than those of any other group of connected graphs, they estimated the Carley-tree contribution to the low temperature series and found that, in a first approximation, the spurious singularities all lie on the circle $u = u_c$ for $q = 4$, 6, 8 and 12. For $q = 4$, there is only one solution; for $q = 6$, there are two at positive and negative axes; for $q = 8$, there are three in the complex u plane; for $q = 12$, five. The distribution of singularities in the complex u plane for simple cubic lattice was shown in figure 21 of Domb [107]. Higher-order approximations move the spurious singularities nearer to the origin. Infinite-order approximations would move the spurious singularities to the origin. From the existence of the non-physical singularity points and its divergence, the radius of the circle of convergence for low-temperature expansions could be zero. This is because there is no special point between the zero and the critical point and, if the radius was not the critical point, it is possible that it would be reduced to zero. In the following, we shall discuss in detail the radius of the circle of convergence for low-temperature expansions.

The irregularity (i.e. the alternating sign) and divergence of the low-temperature expansions in 3D are clearly associated with an unphysical singularity on the negative real axis [107, 319, 320]. One would expect from the tendency of known terms (up to 54th order ($n = 27$) [111, 238]) that the low-temperature series for spontaneous magnetization should alter the signs and rapidly increase the coefficients of the terms, up to infinite terms. This obviously leads to a stronger oscillation and divergence of the spontaneous magnetization, especially, at the high-temperature region (close to the critical point). Thus, it is crucial to find the radius of the circle of convergence of the low-temperature series. From the coefficients m_n of the low-temperature series [111, 238], one can calculate the ratio of m_{n+1}/m_n to evaluate the circle of convergence in accordance with criterion (1) above [315–317]. From table 2, the calculated results from the last known terms are as follows: $-3.3479826\ldots$ for $n = 21$, $-3.3621183\ldots$ for $n = 22$, $-3.3626251\ldots$ for $n = 23$, $-3.3716472\ldots$ for $n = 24$, $-3.3741696\ldots$ for $n = 25$, $-3.3805110\ldots$ for $n = 26\ldots$. Then, one can evaluate the difference $\Delta_{(n+1,n)} = (m_{n+2}/m_{n+1} - m_{n+1}/m_n)$ between the neighbouring ratios m_{n+1}/m_n. It is seen from table 2 that, after the initial oscillation between positive and negative values up to $\Delta_{(21,20)}$, it becomes stable at small negative values: $-0.0141357\ldots$ for $\Delta_{(22,21)}$, $-0.0005068\ldots$ for $\Delta_{(23,22)}$, $-0.0090221\ldots$ for $\Delta_{(24,23)}$, $-0.0025224\ldots$ for $\Delta_{(25,24)}$, $-0.0063414\ldots$ for $\Delta_{(26,25)}\ldots$. It is reasonable that all the higher-order terms would follow this tendency, i.e. the higher-order terms m_{n+1}/m_n would decrease monotonously, by small finite values, with increasing n. Regarding the existence of infinite terms of the exact low-temperature series, it seems reasonable to conclude that the ratio m_{n+1}/m_n would approach negative infinite as n becomes infinite, because small finite values times infinite leads to infinite. For criterion (1), one finds that the radius of the circle of convergence of the low-temperature series is zero. This means that the non-physical singularity on the negative axis approaches zero, taking into account all of the infinite terms of the low-temperature series. There are two possibilities for the circle of convergence of the low-temperature series: a zero radius or a non-zero radius. It is our argument that it would be unreasonable to predict the ratio m_{n+1}/m_n for $n = \infty$ to be about -3.5 simply by extrapolating plots as a function of $1/n$ to zero

Table 2. Low-temperature series coefficients m_n, the ratio m_{n+1}/m_n, the difference $\Delta_{(n+1,n)} = (m_{n+2}/m_{n+1} - m_{n+1}/m_n)$ between the neighbouring ratios m_{n+1}/m_n and $(m_n)^{-1/n}$ for magnetization of the three-dimensional Ising model on a simple cubic lattice. The values for low-temperature series coefficients m_n are taken from table VI of [238].

n	m_n	m_{n+1}/m_n	$\Delta_{(n+1,n)} = (m_{n+2}/m_{n+1} - m_{n+1}/m_n)$	$(m_n)^{-1/n}$
0	1	0	–	1
1	0	–	–	0
2	0	$-\infty$	∞	0
3	−2	0	$-\infty$	0.793700525984099...
4	0	$-\infty$	∞	0
5	−12	−1.166666666666666...	−5.261904761904761...	0.608364341893205...
6	14	−6.428571428571428...	4.295238095238095...	0.644137614709094...
7	−90	−2.133333333333333...	−1.991666666666666...	0.525802320771714...
8	192	−4.125	1.412878787878787...	0.518307324814038...
9	−792	−2.712121212121212...	−0.880057558828508...	0.476342601582425...
10	2148	−3.592178770949720...	0.577404276392955...	0.464297742761535...
11	−7716	−3.014774494556765...	−0.403332289038798...	0.443200975243094...
12	23262	−3.418106783595563...	0.248094709946303...	0.432626129059729...
13	−79512	−3.170012073649260...	−0.188903079452852...	0.419801165692409...
14	252054	−3.358915153102113...	0.106577644774961...	0.411319244095722...
15	−846628	−3.252337508327151...	−0.090946724218825...	0.402550612240097...
16	2753520	−3.343284232545977...	0.044154987939316...	0.395828431381549...
17	−9205800	−3.299129244606661...	−0.045677618649371...	0.389358196365129...
18	30371124	−3.344806863256032...	0.016620758351184...	0.383979226771075...
19	−101585544	−3.328186104904847...	−0.024389916227353...	0.378955133136635...
20	338095596	−3.352576021132200...	0.004593441138821...	0.374582966156199...
21	−1133491188	−3.347982579993378...	−0.014135718971191...	0.370541820614560...
22	3794908752	−3.362118298964570...	−0.00050678373868...	0.366928763492823...
23	−12758932158	−3.362625082703257...	−0.009022115314501...	0.363594050587216...
24	42903505303	−3.371647198017758...	−0.00252237410530...	0.360561596174962...
25	−144655483440	−3.374169572123065...	−0.006341432681172...	0.357755734601860...
26	488092130664	−3.380511004804237...		0.355174876597187...
27	−1650000819068			0.352777263173715...

(though we could not fully exclude this possibility), because there are infinite uncalculated points for plots as a function of n.

One could also try to evaluate the circle of convergence in accordance with criterion (2) above [315–317]. It is clear from table 2 that the value $(m_n)^{-1/n}$ for magnetization of the 3D Ising model on a simple cubic lattice changes from 1 for $n = 0$ to 0.352777263... for $n = 27$. After the initial irregularity, the value $(m_n)^{-1/n}$ decreases monotonously from 0.644137614... for $n = 6$ to 0.352777263... for $n = 27$. It is reasonable to believe that this tendency is valid for all the terms with $n > 27$. Regarding the existence of infinite terms for the low-temperature series, the value $(m_n)^{-1/n}$ could decrease steadily down to zero as n approaches infinite. Once again, one concludes that the radius of the circle of convergence of the low-temperature series could be zero. In other words, either the zero or the non-zero radius is true for the circle of convergence of the low-temperature series. Nevertheless, this needs to be proved rigorously in the future.

If one agreed with the statement above for the zero radius of the circle of convergence, one could discuss further the problems of analytic continuation and

singularities of the low-temperature series. According to the principle of analytic continuation [317], a function that is well defined inside its circle of convergence can be continued well beyond its circle of convergence in all directions where singularities are not encountered. The fact that the function is well defined within the circle of convergence is sufficient to guarantee analytic continuation throughout the remainder of the complex plane, unless such continuation is blocked by singularities. In the present case, because the radius of the circle of convergence is zero, singularities of the low-temperature series are encountered at the origin and, thus, the function is not well defined within the circle of convergence. Therefore, the function cannot be continued well beyond its circle of convergence in any direction, because such continuation is blocked by singularities at the origin. This means that, if one agreed with the zero radius of the circle of convergence, the so-called *exact* low-temperature series could not serve as a standard for judging the correctness of the putative exact solution of the 3D Ising model.

On the other hand, Padé approximants [96, 97] were successful as an effective way of deriving information on the critical behaviour up to the critical point, with very high precision. The Padé approximant method has been applied to overcome difficulties to obtaining more information outside the circle of convergence [96, 97]. However, this method cannot prove/guarantee the continuation or the radius of the circle of convergence of the function, since the Padé approximant can evaluate the series even with the zero radius of the circle of convergence. For instance, for the series $F(z)=1\ -1!\ z+2!\ z^2-3!\ z^3+4!\ z^4-5!\ z^5+6!\ z^6-\ldots$, the Padé approximant can calculate, approximately, its value with very high precision; but the radius of the circle of convergence of this series is zero.

The reason for the zero radius of the circle of convergence of the low-temperature series might be that something is missing in the series as well as in the system. One possibility is the lack of the extra dimension in the 3D Ising system, which is actually hidden in accordance with the existence of the topologic problems. This extra dimension should be introduced to properly account for the low-temperature series; otherwise, the divergent low-temperature series with the zero radius of the circle of convergence are obtained. The inconsistency of the non-relativistic quantum mechanism with the relativity theory, due to the lack of information on the additional dimension as well as the second action of time (i.e.$-\partial^2/\partial t^2$) as discussed above, might be the origin of all the problems (irregularity, divergence, the existence of non-physical singularity point and the zero radius of convergence, etc.) with the low-temperature series expansions when the expansions are employed on the 3D Ising model.

8.2.3. High-temperature expansions. The high-temperature series expansion is an exact expansion that uses the variable $\kappa=\tanh K$, which is small at high temperatures. For the 2D Ising model, it is easy to write down every term of the high-temperature series expansion by accounting for the loops in the 2D lattice. If one took infinite terms of the high-temperature series expansion into account, one would expect that it would fit exactly with the exact solution from infinite temperature down to the critical point. However, for the 3D Ising model, it is a challenge to write down every term of the high-temperature series expansion because considering the polygons becomes tedious and extremely difficult plus the existence

of crosses and knots in the 3D Ising lattice causes the well-known topologic problem. For physical phenomena, where an interaction completely changes the character of the solution, it is necessary to derive a substantial numbers of terms for such perturbation expansions and, if possible, to estimate the asymptotic behaviour of the coefficients. One could not obtain exact information at/near the critical point if one failed to derive the infinite terms of the high-temperature series expansion. As remarked by Domb [107], one should be cautious with series expansions if wrong conclusions are to be avoided; physical insights into the nature of the expected solution should be invoked wherever possible and used to provide consistency checks; methods of series analyses should be tested wherever possible on exact closed form solutions. As revealed in the Appendices and discussed below, the situation with the 3D Ising model is even more pessimistic than indicated above: the putative exact solution could fit well with the high-temperature series expansion only at/near infinite temperature or, from another angle, the high-temperature series expansion could fit well with the putative exact solution only at/near infinite temperature. Once again, there are two possibilities: (1) the high-temperature series expansion may be inexact at finite temperature or (2) the putative exact solution may be incorrect. Considering the possibility of the occurrence of a phase transition at infinite temperature, the high-temperature series expansion could be invalid at finite temperatures.

In other words, it is our opinion that the (albeit exact) high-temperature series cannot serve as an adequate basis for rejecting a putative exact solution of the 3D Ising model. It is true that the high-temperature expansion of the Ising model converges rigorously and the convergent expansions fully define $N^{-1} \ln Z$ in the thermodynamic limit, $N \to \infty$, for all $T > T_c$, as demonstrated for the 2D and 1D models. Note that the convergence and exactness of the high-temperature expansion series do not equate with validity at any temperature range without any conditions. One has to keep in mind that the basis of the high-temperature expansion series is that K or κ have to be small, i.e. K or $\kappa \to 0$. Although the high-temperature expansion series is valid for all $T > T_c$ in the 2D and 1D models, it does not guarantee that the same thing must happen in 3D. The critical point at 2D, located exactly on the circle of convergence, does not guarantee that the same thing must happen in 3D. Actually, in the 2D case, we are extremely lucky because both the high- and low-temperature expansions are exact and convergent, and the critical point is located exactly on the circles of convergence of both expansions. The free energy can be described by a unique function of expansions for the whole temperature range. However, we are not as fortunate in 3D because a non-physical singularity point with $z < 0$ exists. The inexactness, irregularity (i.e. the alternating sign) and divergence of the low-temperature expansions in 3D are clearly associated with an unphysical singularity on the negative real axis [107, 319, 320]. This strongly suggests the existence of such a non-physical singularity point for the high-temperature expansions, since the parameters for the low- and high-temperature expansions are related (the definition of $\kappa = \tanh K = (1-x)/(1+x)$ with $x = e^{-2K}$). This non-physical singularity point could greatly reduce the radius of the convergence of the (still exact) high-temperature series. If the radius of the convergence of the high-temperature series was decreased, it would be zero (or infinitesimal) – a point – because there is no special point between the critical point and infinite temperature.

This is due to the fact that the radius of the convergence of the low-temperature series is also zero, according to the discussion above. Although κ looks convergent as $K \to K_c$, the existence of this non-physical singularity makes such a convergence meaningless. Therefore, it is concluded that the radius of the convergence of either low- or high-temperature series expansions is zero and both series expansions could be inexact at any finite temperatures. The claim that the high-temperature expansion series is valid for all $T > T_c$ in 3D has not yet been proved rigorously. The radius of the convergence of the high-temperature series is the critical temperature of the 2D Ising model and was proved to be true by Onsager's exact solution. Note that the Onsager exact solution served as the standard for judging the validity of high-temperature series in 2D; not inversely. Only the exact solution can serve as the standard for judging its validity in 3D. It is possible that for 3D, the high-temperature expansion series is rigorously valid only at its very high temperature limit. The radius z_0 of convergence may not be finite but infinitesimal, i.e. $z_0 \to 0$. The non-physical singularity point could be located on the circle of convergence with its infinitesimal radius z_0 (being a point at infinite temperature). The physical singularity point, i.e. the critical point, which is our main interest, could be located outside the circle of convergence for the 3D Ising model. This could be why the high-temperature expansion series cannot exactly locate the critical point of the 3D Ising model, which has displayed results no better than with renormalization group techniques. The scenario is that all the configurations used for deriving the high-temperature expansion series (of infinite terms) exist only near infinite temperature (i.e. K or $\kappa \to 0$) in a random fashion, although it is less random than the infinite-temperature state, and many (actually infinite) configurations, as a kind of microstructure, have already emerged. The information from these configurations can be maintained in the exact function and weights in an intriguing way, as revealed in this paper.

The main reason for the zero radius of convergence of the series expansions could be that, in accounting for the terms of these series expansions, the normal procedure does not consider the important hidden intrinsic property of the 3D Ising model. In other words, the interacting spins at the thermodynamic limit in the three dimensions intrinsically hide the topologic knots of interaction, which introduce a comparatively higher energy than the simple sum of the normal loops as calculated in other dimensional models. This intrinsic property is a cooperative non-local phenomenon, which cannot be described properly by these approximations, taking into account only the local environments. The non-local behaviour exists especially and only in the 3D many-body interacting spin system, which can be seen clearly in its complex boundary condition, its topologic problem, etc. The non-local behaviour could be related to the additional dimension, as discussed above. The lack of information on the additional dimension in the non-relativistic quantum mechanism (which is inconsistent with the relativity theory) might be the origin of all the problems (the existence of non-physical singularity point and the zero radius of convergence, etc.) of the series expansions when these are employed on the 3D Ising model, described within the framework of the non-relativistic quantum mechanism.

The difference between low- and high-temperature series expansions is mainly due to their starting states. The high-temperature series expansion starts from the highly random state, where the nonlocal property is negligible, but the

low-temperature series expansion initiates from the completely order state, where the nonlocal property is extremely strong. One could find a mechanism of spontaneously and simultaneously knowing all the high-temperature configurations at a temperature that infinitesimally deviates from infinite, whereas it is impossible to find a mechanism of spontaneously knowing all the low-temperature configurations at a temperature that infinitesimally deviates from zero, owing to the high thermal energy cost up to the critical point. Therefore, the high-temperature series expansions can be exact at a temperature infinitesimally deviating from infinite, whereas the low-temperature series expansions in the previous form cannot be exact at a temperature infinitesimally deviating from zero. The situation at low temperatures is worse than at high temperatures, which may explain why the low-temperature series expansion is not more reliable than the high-temperature series expansion for predicting the critical point and the critical exponents.

One may ask why the high-temperature expansions can be valid for all $T > T_c$ in the 2D and 1D models, but only for $T \to \infty$ in the 3D model. This can be ascribed to differences between the 3D and the other models. The differences between the 2D and 3D Ising models are evident: topologic, symmetric, dimensionality, singularity, ... The following are several general points on this issue. (1) Types of interactions: it is known that the 3D is especially designed for validating the law that the strength of the interaction is inversely proportional to the square of the distance. (2) Types of topologic: the high-level life, such as humans, fish, etc., cannot live in 2D since a 2D gastrointestinal system can divide the body of a 2D fish to separated two parts. Another example is the connection between different points in lattices. The number of direct connections for communication between two lattice points without any cross to other connections in 1D is two; in 2D it is four; in 3D it is infinite. This makes neural networks in high-level life possible only in 3D. Next, let us focus on the Ising model where spins with interactions are located on each lattice point. The intrinsic difference between the 3D and 2D Ising models can be seen clearly by comparing equations (15a) and (15b) with equation (14) in Kaufman's paper [17]. The end factors in equations (15a) and (15b) originate from the boundary condition that many of the bonds are nonplanar and that these bonds cross over those in other planes. This boundary condition in 3D is much more complicated than in the 2D case. To deal with this complex boundary condition, one needs to introduce Conjecture 1 to open the topologic knots. As discussed above, this topologic problem hides another related intrinsic property – all the elements in matrix V are correlated intimately, so that the 3D Ising model has an intrinsic nonlocal property, whereas the 2D model lacks such nonlocal behaviour. This nonlocal property can also be seen from the form of the additional rotation shown in equation (18), where the elements K''' of the additional rotation matrix is a mixture of K, K′ and K″. This nonlocal property is an intrinsic property of the 3D Ising model, with the result that any approximation techniques taking into account the local property only cannot be correct for the 3D Ising model, though these approximates work well for other 2D or 1D models. The only exception is the application of the high-temperature expansions at/near infinite temperature, because there is no interaction at infinite temperature and the interaction is comparatively weak at a temperature infinitesimally deviating from infinite in comparison with temperature. Only at this extremely high-temperature limit can the effect of the nonlocal property be neglected. This also explains why the

low-temperature expansions diverge in 3D, since such nonlocal property is extremely strong at low temperatures.

Furthermore, a serious problem with analysis of the 3D Ising model is the presence of confluent singularities, which are extremely weak or non-existent in the 2D model [111]. Both field theory and high-temperature series analysis suggest a value for the confluent exponent not very different from 0.5. Certainly, the 2D and 3D Ising models are intrinsically different, otherwise the exact solution of the 3D Ising model would have been found immediately after Onsager's discovery. In any case, as with Kramers and Wannier, one can easily locate the critical point. If the critical temperature were, as hoped, the radius of the convergence of the high-temperature series, one would have located the critical point (almost) exactly by this expansion. The well-known group of critical exponents $\alpha = 1/8$, $\beta = 5/16$, $\gamma = 5/4$, $\delta = 5$, $\eta = 0$ and $\nu = 5/8$, obtained by the high-temperature expansion and suggested by Fisher [103] and Domb [107], gives the value of $\eta = 0$, which is the same as predicted by the main field theory and certainly not relevant. The critical exponent η denotes the deviation from the Ornstein–Zernike behaviour, which cannot be zero. All these indicate that the success and optimism of the high-temperature series in other dimensions cannot be simply transplanted to the 3D case. For 4D, it is well known that the mean field theory, which is believed to be the zero-order approximation, can well describe the behaviour. Other approximations, better than the mean field theory, can give good results because they just add higher-order perturbation terms that approach infinitesimal for 4D. To further question why the 3D differs with other dimensions is analogous to asking why we are living in a 3D world. This is beyond the scope of the present paper. All the analyses above indicate that both the low- and high-temperature series expansions may not give the exact information at the critical region of the 3D Ising model.

8.2.4. Monte Carlo simulations. Why can Monte Carlo simulations not provide the exact solution? First, most simulations are limited by the size effects of the model and the power of the computers. It is not possible to perform calculations and simulations on a lattice with the number of spins or atoms, $N \to \infty$, since the number of configurations of the Ising model increases as 2^N. In the finite system that is simulated, the difficulty is that there is no sharp transition between zero and non-zero magnetization or a sharp peak in the specific heat. Therefore, the critical point cannot be located precisely [212]. Furthermore, the absence of a sharp peak in the specific heat hinders an analytical understanding of its singularity at the critical point. Monte Carlo simulations are powerful techniques for numerical calculations, which numerically evaluate canonical thermal averages of some observable A by an approximate one, where M states $\{x_\mu\}$ are selected by importance-sampling process [213]. The importance-sampling process consists of the construction of a Markov chain of states $(x_1 \to x_2 \to \cdots x_\mu \to x_{\mu+1} \to \cdots)$, where a suitable choice of transition probability $W(x_\mu \to x_{\mu+1})$ ensures that, for large enough μ, states x_μ are selected according to the canonical equilibrium probabilities, $P_{\mathrm{eq}}(x_\mu) \propto \exp\{-H(x_\mu)/k_{\mathrm{B}}T\}$. The limitations of Monte Carlo simulations are as follows [213]. (1) Only in the limit $M \to \infty$ we can expect to obtain an exact result, while for finite M a 'statistical error' is expected. The estimation of this error is a very nontrivial matter, since it depends

sensitively on the precise choice of W and subsequent generated states are more or less correlated. It is expected that the 'correlation time' diverges in the thermodynamic limit at a second-order phase transition [321]. (2) While the importance-sampling method guarantees that, for $\mu \to \infty$, the states are selected according to $P_{\text{eq}}(x_\mu)$, but for choices of μ that are not large enough there is still some 'memory' of the (arbitrary) initial state with which the Markov chain was started. The non-equilibrium relaxation time for the system, which relaxed from the initial state towards the correct thermal equilibrium, is divergent at a second-order phase transition in the thermodynamic limit [322]. (3) For realization of the Markov chain, (pseudo-) random numbers are used both for constructing a trail state x'_μ from a given state x_μ and for the decision of whether or not to accept the trial configuration as a new configuration. For instance, in the Metropolis algorithm, this is done if the transition probability W exceeds a random number that is uniformly distributed in the interval from zero to one [193–202]. Evidently, it is necessary to carefully test the quality of the random numbers since bad random numbers cause systematic errors. However, this is again a nontrivial matter, since there is no unique way of testing random-number generators and there is no absolute guarantee that a random-number generator that has passed all the standard tests does not yield random numbers leading to systematic errors in a particular application [234, 323–326] (4) Monte Carlo methods apply to a system of finite size only and the results of calculations near a phase transition are affected by finite size and boundaries. The finite size of the simulated lattice, typically a (hyper-)cubic lattice of linear dimension L with periodic boundary conditions in all lattice directions, causes a systematic rounding and shifting of the critical singularities. This is because singularities of the free energy can only develop in the thermodynamic limit $L \to \infty$. This remark is particularly obvious for the correlation length ξ, which cannot diverge towards infinite in a finite simulation box, so that serious finite-size effects must be expected when the correlation length ξ has grown to a size comparable to L [235, 327–329]. Therefore, the results obtained by Monte Carlo simulations depend sensitively on the numbers of Monte Carlo steps, the linear dimension L of the simulation box with periodic boundary conditions, the non-equilibrium relaxation time of the system and the quality of the random-number generators, etc. Actually, the correlation length diverges to infinite at the critical point of a second-order phase transition; the physical fluctuations in the magnetization become very large near the critical point. These fluctuations cannot be entirely suppressed by the importance sampling. To obtain good averages, the Monte Carlo simulations should be run for an inordinately long time and, unfortunately, for infinite time to reach the exact solution. Most importantly, any approximation method cannot prove exact information at/near the critical point, since whenever the thermodynamic functions have an essential singularity it is difficult to perform any computation by successive approximation because the convergence of approximation by analytic functions in such cases is notoriously slow [13]. Even if we continued to work with the smallest lattices possible, the inclusion of longer-range interactions/correlations would force us to bigger systems and there is a limit to what could be done even with computers many times faster than those currently available. Nowadays, calculations of the Ising models have been performed on lattice sizes of $L = 256$–5888, far from infinite. To date, most 3D simulations with a lattice size lager than 4800 have been short runs,

which could not produce well-equilibrated configurations at the critical point [184, 185, 213]. Normally, increasing the lattice sizes would lower the estimates of the critical point [170, 212, 213], which would push the values in the Binder and Luijten review [213] towards our putative exact solution. For the 2D Ising model, Monte Carlo simulations give much better results [213], not only because much larger lattice sizes can be dealt with but also because there is no topologic problem of crosses and knots. Although the combination of Monte Carlo simulations and renormalization group techniques reduces calculation time and gives better results by allowing a much larger study than is possible by direct summation methods [178, 179, 330], the essential difficulties in the Monte Carlo simulations are not removed. In utilizing Monte Carlo simulations, the accuracy of the calculations can be improved by increasing either the lattice size or the running time of importance sampling, but it is not always explicitly practical to count the lattice states or to determine the critical parameters with more than a handful of lattice sites, on any computer no matter how powerful [21]. Fortunately and unfortunately, this combination contains both the advantages and disadvantages of the renormalization group techniques.

8.2.5. Renormalization group techniques. Why can the renormalization group techniques not give the exact solution? The renormalization group techniques developed by Wilson and others divide roughly into two categories [141–144, 149, 152–160, 192–202, 208–225]. (1) The real-space renormalization group techniques, close in spirit to the original idea of Kadanoff [210, 243, 331], which allow one to simplify calculations of the critical exponents in the critical regime without ever working out the partition function. (2) The field theoretical or k-space renormalization group techniques, as developed by pursuing the analogy between statistical mechanics and quantum field theory. In the former case, we are actually concerned with the construction of new models from old by averaging dynamical variables of the old model to form the block variable of the new model. In the latter case, we are actually concerned with changing the parameters of the Landau–Ginzburg model to experimentally more accessible quantities. Superficially, it seems that there is no connection between the categories of the renormalization group techniques. However, at a deeper level, there is a close connection, because the basic idea is the same and because there are connections between ϕ and a set of block variables [212]. It is believed that in both categories, performing the renormalization reduces the degrees of freedom while losing the information of the system.

For the real-space renormalization techniques, the final results depend sensitively on how to divide Kadanoff blocks, define the effective Hamiltonian, determine the details of the block variables and calculate approximately the partial trace [141–144, 149, 152–160, 208–225]. The larger the Kadanoff blocks, the more accurate the calculations, but the more complicated the procedure. The cumulant expansion during the calculation of the partial trace also causes uncertainty in the results. The more terms remain, the more accurate the final results. The final results would approach the exact solution if and only if the size of the Kadanoff blocks were chosen to be infinite and the infinite terms of the expansion were retained. This is impossible, because many more variables would emerge with the increasing size of the Kadanoff blocks and take into account more terms of the

expansion, which make the calculations extremely difficult. Calculating the critical exponent ν relates the divergence of the correlation length ($\xi \to \infty$) to the temperature, while the calculation of the critical exponents η and δ must work in the limit of $n \to \infty$, where n stands for the number of iterations of the renormalization transformation. For the calculation of the remaining three ($T \neq T_c$) critical exponents β, γ and α, difficulties arise from the fact that, in the regime very close to the critical fixed point, many measurable quantities change drastically in response, not only to small temperature variations near T_c, but also small changes in the parameters appearing in the effective Hamiltonian, remembering that the effective Hamiltonian is temperature-dependent. The critical exponent α proves considerably harder to calculate than the others, because the specific heat is not simply related to the block variables [22]. Moreover, when we renormalize, we know very little about how T and T_c vary, but skip the problem by eliminating T–T_c in favor of the correlation length. All these difficulties imply that it is hard to locate exactly the critical point by real-space renormalization techniques. One should note that the values of the critical point, well-established in two recent review articles [154, 213], vary with a very large deviation. Furthermore, a scientist, not knowing all values of the exact solutions of the critical point and the critical exponents that are strongly correlated, may choose one of these parameters (though an inexact one) as the standard to determine others. This causes serious problems for the accuracy of the calculations, since the high-accurate critical exponents must be determined only at the very narrow temperature interval near to the critical point and the high-accurate critical point can be determined only when the critical exponents used during the calculations are exact.

For the field theoretical or k-space renormalization techniques [141–144, 149, 152–160, 208–225], as one follows the original works [126, 127, 142], one easily discovers that a series of approximations could cause serious problems for the renormalization group calculations. In the first step, high-order contributions to the initial Hamiltonian, which are proportional to $|\vec{s}|^6$, $|\vec{s}|^8$, etc., are neglected for adoption of a continuous local variable or spin $\vec{s}$ with a magnitude constrained by a weight factor for each individual variable $\vec{s}_x$. This point is questionable, especially for the spin 1/2 Ising models where the strong constraint $s = \pm 1$ might still play a special role. These high-order contributions could seriously affect the construction of the reduced Hamiltonian in momentum space for the spin 1/2 Ising models [143]. The high momentum cut-off during the definition of a renormalization group by partial trace over high momentum variables may also cause problems, since, at the critical point, all spin components with long and short wavelengths (or low and high momentums) become comparably dominant. In the final and crucial computational step of realizing the renormalizing group operator by a perturbation expansion of treating the coupling constant u (in field theoretic language) as a small parameter, which leads to a graphical formulation full of Feynman type-integrals, the biggest problem is that the small parameter is not, in fact, a coupling constant, but rather the dimensional difference $\epsilon = 4 - d$ [143]. For the 3D Ising model, $\epsilon = 1$, cannot be treated as a small parameter. It seems that the series expansion for $n = 1$ and $d = 3$ at order ϵ^2 gives the best match of the critical exponent γ to the exact solution. Furthermore, the introduction of Feynman graphical techniques, which were

originally developed for quantum electrodynamics, causes other serious problems of approximations, because iterating a set of non-linear recursion relations (obtained by the linearization of leading order (or even several leading orders) in the coupling constant) many times, causes uncertainty in the final results and, as no one knows how to account for the contributions of all the infinite Feynman graphs, becoming important in the same order at the critical point of the second-order phase transition.

Although the renormalization group theory is described in mathematical terms, it is not rigorous. Besides, we have to make several assumptions. We deal with formal series expansions without knowing anything about their convergence or divergence and the term limit is used without having defined a metric [236]. A serious problem with the renormalization group transformation in real-space or otherwise is that there is no guarantee that they will exhibit fixed points [149]. For some renormalization group transformations, iteration of a critical point does not lead to a fixed point, presumably yielding instead interactions with increasingly long-range forces [236, 332]. There is no known principle for avoiding this possibility and a simple approximation to a transformation can misleadingly give a fixed point, even when the full transformation cannot [144–146]. Nothing is known yet about how the absence of a fixed point would be manifested in Monte Carlo renormalization group computations. Thus, it can be concluded that the high-precision calculations of both the real-space and field theory renormalization group techniques cannot give the exact solution owing to the existence of systematical errors.

We still need to further explain why the high-precision calculations of the renormalization group theory and Monte Carlo simulations cannot give the exact solutions for the critical point and the critical exponents (except for γ). The key factor is that serious systematical errors exist in these techniques, caused by the disadvantages discussed above. These systematical errors are related directly to the initial physical concepts/views and the neglect of important factors during procedures, etc. For instance, linearization during calculations is not very reliable since non-linear terms could become dominant near/at the critical point. Therefore, the systematical errors of the renormalization group theory and Monte Carlo simulations are intrinsic and cannot be removed by efforts to improve, technically, the precision. This means that estimates of the critical point and the critical exponents by various theories and experimental techniques can become more precise but not sufficiently accurate. The situation is similar to that of everyone using a gun of the same kind with very high 'so-called accuracy' (actually, only high precision) and high systematic error, which can shoot 9 points with high precision but never shoot exactly 10 points on the target. However, the renormalization group theory and Monte Carlo simulations are still powerful techniques for the study of critical phenomena as long as the simulations focus only on the critical exponent γ and one keeps in mind that there are systematic errors for the critical point and other critical exponents.

8.2.6. Experimental techniques. Why can experimental techniques not give the exact solution? First of all, the critical regions are very narrow, $\Delta T/T_c = (T - T_c)/T_c \lesssim 10^{-2} \sim 10^{-1}$ [105]. The temperature difference ΔT can be measured much more accurately than the temperature T itself. The major experimental uncertainty is the relative location of T_c itself [105]. For instance, in

specific heat measurement, a rounded peak is often observed, making the precise location of the critical point uncertain. In resonance experiments, the lines of both the order and disorder phases often overlap in a small temperature region close to the critical point. Measurements in applied magnetic field require the extrapolation to zero field to fix the critical point, introducing further uncertainty. The determinations of critical exponents for bulk even involve extrapolations to zero internal field values. The choice of the critical region and the critical point are interdependent and affect the evaluation of the critical exponents. Furthermore, the domains often exist in ferromagnets and the domain walls serve to break up the long-range correlations so essential to the critical behaviour. For experiments, it is essential to ensure that the domains should be larger than the theoretical coherence length, but it is infinite at the critical point. The existence of long-range interactions and magnetic anisotropy in the real materials may affect the critical behaviour. Impurities in the magnet sample may seriously affect the value of the critical temperature; thus, good measurements require the use of single crystals of extreme purity and well-defined geometry. Last but not least, the spontaneous magnetostriction alters the lattice parameters of the materials at the critical regime. This effect should be included in the analysis of precise data, to compare with a theory that has fixed lattice constants. In every case, it is necessary to be convinced either that the transition is second order or that the latent heat in a first-order transition is too small to change the critical behaviour under study, since the connection between the critical effects and lattice size and shape can in some cases make the transition first-order [105]. It is well-known that the accuracy of experiments is less than that of theories. As stated by Vicentini-Missoni [268], good data in the critical region are available only for a few substances. All the above factors block the accurate determination of critical exponents in real materials, though the accuracy of the experimental techniques has improved greatly over the past decades.

8.2.7. More general discussions. We still need to further explain why, over the years, the multitude of separate determinations of these critical exponents by various independent scientists using completely different techniques (Monte Carlo simulations, high- and low-temperature expansions, renormalization group field theory and experiments) coincide. Superficially, all these different techniques are independent. At a deeper level, they are related and connected closely. Nowadays, it is believed that the field theory renormalization group technique gives the most accurate estimates among all these approximation techniques [154, 212, 213]. The coincidence in the results of the Gell–Mann and Low approach with the Kadanoff–Wilson method seems, at first sight, accidental. As mentioned above, the field-theory renormalization group technique is connected with the real-space renormalization group technique, since they share the general idea of the renormalization group and there are connections between the variables [212]. Di Castro and Jona-Lasinio [333] made an effort to underline the deep conceptual unity which is implicit in various aspects of the renormalization group idea by explicitly making a connection between the Kadanoff–Wilson and the Gell–Mann–Low approaches. With the exception of the spaces where the renormalization group techniques are performed, the concepts, as well as the processes, of the two techniques are very similar and closely related.

For instance, the model Hamiltonian, describing either a relativistic field-theory model in $d-1$ space and one time dimension or a classic ferromagnet in d-space dimension of Ising-type for $n=1$, is actually the same [333, 334]. Dividing the Kadanoff blocks in real-space corresponds to cutting off the momentums in k-space; both methods lead to an asymptotically scaling invariant theory with equal critical exponents, at least in the first few orders in the ε-expansion. The Monte Carlo technique and its related renormalization group techniques share the disadvantages of the Monte Carlo process. Even the low- and high-temperature series expansions are related closely to the field theories [142]. Studying the possible phases of interacting constituents in a high or low temperature equalizes, in field theoretic language, to study strongly cut-off field theories, as what the field theory renormalization technique does for the critical point.[142] It is well-known that the low-temperature expansions have the lowest precision among all the theoretical techniques, while the accuracy of experiments is lower than that of theories. Although separate determinations of these critical exponents were carried out independently, during the processes of determination and publication, scientists like to refer to the published or well-established data. For instance, a scientist working on the Monte Carlo technique may proceed in steps, using the values of the critical exponents from the field-theory renormalization as initial guesses, to obtain a good first estimate of his own calculation and avoid ambiguities in the fitting procedure [213]. A scientist, who is doing experiments, may also be asked to compare (or match) with well-established theoretical values. Almost all scientists in the field have pre-set the existence of a non-zero value of the critical exponent α for fitting the experimental data or calculating the critical parameters. Almost all scientists in the field use the scaling laws to determine other retained critical exponents from part of the calculated critical exponents, in most cases, including the critical exponent α (pre-set already to be non-zero). At the deepest level, all these theoretical techniques have the same problem of neglecting the high-order terms, the size effects and the knot effects, etc. Evidently, all these terms/effects, which might be negligible in other cases, become comparable with the leading terms at/near the critical point of the second-order phase transition in the thermodynamic limit for the 3D case. Such neglect results in systematical errors. Furthermore, it could be that, typically, these approximation calculations are, in principle, straightforward; however, the increased labour necessary for calculating each succeeding coefficient is large [315]. Normally, computation of the coefficient a_{n+1} in series methods should involve at least as much labour as the cumulative calculation of a_0, $a_1, \ldots, a_n$. Thus, while there is, in principle, no limit to the number of calculable coefficients, in practice, there is a sharp upper boundary $a_{n\,\max}$ [315]. Typically, the first few coefficients are trivial and no special methodology is necessary. However, in higher orders, the bookkeeping is extremely involved and scrupulous accuracy is necessary in determining the coefficients, as extrapolative analysis of the computed coefficients makes critical-point behaviour exceedingly sensitive to tiny fractional changes in the last few available coefficients. For these reasons, it is of paramount importance to have a well-defined, systematic procedure for computing coefficients, which incorporates as many short cuts as possible and minimizes the opportunity for careless error. However, the position is less satisfactory for 3D lattices where the series converge more slowly than those of 2D lattices [107]. This is true, not only for

the series methods, such low- and high-temperature series expansions, but also for the renormalization group techniques that actually involve the spirit of the series methods. The existence of the sharp upper boundary in determining the coefficients could be why, over years of experimentation by various independent scientists using completely different techniques, the multitude of separate determinations of the critical exponents coincide.

After six decades, since Onsager's solution to the 2D Ising model was reported in 1944, the exact calculation of properties of the 3D version has proved hopelessly difficult. Onsager himself realized immediately that the 3D Ising model cannot be solved exactly using only the procedure he developed for the 2D version. The application of the algebraic method to the 3D problem is seriously hindered at an early stage because the operators of interest generate a large Lie algebra, which is very difficult to deal with [59]. It seems impossible to locate exactly the critical point of the 3D Ising model simply by the dual transformation, which was used by Kramers and Wannier [14, 15] to locate exactly the critical point of the 2D Ising model. This is because the symmetry for the dual transformation of the 2D Ising model is broken down by the introduction of the third dimension. The combinatorial method of counting the closed graph, developed by Kac and Ward [60], cannot be adapted in any obvious way to the 3D problem, since it introduces some problems in topology that have not been rigorously solved. Actually, their success to simplify the procedure to re-derive the Onsager results was, in large measure, due to knowing the answer and they were, in fact, guided by this knowledge [104, 335]. Feynman provided the key technical formulation for the needed missing lemma [104, 335], the so-called Feynman's conjecture, which eventually was proved by Sherman [240, 241], making the Kac–Ward method completely rigorous. It has been rather puzzling that the two methods for finding the exact solutions for the Ising problem, namely the algebraic method of Onsager and the combinatorial method employing Pfaffians, have exactly the same range of application, although they appear so different in approach. As remarked by Hurst [336], problems which yield to one method yield to the other, while problems which are not tractable by one approach also fail to be exactly solved by the other, although the reasons for this failure appear to have completely different mathematic origins. On the one hand, Ising problems, which cannot be solved by the Pfaffian method, are characterized by the appearance of crossed bonds that produce unwanted negative signs in the combinatorial generating functions. Such crossed bonds are usually manifestations of the topological structure of the lattice being investigated, i.e. the 3D simple cubic lattice. On the other hand, the Onsager approach breaks down because the Lie algebra encountered in the solution process cannot be decomposed into sufficiently simple algebra. It is usually stated that such complicated algebra occur only when the corresponding lattice has crossed bonds. Barahona and Istrial proved that the general, spin glass 3D Ising model belongs to a class of problems that theorists believe will remain unsolved forever, by translating the Ising model into terms of graph theory [337–340]. What they proved was that computing the energy states for the general, spin glass 3D Ising model is what computer scientists call an NP-complete problem - one of a class of recalcitrant calculations that theorists believe can be solved only by arduous brute force computations. This is because the 3D lattices are inherently nonplanar and any nonplanar graph throws up a barrier of computational intractability. Following the

fundamental results of Onsager [13], Kac and Ward [60, 335], Feynman [341], Kasteleyn [245, 246, 342], Temperley [343], Hurst and Green [244] and Barahona [337], Istrail showed that the essential ingredient in the NP-completeness of the Ising model is nonplanarity. This criterion includes two-dimensional models with next nearest-neighbour interactions, in addition to the nearest-neighbour kind, which researchers had found as vexing to solve as their three-dimensional cousins. Every nonplanar lattice in two or three dimensions, as Istrail showed, contains a subdivision of an infinite graph he called the 'basic Kuratowskian' [338]. For the basic Kuratowskian with weights -1, 0, and 1 assigned to the edges, the problem of computing a minimum weight 'cut' (i.e. set of edges joining vertices in opposite states) is NP-complete. The calculation of the partition function for four spin glass 3D Ising models with $\{-J, 0, +J\}$ interactions, with $\{-J, 0\}$ interactions, with $\{0, +J\}$ interactions and with $\{-J, +J\}$ interactions is NP-complete, since their crystal lattice is non-planar. Istrail claimed that the problem falls into the 'computationally intractable' class of conundrums that are too complex to be solved on any realistic timescale. NP-completeness, however, does not mean things are completely hopeless. The complexity only prevents algorithms from solving all instances of the problem in polynomial time [340]. Moreover, such NP-completeness, from the point view of computer sciences, cannot be fully used to judge the advances in mathematics which are needed to uncover the exact solution. Finally, as Istrail noted, it might still be possible to find exact answers for some special cases of the Ising model and, in particular, Ising's original, ferromagnetic 3D model, in which all coupling constants are equal (and positive), may turn out to be simple enough to solve within polynomial time [339, 340]. Fortunately, what we have attempted to exactly solve here is the only possibility for exact answers, as Istrail indicated – the ferromagnetic 3D Ising model. The key to all the algebraic, combinatorial and topologic problems listed above for solving exactly the 3D Ising model is the introduction of our first conjecture. The large Lie algebra can be decomposed into sufficiently simple algebra by introducing the additional rotation in the physical space with higher dimensions, while it also serves to open the crosses/knots to solve the combinatorial and topologic problems. In fact, it is our hope that the putative exact solution of the 3D Ising model reported in this work would provide the key to efficient algorithms for solving thousands of other computational problems, ranging from factoring large numbers to the notorious travelling salesman problem [340].

The key point is how to properly judge the correctness of a putative exact solution. Where no one knows the standard of such judgment, the proper steps are to judge the correctness of the assumption/conception/conjecture and the deriving procedure. If there is nothing wrong with the assumption/conception/conjecture and the deriving procedure, one should accept the correctness of the final results. Any theories (even those as great as Einstein's general relativity) should have their own assumptions, conceptions, conjectures or whatever the starting point. One should allow the existence of such starting points. In the present case, the only starting points are the two conjectures. Conjecture 1 is based on the well-known fact in topologic, namely, the knots in a 3D space can be opened by a rotation in a 4D space, which is introduced to deal with the well-known topologic problem as well as the non-local property of the 3D model. As mentioned above, the introduction of the additional dimension is not contradictory with the existence of four noncompact

space-dimensions, as introduced in Kaluza and Klein's theory for unifying electromagnetism and gravity, and also string theories. Alternatively, one could also treat the additional dimension just as a pure mathematic structure or a boundary condition. The introduction of the weights on the eigenvectors, as stated in conjecture 2, is a very common technique in either physics or mathematics. The detailed calculation of the weights could provide a mechanism for the high-temperature series expansion being exact at a temperature infinitesimally deviating from infinite, even where its radius of the convergence is reduced to zero/infinitesimal. After the introduction of the two conjectures, the deriving procedure simply follows those used by Onsager, Kaufman, Yang, Fisher, *et al*. If one could not point out the incorrectness of the two conjectures and the deriving procedure, one would have to accept the correctness of the final solution as the immediate consequence of the conjectures and procedure.

The principles for judging the correctness of a theory are: (1) self-consistency, (2) compatibility, (3) simplicity and (4) consistency with experiments. The present work is self-consistent, compatible with the exact solution of the 2D Ising model. The present procedure is very simple and elegant, only by the introduction of the two conjectures, while most steps of the procedure directly follow what others employed for the 2D Ising model. That is, employing new initial conditions as the least possible, deriving new final results as the richest possible. A good theory indeed! The results obtained are consistent with the results of carefully performed experiments, although the precision of experiments on the critical phenomena is comparatively low.

8.3. *Symmetry, uniqueness and beauty of the solution*

Finally, we need to check the symmetry and uniqueness of the putative exact solution. For a rectangular lattice, the critical temperatures determined by $\mathrm{K}^* = K'$ or $K'^* = K$ coincide. When one interchanges the roles of K and K' (in case of $K \neq K'$), however, the eigenvalues and the specific heat of the 2D system could be different by a factor [13, 17]. The dual transformation is valid for the rectangular lattice, from which one can also derive another condition of $\sinh 2K \cdot \sinh 2\mathrm{K}' = 1$ for the critical temperature [13, 17]. For simple orthorhombic lattices, $K^* = K' + K'' + (K'K''/K)$ is one of the relations for their Curie temperatures. Dual transformation is held for interchanging the roles of K and $K' + K'' + (K'K''/K)$, i.e. $[K' + K'' + (K'K''/K)]^* = K$, from which the condition of $\sinh 2K \cdot \sinh 2(K' + K'' + (K'K''/K)) = 1$ can be derived for the critical temperature. Similarly, when one interchanges the roles of K and $K' + K'' + (K'K''/K)$, the eigenvalues and the specific heat of the 3D system could be different by a factor. Note that the dual transformation is held only for interchanging the roles of K and $K' + K'' + (K'K''/K)$, not for interchanging the roles of K and K' (or K''). This makes the 3D system very complicated. For a simple cubic lattice, $K = K' = K''$, the critical temperatures determined by the procedure, setting one of the three crystallographic axes as the starting point of the diagonalization (or the standard axis of the procedure), coincide, certainly at the golden ratio. However, for the simple orthorhombic Ising model with less symmetry, although the form of $KK^* = KK' + KK'' + K'K''$ is very symmetric, if we interchanged

the role of K with K' (or K$''$) at the beginning of the procedure, the final results would be different. For instance, if we selected the axis of K' to define K'^* as $e^{-2K'} \equiv \tanh K'^*$, the critical temperature of the simple orthorhombic Ising model would be determined by the relation of $K'K'^* = KK' + K'' + K'K''$, which differs from that determined by $KK^* = KK' + KK'' + K'K''$. As K' is smaller than K, the former critical temperature is higher than the latter. Namely, the critical temperature depends on which crystallographic axis of the lattice is set as the standard axis of the procedure. The critical temperature derived from $KK^* = KK' + K'' + K'K''$ is the lowest, as K is the largest among K, K' and K''. It is bewildering that we have not succeeded in equalizing the critical points or other physical quantities where there are differences between K, K' and K'', which are obtained by setting different axes as standard. It will be shown in the following discussion that lack of uniqueness of the solution is ascribed to the intrinsic character of the 3D Ising lattice. From the condition for the critical temperature of the rectangular lattice, $K^* = K'$ (or $K'^* = K$), we have $K^*/K = K'/K$ (or $K'^*/K' = K/K'$) and $K^* K'^* = KK'$. One could map the points in the subspace of $K'/K < 1$ in the parametric axis of K'/K one to one into the subspace of $K/K' > 1$ in the parametric axis of K/K'. Considering the parametric axis of K'/K, the duality transformation is held for the parameters in two subspace separated by the point $K'/K = 1$, at which the silver solution is located for the square Ising lattice (the most symmetric in the 2D system). Note that the silver ratio is actually the largest solution for the 2D Ising system, if we always set the larger from K and K' as the standard axis. This means that any solution higher than the silver ratio would be forbidden for the 2D Ising lattice if we started our procedure in this way. From the conditions for the critical temperature of the simple orthorhombic Ising lattices, we have $K^*/K = K'/K + K''/K + K'K''/K^2$ and $KK^* = K'K'^* = K''K''^*$. The condition of $KK^* = K'K'^* = K''K''^*$ for the 3D Ising system differs with $K^*K'^* = KK'$ for the 2D Ising system. Nevertheless, the duality transformation is held for the parameters in two subspaces separated by the curve of $K'/K + K''/K + K'K''/K^2 = 1$ in the parametric plane $K'/K \sim K''/K$. Actually, all the points at the curve of $K'/K + K''/K + K'K''/K^2 = 1$ (the dashed curve in figure 4) correspond to the simple orthorhombic Ising lattices with the critical temperature of the silver solution. However, the golden solution for the simple cubic Ising lattice (the most symmetric in the 3D system) is not located at the line of $K'/K + K''/K + K'K''/K^2 = 1$, but at the point (1, 1) (the star in figure 4) in the parametric plane $K'/K \sim K''/K$. The subspace determined by $K'/K + K''/K + K'K''/K^2 < 1 \cap K'/K > 0 \cap K''/K > 0$ does not coincide exactly with that determined by $0 < K'/K < 1 \cap 0 < K''/K < 1$, which can be mapped fully one to one into the subspace determined by $K''/K' < \mathrm{K}/\mathrm{K}' \cap \mathrm{K}/\mathrm{K}' > 1 \cap K''/K' > 1 \cap K''/K' > 0$ in the parametric plane $K/K' \sim K''K'$. This illustrates clearly that lack of uniqueness of the solution is an intrinsic character of the 3D Ising lattice. Even if the term of the additional rotation $K'K''/\mathrm{K}$ was not included in our calculation, lack of unification of the solution would still be true. At the very beginning of our procedure, the conditions of $K \geq K'$ and $K \geq K''$ (i.e. $0 \leq K'/K \leq 1 \cap 0 \leq K''/K \leq 1$ in the parametric plane $K'/K \sim K''/K$) are fixed to be held, which is very important because if one loosens them, the solution would be not unique but physically meaningless. Taken as a reasonable explanation, we must assume that K''' is not larger than either K' or K'', considering that the additional rotation is performed in a

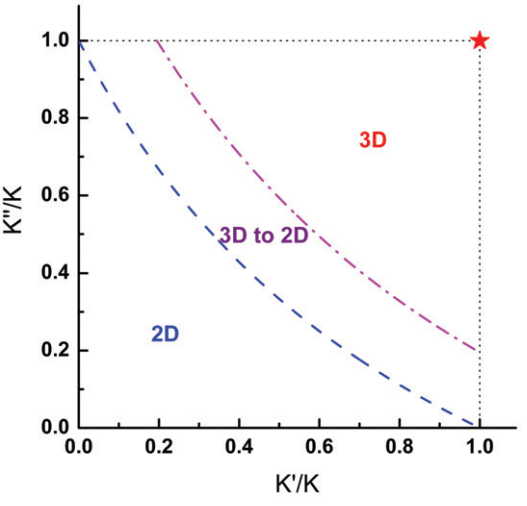

Figure 4. Phase diagram in the parametric plane $(K'/K) \sim (K''/K)$ of the simple orthorhombic Ising lattices. The golden solution for the simple cubic Ising lattice is located by the star (1, 1). The dashed curve of $(K'/K) + (K''/K) + (K'K''/K^2) = 1$ corresponds to the points at the critical temperature of the silver solution. The area between the dashed and the dash/dot curve of $(K'/K) + (K''/K) + (K'K''/K^2) \approx 1.39$ is for the 3D to 2D crossover phenomenon. All the points below the dashed curve have the 2D critical exponent, while all the points above the dash/dot curve behave as a real 3D system.

curled-up dimension. At the beginning of the diagonalization procedure, we have to set up only the largest among K, K' and K'' as the standard axis for the definition of K^*, because the solution obtained in this way is the lowest. In this way, the points in the area of $0 \leq K'/K \leq 1 \cap 0 \leq K''/K \leq 1$ in the parametric plane $K'/K \sim K''/K$ (see figure 4) can fully represent all the possible parameters for the 3D simple orthorhombic Ising lattices. It is obvious that the simple cubic lattice with the highest symmetry has the highest critical temperature, at the golden ratio. In other words, if the 3D lattice is asymmetric with difference between K, K' and K'', the critical temperature will be lower than the golden ratio, as the largest among K, K' and K'' is always set as the standard axis. This means that any solution higher than the golden ratio is forbidden for the 3D simple orthorhombic Ising lattices due to lack of physical significance. This is reasonable since the simple cubic lattice with the highest symmetry is the system with the most obvious characters of the three dimensions and the 3D lattice with less symmetry is more or less closer to the 1D or 2D system. As shown in figure 1, if one fixes K and sets $K' = K''$, the critical point decreases with decreasing K' and K'' to disappear as no ordering occurs in the 1D system. However, on the other hand, if one fixed $K' = \mathrm{K}$, the critical point of the simple tetragonal lattices would decrease from the golden ratio of the simple cubic lattice to the silver ratio of the square lattice with decreasing K''.

One of the most remarkable aspects of the golden ratio is the proportion inherent in it. The golden ratio always surprisingly appears at the crosspoint of the simple and complex, classic geometry and irregular geometry [344]. Most people are familiar with the golden ratio since it is one of the most ubiquitous irrational numbers known to man. Actually, it is the most irrational number ever and it is related to the beauty

of nature, such as the golden section, the golden angle, the golden ellipse, the golden triangle, the golden rectangle, the pentagram, the golden spiral, etc. The famous Fibonacci sequence and the golden ratio are intertwined. The golden ratio occurs in the structure of both plants and animals –the best known example being the nautilus shell. The system trends to equilibrium at a state with minimizing the cost of free energy. It is thought that a system with a golden ratio may stand for such a state [344]. The various golden ratios that appear in real life may originate from one essential source: competition between interaction energy and thermal activity balances at the critical temperature of the golden ratio for the most symmetric 3D Ising lattice. Natural symmetry is the most important for physical properties of a system. It has been noticed that the golden ratio solution appears for the Curie temperature of the 2D rectangular Ising lattice with $K' = 3K$, which has less symmetry than the square Ising lattice with the silver ratio solution and, therefore, the golden ratio solution can be excluded from the 2D system, as discussed above. This beautiful solution of the golden ratio corresponds only to the critical temperature of the most symmetric 3D simple cubic Ising system. The more symmetric, the more beautiful. This is the nature of our symmetric three dimensions, the nature of the world we are living.

9. Conclusions

A putative exact solution of the 3D Ising model on simple orthorhombic lattices has been derived explicitly. The partition function of the 3D simple orthorhombic Ising model has been evaluated by spinor analysis, by introducing the two conjectures employing an additional rotation in the fourth curled-up dimension and weight factors on the eigenvectors. The partition function of the 3D simple orthorhombic Ising model have been dealt with within a $(3+1)$-dimensional framework with different weight factors on the eigenvectors. The relation of $KK^* = KK' + KK'' + K'K''$ or $\sinh 2K \cdot \sinh 2(K' + K'' + (K'K''/K)) = 1$ would be valid for the critical temperature of the simple orthorhombic Ising model, if the two conjectures were true. For the simple cubic Ising lattice, the putative critical point is located exactly at the golden ratio $x_c = e^{-2K_c} = (\sqrt{5} - 1)/2$, as derived from $K^* = 3K$ or $\sinh 2K \cdot \sinh 6K = 1$. The specific heat of the simple orthorhombic Ising lattices shows a logarithmic singularity at the critical point of the phase transition, however, also based on the validity of the conjectures. The putative exact value for the critical temperature is lower than all approximation values, as it should be. As we always set the largest among K, K' and K'' as the standard axis for the definition of K^*, any solution higher than the golden (or silver) ratio would be forbidden for the 3D (or 2D) Ising lattices. The golden (or silver) ratio is the largest solution for the critical temperature of the 3D (or 2D) Ising system, corresponding to the most symmetric, simple cubic (or square) lattice. Natural symmetry is most important for the physical properties of the system. The most symmetric, the most beautiful. The spontaneous magnetization of the 3D simple orthorhombic Ising ferromagnet has been derived by the perturbation procedure, following introduction of the conjectures. The spin correlation functions have been discussed in terms of the Pfaffians, by defining the effective

skew-symmetric matrix A_{eff}. The true range κ_x of the correlation and the susceptibility of the 3D simple orthorhombic Ising system have been determined by procedures similar to those used for the two-dimensional Ising system. The putative critical exponents for the 3D simple orthorhombic Ising lattices have been derived explicitly to be $\alpha = 0$, $\beta = 3/8$, $\gamma = 5/4$, $\delta = 13/3$, $\eta = 1/8$ and $\nu = 2/3$, showing universality behaviour and satisfying the scaling laws. These exact values for the critical exponents of the 3D Ising lattice are located between those for the 2D and (mean field) 4D Ising lattice. These critical exponents are close to approximation values and experimental data. The exact solutions have been judged by several criteria. The reasons for the deviations in the approximation results and experimental data from the putative exact solutions are interpreted. The simple cubic lattice with the highest symmetry is the most obvious characteristic of the three dimensions and the 3D lattice with less symmetry is closer to the 1D or 2D lattice. The 3D-to-2D crossover phenomenon differs from the 2D-to-1D crossover phenomenon and there is a gradual crossover of the exponents from 3D to 2D values. Special attention has also been paid to the extra energy caused by the introduction of the fourth curled-up dimension; the chaotic states at/near infinite temperature as revealed by the introduction of weight factors on the eigenvectors. The physics beyond the conjectures and the existence of the extra dimension are discussed, with referring to the quantum mechanism. The present work not only has significance in statistic physics and condensed matter physics but also bridges the gap between the fields of quantum field theory, cosmology theory, high-energy particle physics, graph theory and computer sciences. Our results, which have aesthetic appeal, reveal the nature of nature: simple, symmetric and beautiful.

Acknowledgements

The author acknowledges the continuous support of the National Natural Science Foundation of China since 1990 (under grant numbers 59001452, 59371015, 19474052, 59421001, 59725103, 59871054, 59831010, 50171070, 10274087, 10674139, 50331030, and 50332020) and the support of the Sciences and Technology Commission of Shenyang since 1994. He is grateful to Fei Yang for understanding, encouragement, support and discussion.

Appendix A

The effects of the rotations ω_{2t_y} and ω_{2t_z} with their weight factors w_y and w_z are discussed as follows. It is not surprising that things can come out of nothing in nature. The addition of the fourth curled-up dimension expands the 3D physical world to a higher-dimensional world so that it is necessary to introduce the weights w_y and w_z to effectively equalize it with the original system. The weights defined in Conjecture 2 vary in range $[-1, 1]$. They can be equal to $0, \pm 1$, and any values between 0 and ± 1. They could interchange their roles (and values) at any time, from the point of view of symmetry. In this way, the system studied is always

$(3+1)$-dimensional, even where any of the weights occasionally equals zero. A 'zero' weight factor w_y or w_z still acting with other dimensions is no more mystical than Euler's equation $e^{i\pi}+1=0$: an imaginary number interacting with real numbers to produce nothing.

The partition function of the 3D simple cubic Ising lattice could be expressed as (74):

$$N^{-1}\ln Z = \ln 2 + \frac{1}{2(2\pi)^4}\int_{-\pi}^{\pi}\int_{-\pi}^{\pi}\int_{-\pi}^{\pi}\int_{-\pi}^{\pi}\ln[\cosh 2K\cosh 6K - \sinh 2K\cos\omega' - \sinh 6K\left(w_x\cos\omega_x + w_y\cos\omega_y + w_z\cos\omega_z\right)] \times d\omega' d\omega_x d\omega_y d\omega_z \tag{A1}$$

where $w_x=1$ and

$$w_y = w_z = \pm\sqrt{\sum_{i=0}^{\infty} b_i\kappa_i^{2i}}, \tag{A2}$$

with $b_0=7/18$, $b_1=-4025/216$, $b_2=62125/432$, $b_3=-315237349/31104$, $b_4=-196961527937/186624$, $b_5=-81949884191959/746496$, $b_6=-1598437187231\,21207/13436928$, $b_7=-8878670776134424776 77/644972544$, $b_8=-216261883802\,726526301599/1289945088$, $b_9=-27308340932849690181428182 53/139314069504$, $b_{10}=-93129271468013060891310550 9313/278628139008$, ...

Ansatz 1: All the coefficients b_i for the terms embodied in w_y and w_z are negative for $i\geq 1$.

There is no mathematical problem in the introduction of the weights w_x, w_y and w_z, which is used to embody some information of the high-temperature terms. Clearly, the close form of the free energy has been found for the 3D Ising model from $T=0$ to any finite temperatures and also at infinite temperature ($\kappa=0$), with the exception of near-infinite temperature ($\kappa\to 0$). Actually, in principle, we could account for all of the infinite terms for near-infinite temperature based on the law of high-temperature expansion (though extremely difficulty). The coefficients b_i can be determined exactly for higher orders as long as the corresponding terms of the high-temperature expansion are determined. One would estimate how the higher-order terms appear from these existing terms. All the coefficients for the terms up to b_{10}, except for b_0, embodied in w_y and w_z are negative. Ansatz 1 is introduced to extend this tendency to all the terms inside the square root. The ratio of b_{i+1}/b_i varies in the range 70 – 171 for $i\geq 2$. One could expect that all the coefficients b_i for $i>10$ are negative, with the ratios of b_{i+1}/b_i in the order of hundreds. Actually, these facts can be proved by evaluating the higher-order coefficients b_i approximately with high precision, even without having information on higher-order terms of the high temperature expansion. This is because, in the procedure of determining each coefficient b_i, there is always a term which does not relate to any lower-order coefficients, but appears to compensate most of the contribution of the high-order terms of the high-temperature expansion. Furthermore, the terms that relate directly to lower-order coefficients are dominant for the higher-order coefficient b_i. Thus, near infinite temperature ($\kappa\to 0$), the effects of the high-order terms (higher than 22nd) are extremely small, which can be neglected in a certain sense. Therefore,

these infinite terms of the high-temperature expansion can be embodied into the close square form of the weight factors.

One could estimate how the weights appear from these existed terms, supposing Ansatz 1 *is* true. Note that the weights $w_y = w_z = \pm\sqrt{7/18}$ at infinite temperature as $\kappa = 0$. The weights w_y and w_z approach zero identically when the temperature of the system becomes infinitesimal below infinite (i.e. $\kappa \to \neq 0$ and infinitesimal) because, if Ansatz 1 were true, the truncated sums in (A.2) would become negative, making the square root to be imagined and physically not meaningful. This indicates that the weights w_y and w_z are always equal to zero at any finite temperatures.

By the following procedure, we will show that at/near infinite temperature, the exact solution for the partition function of the 3D simple cubic Ising lattice fits exactly to the high-temperature series expansion [80, 93, 107, 111]. Equation (A1) can be expressed as:

$$\begin{aligned}\ln\lambda - \ln 2(\cosh 2K\cosh 6K)^{1/2} &= \frac{1}{2(2\pi)^4}\int_0^{\pi}\int_0^{\pi}\int_0^{\pi}\int_0^{\pi} \ln[1 - 2\kappa_{3D}\cos\omega' - 2\kappa'_{3D}(w_x\cos\omega_x + w_y\cos\omega_y \\ &\quad + w_z\cos\omega_z)]d\omega' d\omega_x d\omega_y d\omega_z \end{aligned} \tag{A3}$$

Here $\lambda = Z^{1/N}$,

$$\begin{aligned}\kappa_{3D} &= \frac{\tanh 2K}{2\cosh 6K} = \frac{\kappa(1 - 3\kappa^2 + 3\kappa^4 - \kappa^6)}{1 + 16\kappa^2 + 30\kappa^4 + 16\kappa^6 + \kappa^8} \\ &= \kappa - 19\kappa^3 + 277\kappa^5 - 3879\kappa^7 + 54057\kappa^9 - 752955\kappa^{11} + 10487357\kappa^{13} \\ &\quad - 146070095\kappa^{15} + 2034494033\kappa^{17} - 28336846435\kappa^{19} + 394681356133\kappa^{21} + \cdots \end{aligned} \tag{A4}$$

and

$$\begin{aligned}\kappa'_{3D} &= \frac{\tanh 6K}{2\cosh 2K} = \frac{\kappa(3 + 7\kappa^2 - 7\kappa^4 - 3\kappa^6)}{1 + 16\kappa^2 + 30\kappa^4 + 16\kappa^6 + \kappa^8} \\ &= 3\kappa - 41\kappa^3 + 559\kappa^5 - 7765\kappa^7 + 108123\kappa^9 - 1505921\kappa^{11} + 20974727\kappa^{13} \\ &\quad - 292140205\kappa^{15} + 4068988083\kappa^{17} - 56673692889\kappa^{19} + 789362712287\kappa^{21} \ldots \end{aligned} \tag{A5}$$

with $\kappa = \tanh K$. Then, one can calculate immediately the high-order terms ${\kappa_{3D}}^2$, ${\kappa_{3D}}^4$, ${\kappa_{3D}}^6$, ${k_{3D}}^8, \ldots$; ${\kappa'_{3D}}^2$, ${\kappa'_{3D}}^4$, ${\kappa'_{3D}}^6$, ${\kappa'_{3D}}^8, \ldots$; ${\kappa_{3D}}^2{\kappa'_{3D}}^2$, ${\kappa_{3D}}^4{\kappa'_{3D}}^2$, ${\kappa_{3D}}^6{\kappa'_{3D}}^2, \ldots$; ${\kappa_{3D}}^2{\kappa'_{3D}}^4$, ${\kappa_{3D}}^4{\kappa'_{3D}}^4$, ${\kappa_{3D}}^6{\kappa'_{3D}}^4, \ldots$; ... The left side of the equation above for the partition function is re-written as:

$$\begin{aligned}&\ln\lambda - \ln\left[2\cosh^3 K\left(\frac{1 + 16\kappa^2 + 30\kappa^4 + 16\kappa^6 + \kappa^8}{1 - \kappa^2}\right)^{1/2}\right] \\ &= \ln\lambda - \ln\left[2\cosh^3 K\left(1 + \frac{17}{2}\kappa^2 - \frac{101}{8}\kappa^4 + \frac{2221}{16}\kappa^6 - \frac{157133}{128}\kappa^8\right.\right. \\ &\quad + \frac{3128095}{256}\kappa^{10} - \frac{132058577}{1024}\kappa^{12} + \frac{2909991333}{2048}\kappa^{14} \\ &\quad - \frac{529380209469}{32768}\kappa^{16} + \frac{12331364457995}{65536}\kappa^{18} - \frac{585509987761867}{262144}\kappa^{20} \\ &\quad \left.\left. + \frac{14115585949315307}{524288}\kappa^{22} + \cdots\right)\right] \end{aligned} \tag{A6}$$

Expanding the logarithmic function on the right-hand side of the expression for the partition function by $\ln(1-x) = -\sum_{n=1}^{\infty} x^n/n$ yields:

$$-\sum_{n=1}^{\infty}\frac{1}{n}\cdot\sum_{p+q+r+s=n}\frac{n!}{p!q!r!s!}\cdot 2^n\kappa_{3D}^{p}\kappa_{3D}^{\prime(q+r+s)}\cdot f^{(r+s)} \cdot\cos^p\omega'\cos^q\omega_x\cos^r\omega_y\cos^s\omega_z \tag{A7}$$

and then integrating each term results in:

$$\begin{aligned}
&-\left\{\frac{1}{2}\left(\kappa_{3D}^2+\kappa_{3D}^{\prime 2}\right)+f^2\kappa_{3D}^{\prime 2}\right\}\\
&-\left\{\left[\frac{3}{4}\left(\kappa_{3D}^4+\kappa_{3D}^{\prime 4}\right)+3\kappa_{3D}^2\kappa_{3D}^{\prime 2}\right]+6f^2\left(\kappa_{3D}^2\kappa_{3D}^{\prime 2}+\kappa_{3D}^{\prime 4}\right)+4.5f^4\kappa_{3D}^{\prime 4}\right\}\\
&-\left\{\left[\frac{5}{3}\left(\kappa_{3D}^6+\kappa_{3D}^{\prime 6}\right)+15\left(\kappa_{3D}^4\kappa_{3D}^{\prime 2}+\kappa_{3D}^2\kappa_{3D}^{\prime 4}\right)\right]\right.\\
&\left.+f^2\left[30\left(\kappa_{3D}^4\kappa_{3D}^{\prime 2}+\kappa_{3D}^{\prime 6}\right)+120\kappa_{3D}^2\kappa_{3D}^{\prime 4}\right]+90f^4\left(\kappa_{3D}^2\kappa_{3D}^{\prime 4}+\kappa_{3D}^{\prime 6}\right)+\frac{100}{3}f^6\kappa_{3D}^{\prime 6}\right\}\\
&-\left\{\left[\frac{35}{8}\left(\kappa_{3D}^8+\kappa_{3D}^{\prime 8}\right)+70\left(\kappa_{3D}^6\kappa_{3D}^{\prime 2}+\kappa_{3D}^2\kappa_{3D}^{\prime 6}\right)+\frac{315}{2}\kappa_{3D}^4\kappa_{3D}^{\prime 4}\right]\right.\\
&+f^2\left[140\left(\kappa_{3D}^6\kappa_{3D}^{\prime 2}+\kappa_{3D}^{\prime 8}\right))+1260\left(\kappa_{3D}^4\kappa_{3D}^{\prime 4}+\kappa_{3D}^2\kappa_{3D}^{\prime 6}\right)\right]\\
&+f^4\left[945\left(\kappa_{3D}^4\kappa_{3D}^{\prime 4}+\kappa_{3D}^{\prime 8}\right)+3780\kappa_{3D}^2\kappa_{3D}^{\prime 6}\right]+1400f^6\left(\kappa_{3D}^2\kappa_{3D}^{\prime 6}+\kappa_{3D}^{\prime 8}\right)+306.25f^8\kappa_{3D}^{\prime 8}\Big\}\\
&-\left\{\left[\frac{63}{5}\left(\kappa_{3D}^{10}+\kappa_{3D}^{\prime 10}\right)+315\left(\kappa_{3D}^8\kappa_{3D}^{\prime 2}+\kappa_{3D}^2\kappa_{3D}^{\prime 8}\right)+1260\left(\kappa_{3D}^6\kappa_{3D}^{\prime 4}+\kappa_{3D}^4\kappa_{3D}^{\prime 6}\right)\right]\right.\\
&+f^2\left[630\left(\kappa_{3D}^8\kappa_{3D}^{\prime 2}+\kappa_{3D}^{\prime 10}\right))+10080\left(\kappa_{3D}^6\kappa_{3D}^{\prime 4}+\kappa_{3D}^2\kappa_{3D}^{\prime 8}\right)+22680\kappa_{3D}^4\kappa_{3D}^{\prime 6}\right]\\
&+f^4\left[7560\left(\kappa_{3D}^6\kappa_{3D}^{\prime 4}+\kappa_{3D}^{\prime 10}\right)+68040\left(\kappa_{3D}^4\kappa_{3D}^{\prime 6}+\kappa_{3D}^2\kappa_{3D}^{\prime 8}\right)\right]\\
&+f^6\left[25200\left(\kappa_{3D}^4\kappa_{3D}^{\prime 6}+\kappa_{3D}^{\prime 10}\right)+100800\kappa_{3D}^2\kappa_{3D}^{\prime 8}\right]\\
&\left.+22050f^8\left(\kappa_{3D}^2\kappa_{3D}^{\prime 8}+\kappa_{3D}^{\prime 10}\right)+3175.2f^{10}\kappa_{3D}^{\prime 10}\right\}\\
&-\left\{\left[\frac{77}{2}\left(\kappa_{3D}^{12}+\kappa_{3D}^{\prime 12}\right)+1386\left(\kappa_{3D}^{10}\kappa_{3D}^{\prime 2}+\kappa_{3D}^2\kappa_{3D}^{\prime 10}\right)\right.\right.\\
&\left.+8662.5\left(\kappa_{3D}^8\kappa_{3D}^{\prime 4}+\kappa_{3D}^4\kappa_{3D}^{\prime 8}\right)+15400\kappa_{3D}^6\kappa_{3D}^{\prime 6}\right]\\
&+f^2\left[2772\left(\kappa_{3D}^{10}\kappa_{3D}^{\prime 2}+\kappa_{3D}^{\prime 12}\right)+69300\left(\kappa_{3D}^8\kappa_{3D}^{\prime 4}+\kappa_{3D}^2\kappa_{3D}^{\prime 10}\right)\right.\\
&\left.+277200\left(\kappa_{3D}^6\kappa_{3D}^{\prime 6}+\kappa_{3D}^4\kappa_{3D}^{\prime 8}\right)\right]\\
&+f^4\left[51975\left(\kappa_{3D}^8\kappa_{3D}^{\prime 4}+\kappa_{3D}^{\prime 12}\right)+831600\left(\kappa_{3D}^6\kappa_{3D}^{\prime 6}+\kappa_{3D}^2\kappa_{3D}^{\prime 10}\right)+1871100\kappa_{3D}^4\kappa_{3D}^{\prime 8}\right]\\
&+f^6\left[308000\left(\kappa_{3D}^6\kappa_{3D}^{\prime 6}+\kappa_{3D}^{\prime 12}\right)+2772000\left(\kappa_{3D}^4\kappa_{3D}^{\prime 8}+\kappa_{3D}^2\kappa_{3D}^{\prime 10}\right)\right]\\
&+f^8\left[606375\left(\kappa_{3D}^4\kappa_{3D}^{\prime 8}+\kappa_{3D}^{\prime 12}\right)+2425500\kappa_{3D}^2\kappa_{3D}^{\prime 10}\right]
\end{aligned}$$

$$
\begin{aligned}
&+ 349272f^{10}\left(\kappa_{3D}^{2}\kappa_{3D}'^{10} + \kappa_{3D}'^{12}\right) + 35574f^{12}\kappa_{3D}'^{12}\Big\} \\
&- \Bigg\{\Bigg[\frac{858}{7}\left(\kappa_{3D}^{14} + \kappa_{3D}'^{14}\right) + 6006\left(\kappa_{3D}^{12}\kappa_{3D}'^{2} + \kappa_{3D}^{2}\kappa_{3D}'^{12}\right) \\
&+ 54054\left(\kappa_{3D}^{10}\kappa_{3D}'^{4} + \kappa_{3D}^{4}\kappa_{3D}'^{10}\right) + 150150\left(\kappa_{3D}^{8}\kappa_{3D}'^{6} + \kappa_{3D}^{6}\kappa_{3D}'^{8}\right)\Big] \\
&+ f^{2}\big[12012\left(\kappa_{3D}^{12}\kappa_{3D}'^{2} + \kappa_{3D}'^{14}\right) + 432432\left(\kappa_{3D}^{10}\kappa_{3D}'^{4} + \kappa_{3D}^{2}\kappa_{3D}'^{12}\right) \\
&+ 2702700\left(\kappa_{3D}^{8}\kappa_{3D}'^{6} + \kappa_{3D}^{4}\kappa_{3D}'^{10}\right) + 4804800\kappa_{3D}^{6}\kappa_{3D}'^{8}\big] \\
&+ f^{4}\big[324324\left(\kappa_{3D}^{10}\kappa_{3D}'^{4} + \kappa_{3D}'^{14}\right) + 8108100\left(\kappa_{3D}^{8}\kappa_{3D}'^{6} + \kappa_{3D}^{2}\kappa_{3D}'^{12}\right) \\
&+ 32432400\left(\kappa_{3D}^{6}\kappa_{3D}'^{8} + \kappa_{3D}^{4}\kappa_{3D}'^{10}\right)\big] \\
&+ f^{6}\big[3003000\left(\kappa_{3D}^{8}\kappa_{3D}'^{6} + \kappa_{3D}'^{14}\right) + 48048000\left(\kappa_{3D}^{6}\kappa_{3D}'^{8} + \kappa_{3D}^{2}\kappa_{3D}'^{12}\right) \\
&+ 108108000\kappa_{3D}^{4}\kappa_{3D}'^{10}\big] \\
&+ f^{8}\big[10510500\left(\kappa_{3D}^{6}\kappa_{3D}'^{8} + \kappa_{3D}'^{14}\right) + 94594500\left(\kappa_{3D}^{4}\kappa_{3D}'^{10} + \kappa_{3D}^{2}\kappa_{3D}'^{12}\right)\big] \\
&+ f^{10}\big[13621608\left(\kappa_{3D}^{4}\kappa_{3D}'^{10} + \kappa_{3D}'^{14}\right) + 54486432\kappa_{3D}^{2}\kappa_{3D}'^{12}\big] \\
&+ 5549544f^{12}\left(\kappa_{3D}^{2}\kappa_{3D}'^{12} + \kappa_{3D}'^{14}\right) + 420665\frac{1}{7}f^{14}\kappa_{3D}'^{14}\Bigg\} \\
&- \Bigg\{\Bigg[\frac{6435}{16}\left(\kappa_{3D}^{16} + \kappa_{3D}'^{16}\right) + 25740\left(\kappa_{3D}^{14}\kappa_{3D}'^{2} + \kappa_{3D}^{2}\kappa_{3D}'^{14}\right) \\
&\qquad + 315315\left(\kappa_{3D}^{12}\kappa_{3D}'^{4} + \kappa_{3D}^{4}\kappa_{3D}'^{12}\right) + 1261260\left(\kappa_{3D}^{10}\kappa_{3D}'^{6} + \kappa_{3D}^{6}\kappa_{3D}'^{10}\right) \\
&\qquad + \frac{7882875}{4}\kappa_{3D}^{8}\kappa_{3D}'^{8}\Bigg] \\
&+ f^{2}\big[51480\left(\kappa_{3D}^{14}\kappa_{3D}'^{2} + \kappa_{3D}'^{16}\right) + 2522520\left(\kappa_{3D}^{12}\kappa_{3D}'^{4} + \kappa_{3D}^{2}\kappa_{3D}'^{14}\right) \\
&+ 22702680\left(\kappa_{3D}^{10}\kappa_{3D}'^{6} + \kappa_{3D}^{4}\kappa_{3D}'^{12}\right) + 63063000\left(\kappa_{3D}^{8}\kappa_{3D}'^{8} + \kappa_{3D}^{6}\kappa_{3D}'^{10}\right)\big] \\
&+ f^{4}\big[1891890\left(\kappa_{3D}^{12}\kappa_{3D}'^{4} + \kappa_{3D}'^{16}\right) + 68108040\left(\kappa_{3D}^{10}\kappa_{3D}'^{6} + \kappa_{3D}^{2}\kappa_{3D}'^{14}\right) \\
&+ 425675250\left(\kappa_{3D}^{8}\kappa_{3D}'^{8} + \kappa_{3D}^{4}\kappa_{3D}'^{12}\right) + 756756000\kappa_{3D}^{6}\kappa_{3D}'^{10}\big] \\
&+ f^{6}\big[25225200\left(\kappa_{3D}^{10}\kappa_{3D}'^{6} + \kappa_{3D}'^{16}\right) + 630630000\left(\kappa_{3D}^{8}\kappa_{3D}'^{8} + \kappa_{3D}^{2}\kappa_{3D}'^{14}\right) \\
&+ 2522520000\left(\kappa_{3D}^{6}\kappa_{3D}'^{10} + \kappa_{3D}^{4}\kappa_{3D}'^{12}\right)\big] \\
&+ f^{8}\big[137950312.5\left(\kappa_{3D}^{8}\kappa_{3D}'^{8} + \kappa_{3D}'^{16}\right) + 2207205000\left(\kappa_{3D}^{6}\kappa_{3D}'^{10} + \kappa_{3D}^{2}\kappa_{3D}'^{14}\right) \\
&+ 4966211250\kappa_{3D}^{4}\kappa_{3D}'^{12}\big] \\
&+ f^{10}\big[317837520\left(\kappa_{3D}^{6}\kappa_{3D}'^{10} + \kappa_{3D}'^{16}\right) + 2860537680\left(\kappa_{3D}^{4}\kappa_{3D}'^{12} + \kappa_{3D}^{2}\kappa_{3D}'^{14}\right)\big] \\
&+ f^{12}\big[291351060\left(\kappa_{3D}^{4}\kappa_{3D}'^{12} + \kappa_{3D}'^{16}\right) + 1165404240\kappa_{3D}^{2}\kappa_{3D}'^{14}\big] \\
&+ 88339680f^{14}\left(\kappa_{3D}^{2}\kappa_{3D}'^{14} + \kappa_{3D}'^{16}\right) + 5176153.125f^{16}\kappa_{3D}'^{16}\Big\}
\end{aligned}
$$

$$
\begin{aligned}
&- \left\{\left[\frac{12155}{9}\left(\kappa_{3D}^{18}+\kappa_{3D}^{\prime 18}\right)+109395\left(\kappa_{3D}^{16}\kappa_{3D}^{\prime 2}+\kappa_{3D}^{2}\kappa_{3D}^{\prime 16}\right)\right.\right.\\
&+1750320\left(\kappa_{3D}^{14}\kappa_{3D}^{\prime 4}+\kappa_{3D}^{4}\kappa_{3D}^{\prime 14}\right)\\
&\left.+9529520\left(\kappa_{3D}^{12}\kappa_{3D}^{\prime 6}+\kappa_{3D}^{6}\kappa_{3D}^{\prime 12}\right)+21441420\left(\kappa_{3D}^{10}\kappa_{3D}^{\prime 8}+\kappa_{3D}^{8}\kappa_{3D}^{\prime 10}\right)\right]\\
&+f^{2}\left[218790\left(\kappa_{3D}^{16}\kappa_{3D}^{\prime 2}+\kappa_{3D}^{\prime 18}\right)+14002560\left(\kappa_{3D}^{14}\kappa_{3D}^{\prime 4}+\kappa_{3D}^{2}\kappa_{3D}^{\prime 16}\right)\right.\\
&+171531360\left(\kappa_{3D}^{12}\kappa_{3D}^{\prime 6}+\kappa_{3D}^{4}\kappa_{3D}^{\prime 14}\right)+686125440\left(\kappa_{3D}^{10}\kappa_{3D}^{\prime 8}+\kappa_{3D}^{6}\kappa_{3D}^{\prime 12}\right)\\
&\left.+1072071000\kappa_{3D}^{8}\kappa_{3D}^{\prime 10}\right]\\
&+f^{4}\left[10501920\left(\kappa_{3D}^{14}\kappa_{3D}^{\prime 4}+\kappa_{3D}^{\prime 18}\right)+514594080\left(\kappa_{3D}^{12}\kappa_{3D}^{\prime 6}+\kappa_{3D}^{2}\kappa_{3D}^{\prime 16}\right)\right.\\
&\left.+4631346720\left(\kappa_{3D}^{10}\kappa_{3D}^{\prime 8}+\kappa_{3D}^{4}\kappa_{3D}^{\prime 14}\right)+12864852000\left(\kappa_{3D}^{8}\kappa_{3D}^{\prime 10}+\kappa_{3D}^{6}\kappa_{3D}^{\prime 12}\right)\right]\\
&+f^{6}\left[190590400\left(\kappa_{3D}^{12}\kappa_{3D}^{\prime 6}+\kappa_{3D}^{\prime 18}\right)+6861254400\left(\kappa_{3D}^{10}\kappa_{3D}^{\prime 8}+\kappa_{3D}^{2}\kappa_{3D}^{\prime 16}\right)\right.\\
&\left.+42882840000\left(\kappa_{3D}^{8}\kappa_{3D}^{\prime 10}+\kappa_{3D}^{4}\kappa_{3D}^{\prime 14}\right)+76236160000\kappa_{3D}^{6}\kappa_{3D}^{\prime 12}\right]\\
&+f^{8}\left[1500899400\left(\kappa_{3D}^{10}\kappa_{3D}^{\prime 8}+\kappa_{3D}^{\prime 18}\right)+37522485000\left(\kappa_{3D}^{8}\kappa_{3D}^{\prime 10}+\kappa_{3D}^{2}\kappa_{3D}^{\prime 16}\right)\right.\\
&\left.+150089940000\left(\kappa_{3D}^{6}\kappa_{3D}^{\prime 12}+\kappa_{3D}^{4}\kappa_{3D}^{\prime 14}\right)\right]\\
&+f^{10}\left[5403237840\left(\kappa_{3D}^{8}\kappa_{3D}^{\prime 10}+\kappa_{3D}^{\prime 18}\right)+86451805440\left(\kappa_{3D}^{6}\kappa_{3D}^{\prime 12}+\kappa_{3D}^{2}\kappa_{3D}^{\prime 16}\right)\right.\\
&\left.+194516562240\kappa_{3D}^{4}\kappa_{3D}^{\prime 14}\right]\\
&+f^{12}\left[8805276480\left(\kappa_{3D}^{6}\kappa_{3D}^{\prime 12}+\kappa_{3D}^{\prime 18}\right)+79247488320\left(\kappa_{3D}^{4}\kappa_{3D}^{\prime 14}+\kappa_{3D}^{2}\kappa_{3D}^{\prime 16}\right)\right]\\
&+f^{14}\left[6007098240\left(\kappa_{3D}^{4}\kappa_{3D}^{\prime 14}+\kappa_{3D}^{\prime 18}\right)+24028392960\kappa_{3D}^{2}\kappa_{3D}^{\prime 16}\right]\\
&\left.+1407913650f^{16}\left(\kappa_{3D}^{2}\kappa_{3D}^{\prime 16}+\kappa_{3D}^{\prime 18}\right)+65664011\frac{1}{9}f^{18}\kappa_{3D}^{\prime 18}\right\}\\
&-\left\{\left[4618.9\left(\kappa_{3D}^{20}+\kappa_{3D}^{\prime 20}\right)+461890\left(\kappa_{3D}^{18}\kappa_{3D}^{\prime 2}+\kappa_{3D}^{2}\kappa_{3D}^{\prime 18}\right)\right.\right.\\
&+\frac{18706545}{2}\left(\kappa_{3D}^{16}\kappa_{3D}^{\prime 4}+\kappa_{3D}^{4}\kappa_{3D}^{\prime 16}\right)+66512160\left(\kappa_{3D}^{14}\kappa_{3D}^{\prime 6}+\kappa_{3D}^{6}\kappa_{3D}^{\prime 14}\right)\\
&\left.+203693490\left(\kappa_{3D}^{12}\kappa_{3D}^{\prime 8}+\kappa_{3D}^{8}\kappa_{3D}^{\prime 12}\right)+\frac{1466593128}{5}\kappa_{3D}^{10}\kappa_{3D}^{\prime 10}\right]\\
&+f^{2}\left[923780\left(\kappa_{3D}^{18}\kappa_{3D}^{\prime 2}+\kappa_{3D}^{\prime 20}\right)+74826180\left(\kappa_{3D}^{16}\kappa_{3D}^{\prime 4}+\kappa_{3D}^{2}\kappa_{3D}^{\prime 18}\right)\right.\\
&+1197218880\left(\kappa_{3D}^{14}\kappa_{3D}^{\prime 6}+\kappa_{3D}^{4}\kappa_{3D}^{\prime 16}\right)+6518191680\left(\kappa_{3D}^{12}\kappa_{3D}^{\prime 8}+\kappa_{3D}^{6}\kappa_{3D}^{\prime 14}\right)\\
&\left.+14665931280\left(\kappa_{3D}^{10}\kappa_{3D}^{\prime 10}+\kappa_{3D}^{8}\kappa_{3D}^{\prime 12}\right)\right]\\
&+f^{4}\left[56119635\left(\kappa_{3D}^{16}\kappa_{3D}^{\prime 4}+\kappa_{3D}^{\prime 20}\right)+3591656640\left(\kappa_{3D}^{14}\kappa_{3D}^{\prime 6}+\kappa_{3D}^{2}\kappa_{3D}^{\prime 18}\right)\right.\\
&+43997793840\left(\kappa_{3D}^{12}\kappa_{3D}^{\prime 8}+\kappa_{3D}^{4}\kappa_{3D}^{\prime 16}\right)+175991175360\left(\kappa_{3D}^{10}\kappa_{3D}^{\prime 10}+\kappa_{3D}^{6}\kappa_{3D}^{\prime 14}\right)\\
&\left.+274986211500\kappa_{3D}^{8}\kappa_{3D}^{\prime 12}\right]\\
&+f^{6}\left[1330243200\left(\kappa_{3D}^{14}\kappa_{3D}^{\prime 6}+\kappa_{3D}^{\prime 20}\right)+65181916800\left(\kappa_{3D}^{12}\kappa_{3D}^{\prime 8}+\kappa_{3D}^{2}\kappa_{3D}^{\prime 18}\right)\right.
\end{aligned}
$$

$$
\begin{aligned}
&+ 586637251200\left(\kappa_{3D}^{10}\kappa_{3D}'^{10} + \kappa_{3D}^{4}\kappa_{3D}'^{16}\right) + 1629547920000\left(\kappa_{3D}^{8}\kappa_{3D}'^{12} + \kappa_{3D}^{6}\kappa_{3D}'^{14}\right)\Big] \\
&+ f^{8}\Big[14258544300\left(\kappa_{3D}^{12}\kappa_{3D}'^{8} + \kappa_{3D}'^{20}\right) + 513307594800\left(\kappa_{3D}^{10}\kappa_{3D}'^{10} + \kappa_{3D}^{2}\kappa_{3D}'^{18}\right) \\
&+ 3208172467500\left(\kappa_{3D}^{8}\kappa_{3D}'^{12} + \kappa_{3D}^{4}\kappa_{3D}'^{16}\right) + 5703417720000\kappa_{3D}^{6}\kappa_{3D}'^{14}\Big] \\
&+ f^{10}\Big[73916293651.2\left(\kappa_{3D}^{10}\kappa_{3D}'^{10} + \kappa_{3D}'^{20}\right) + 1847907341280\left(\kappa_{3D}^{8}\kappa_{3D}'^{12} + \kappa_{3D}^{2}\kappa_{3D}'^{18}\right) \\
&+ 7391629365120\left(\kappa_{3D}^{6}\kappa_{3D}'^{14} + \kappa_{3D}^{4}\kappa_{3D}'^{16}\right)\Big] \\
&+ \mathrm{f}^{12}\Big[188212784760\left(\kappa_{3D}^{8}\kappa_{3D}'^{12} + \kappa_{3D}'^{20}\right) + 3011404556160\left(\kappa_{3D}^{6}\kappa_{3D}'^{14} + \kappa_{3D}^{2}\kappa_{3D}'^{18}\right) \\
&+ 6775660251360\kappa_{3D}^{4}\kappa_{3D}'^{16}\Big] \\
&+ f^{14}\Big[228269733120\left(\kappa_{3D}^{6}\kappa_{3D}'^{14} + \kappa_{3D}'^{20}\right) + 2054427598080\left(\kappa_{3D}^{4}\kappa_{3D}'^{16} + \kappa_{3D}^{2}\kappa_{3D}'^{18}\right)\Big] \\
&+ f^{16}\Big[120376617075\left(\kappa_{3D}^{4}\kappa_{3D}'^{16} + \kappa_{3D}'^{20}\right) + 481506468300\kappa_{3D}^{2}\kappa_{3D}'^{18}\Big] \\
&+ 22457091800f^{18}\left(\kappa_{3D}^{2}\kappa_{3D}'^{18} + \kappa_{3D}'^{20}\right)\Big) + 853369488.4f^{20}\kappa_{3D}'^{20}\Big\} \\
&- \Bigg\{\Bigg[\frac{176358}{11}\left(\kappa_{3D}^{22} + \kappa_{3D}'^{22}\right) + 1939938\left(\kappa_{3D}^{20}\kappa_{3D}'^{2} + \kappa_{3D}^{2}\kappa_{3D}'^{20}\right) \\
&+ 48498450\left(\kappa_{3D}^{18}\kappa_{3D}'^{4} + \kappa_{3D}^{4}\kappa_{3D}'^{18}\right) + 436486050\left(\kappa_{3D}^{16}\kappa_{3D}'^{6} + \kappa_{3D}^{6}\kappa_{3D}'^{16}\right) \\
&+ 1745944200\left(\kappa_{3D}^{14}\kappa_{3D}'^{8} + \kappa_{3D}^{8}\kappa_{3D}'^{14}\right) + 3422050632\left(\kappa_{3D}^{12}\kappa_{3D}'^{10} + \kappa_{3D}^{10}\kappa_{3D}'^{12}\right)\Big] \\
&+ f^{2}[3879876\left(\kappa_{3D}^{20}\kappa_{3D}'^{2} + \kappa_{3D}'^{22}\right) + 387987600\left(\kappa_{3D}^{18}\kappa_{3D}'^{4} + \kappa_{3D}^{2}\kappa_{3D}'^{20}\right) \\
&+ 7856748900\left(\kappa_{3D}^{16}\kappa_{3D}'^{6} + \kappa_{3D}^{4}\kappa_{3D}'^{18}\right) + 55870214400\left(\kappa_{3D}^{14}\kappa_{3D}'^{8} + \kappa_{3D}^{6}\kappa_{3D}'^{16}\right) \\
&+ 171102531600\left(\kappa_{3D}^{12}\kappa_{3D}'^{10} + \kappa_{3D}^{8}\kappa_{3D}'^{14}\right) + 246387645504\kappa_{3D}^{10}\kappa_{3D}'^{12}\Big] \\
&+ f^{4}\Big[290990700\left(\kappa_{3D}^{18}\kappa_{3D}'^{4} + \kappa_{3D}'^{22}\right) + 23570246700\left(\kappa_{3D}^{16}\kappa_{3D}'^{6} + \kappa_{3D}^{2}\kappa_{3D}'^{20}\right) \\
&+ 377123947200\left(\kappa_{3D}^{14}\kappa_{3D}'^{8} + \kappa_{3D}^{4}\kappa_{3D}'^{18}\right) + 2053230379200\left(\kappa_{3D}^{12}\kappa_{3D}'^{10} + \kappa_{3D}^{6}\kappa_{3D}'^{16}\right) \\
&+ 4619768353200\left(\kappa_{3D}^{10}\kappa_{3D}'^{12} + \kappa_{3D}^{8}\kappa_{3D}'^{14}\right)\Big] \\
&+ f^{6}\Big[8729721000\left(\kappa_{3D}^{16}\kappa_{3D}'^{6} + \kappa_{3D}'^{22}\right) + 558702144000\left(\kappa_{3D}^{14}\kappa_{3D}'^{8} + \kappa_{3D}^{2}\kappa_{3D}'^{20}\right) \\
&+ 6844101264000\left(\kappa_{3D}^{12}\kappa_{3D}'^{10} + \kappa_{3D}^{4}\kappa_{3D}'^{18}\right) + 27376405056000\left(\kappa_{3D}^{10}\kappa_{3D}'^{12} + \kappa_{3D}^{6}\kappa_{3D}'^{16}\right) \\
&+ 42775632900000\kappa_{3D}^{8}\kappa_{3D}'^{14}\Big] \\
&+ f^{8}\Big[122216094000\left(\kappa_{3D}^{14}\kappa_{3D}'^{8} + \kappa_{3D}'^{22}\right) + 5988588606000\left(\kappa_{3D}^{12}\kappa_{3D}'^{10} + \kappa_{3D}^{2}\kappa_{3D}'^{20}\right) \\
&+ 53897297454000\left(\kappa_{3D}^{10}\kappa_{3D}'^{12} + \kappa_{3D}^{4}\kappa_{3D}'^{18}\right) + 149714715150000\left(\kappa_{3D}^{8}\kappa_{3D}'^{14} + \kappa_{3D}^{6}\kappa_{3D}'^{16}\right)\Big] \\
&+ f^{10}\Big[862356759264\left(\kappa_{3D}^{12}\kappa_{3D}'^{10} + \kappa_{3D}'^{22}\right) + 31044843333504\left(\kappa_{3D}^{10}\kappa_{3D}'^{12} + \kappa_{3D}^{2}\kappa_{3D}'^{20}\right) \\
&+ 194030270834400\left(\kappa_{3D}^{8}\kappa_{3D}'^{14} + \kappa_{3D}^{4}\kappa_{3D}'^{18}\right) + 344942703705600\kappa_{3D}^{6}\kappa_{3D}'^{16}\Big] \\
&+ f^{12}\Big[3161974783968\left(\kappa_{3D}^{10}\kappa_{3D}'^{12} + \kappa_{3D}'^{22}\right) + 79049369599200\left(\kappa_{3D}^{8}\kappa_{3D}'^{14} + \kappa_{3D}^{2}\kappa_{3D}'^{20}\right) \\
&+ 316197478396800\left(\kappa_{3D}^{6}\kappa_{3D}'^{16} + \kappa_{3D}^{4}\kappa_{3D}'^{18}\right)\Big]
\end{aligned}
$$

$$
\begin{aligned}
&+f^{14}\left[5992080494400\left(\kappa_{3D}^{8}\kappa_{3D}'^{14}+\kappa_{3D}'^{22}\right)+95873287910400\left(\kappa_{3D}^{6}\kappa_{3D}'^{16}+\kappa_{3D}^{2}\kappa_{3D}'^{20}\right)\right.\\
&\left.+215714897798400\kappa_{3D}^{4}\kappa_{3D}'^{18}\right]\\
&+f^{16}\left[5617575463500\left(\kappa_{3D}^{6}\kappa_{3D}'^{16}+\kappa_{3D}'^{22}\right)+50558179171500\left(\kappa_{3D}^{4}\kappa_{3D}'^{18}+\kappa_{3D}^{2}\kappa_{3D}'^{20}\right)\right]\\
&+f^{18}\left[2357994639000\left(\kappa_{3D}^{4}\kappa_{3D}'^{18}+\kappa_{3D}'^{22}\right)+9431978556000\kappa_{3D}^{2}\kappa_{3D}'^{20}\right]\\
&+358415185128f^{20}\left(\kappa_{3D}^{2}\kappa_{3D}'^{20}+\kappa_{3D}'^{22}\right)+11309870605\frac{1}{11}f^{22}\kappa_{3D}'^{22}\Bigg\}
\end{aligned}
\tag{A8}
$$

with $f\equiv w_v=w_z$. One needs to put the expansions for $\kappa_{3\mathrm{D}}$ and $\kappa'_{3\mathrm{D}}$ (and also high-order terms) into the expression (A8). The algebra is straightforward and one arrives:

$$
\begin{aligned}
&-\frac{17}{2}\kappa^2+\frac{207}{4}\kappa^4-\frac{2573}{6}\kappa^6+\frac{39135}{8}\kappa^8-\frac{504377}{10}\kappa^{10}+\frac{7589331}{12}\kappa^{12}\\
&-\frac{97218677}{14}\kappa^{14}+\frac{1488554079}{16}\kappa^{16}-\frac{18520701857}{18}\kappa^{18}\\
&+\frac{295407516807}{20}\kappa^{20}-\frac{3466155691037}{22}\kappa^{22}+\cdots
\end{aligned}
\tag{A9}
$$

Re-writing this equation in logarithmic form yields:

$$
\begin{aligned}
&\ln\left[1-\frac{17}{2}\kappa^2+\frac{703}{8}\kappa^4-\frac{15537}{16}\kappa^6+\frac{1531259}{128}\kappa^8-\frac{37568183}{256}\kappa^{10}\right.\\
&+\frac{1944333867}{1024}\kappa^{12}-\frac{49369925777}{2048}\kappa^{14}+\frac{10486210475347}{32768}\kappa^{16}\\
&-\frac{270077234947067}{65536}\kappa^{18}+\frac{14620934319382209}{262144}\kappa^{20}\\
&\left.-\frac{377787247047993783}{524288}\kappa^{22}+\cdots\right]
\end{aligned}
\tag{A10}
$$

Then, from (A6) and (A10), one derives:

$$
\begin{aligned}
\ln\lambda&=\ln\left[2\cosh^3 K\left(1+\frac{17}{2}\kappa^2-\frac{101}{8}\kappa^4+\frac{2221}{16}\kappa^6-\frac{157133}{128}\kappa^8\right.\right.\\
&+\frac{3128095}{256}\kappa^{10}-\frac{132058577}{1024}\kappa^{12}+\cdots\Big)\\
&\times\left(1-\frac{17}{2}\kappa^2+\frac{703}{8}\kappa^4-\frac{15537}{16}\kappa^6+\frac{1531259}{128}\kappa^8-\frac{37568183}{256}\kappa^{10}\right]\\
&\left.+\frac{1944333867}{1024}\kappa^{12}-\cdots\right)\Bigg]\\
&=\ln\left[2\cosh^3 K\left(1+3\kappa^4+22\kappa^6+192\kappa^8+2046\kappa^{10}+24853\kappa^{12}\right.\right.\\
&+329334\kappa^{14}+4649601\kappa^{16}+68884356\kappa^{18}+1059830112\kappa^{20}\\
&\left.\left.+16809862992\kappa^{22}+\cdots\right)\right]
\end{aligned}
\tag{A11}
$$

The result is equal, term by term, to the high-temperature series expansion at its high-temperature limit [80,93,107,111]:

$$\lambda = Z^{1/N} = 2\cosh^3 K\big[1 + 3\kappa^4 + 22\kappa^6 + 192\kappa^8 + 2046\kappa^{10} + 24853\kappa^{12} + 329334\kappa^{14} + 4649601\kappa^{16} + 68884356\kappa^{18} + 1059830112\kappa^{20} + 16809862992\kappa^{22} + \cdots\big] \tag{A12}$$

For finite temperatures, the partition function can be expanded as:

$$\lambda = Z^{1/N} = 2\cosh^3 K\bigg[1 + \frac{7}{2}\kappa^2 + \frac{87}{8}\kappa^4 + \frac{3613}{48}\kappa^6 + \frac{170209}{384}\kappa^8 + \frac{929761}{256}\kappa^{10} + \frac{318741323}{9216}\kappa^{12} + \frac{6705494087}{18432}\kappa^{14} + \frac{411207879769}{98304}\kappa^{16} + \frac{270525364951805}{5308416}\kappa^{18} + \frac{13788821925530329}{21233664}\kappa^{20} + \frac{121443302317649443}{14155776}\kappa^{22} + \cdots\bigg] \tag{A13}$$

From another angle, one realizes that the high-temperature series expansion could fit well with the putative exact solution only at/near infinite temperature, if one assumes the putative exact solution to be correct. Possibly, the high-temperature series expansion would be valid only at/near infinite temperature. However, the appearance of fraction numbers in (A13) suggests that κ_{3D} and κ'_{3D}, instead of κ, might be a good basis of the series expansion for the exact solution.

Appendix B

One could also prove that the putative exact solution well reproduces the results of the high-temperature series expansion at/near infinite temperature for the simple orthorhombic Ising lattices. According to equation (49), the partition function for the simple orthorhombic Ising lattices could be expressed as:

$$N^{-1}\ln Z = \ln 2 + \frac{1}{2(2\pi)^4}\int_{-\pi}^{\pi}\int_{-\pi}^{\pi}\int_{-\pi}^{\pi}\int_{-\pi}^{\pi}\ln[\cosh 2K\cosh 2(K' + K'' + K''') - \sinh 2K\cos\omega' - \sinh 2(K' + K'' + K''') \times \left(w_x\cos\omega_x + w_y\cos\omega_y + w_z\cos\omega_z\right)]d\omega' d\omega_x d\omega_y d\omega_z \tag{B1}$$

with $w_x = 1$ and:

$$w_y = w_z = \pm\sqrt{A_0 - A_1 - A_2 - \cdots}, \tag{B2}$$

where the leading terms are as follows:

$$A_0 = \frac{\kappa_4^2 + 2\kappa_2\kappa_3 + 2\kappa_3\kappa_4 + 2\kappa_4\kappa_2}{2(\kappa_2 + \kappa_3 + \kappa_4)^2}, \tag{B3a}$$

$$A_1 = -\frac{1}{8(\kappa_2+\kappa_3+\kappa_4)^3}\big[23\kappa_4^5 + 115\kappa_2\kappa_4^4 + 115\kappa_3\kappa_4^4 + 32\kappa_2^4\kappa_4 + 32\kappa_3^4\kappa_4 + 32\kappa_2^4\kappa_3 + 32\kappa_2\kappa_3^4 + 128\kappa_2^3\kappa_3^2 + 128\kappa_2^2\kappa_3^3 + 136\kappa_2^3\kappa_4^2 + 136\kappa_3^3\kappa_4^2 + 196\kappa_2^2\kappa_4^3 + 196\kappa_3^2\kappa_4^3 + 596\kappa_2\kappa_3^2\kappa_4^2 + 596\kappa_2^2\kappa_3\kappa_4^2 + 528\kappa_2^2\kappa_3^2\kappa_4 + 460\kappa_2\kappa_3\kappa_4^3 + 272\kappa_2^3\kappa_3\kappa_4 + 272\kappa_2\kappa_3^3\kappa_4\big] \tag{B3b}$$

$$\begin{aligned} A_2 = -\frac{1}{16(\kappa_2+\kappa_3+\kappa_4)^4}\big[&472\kappa_2^6\kappa_4^2 + 472\kappa_3^6\kappa_4^2 + 464\kappa_2^6\kappa_3^2 + 464\kappa_2^2\kappa_3^6 + 1040\kappa_2^3\kappa_3^5 \\ &+ 1040\kappa_2^5\kappa_3^3 + 752\kappa_2^5\kappa_4^3 + 752\kappa_3^5\kappa_4^3 + 1376\kappa_2^4\kappa_3^4\kappa_4^4 + 472\kappa_2^4\kappa_4^4 \\ &+ 472\kappa_3^4\kappa_4^4 + 944\kappa_2^6\kappa_3\kappa_4 + 944\kappa_2\kappa_3^6\kappa_4 + 2320\kappa_2\kappa_3^5\kappa_4^2 + 2320\kappa_2^5\kappa_3\kappa_4^2 \\ &+ 2608\kappa_2^5\kappa_3^2\kappa_4 + 2608\kappa_2^2\kappa_3^5\kappa_4 + 52\kappa_2^2\kappa_3^2\kappa_4^4 + 4712\kappa_2^2\kappa_3^4\kappa_4^2 + 4712\kappa_2^4\kappa_3^2\kappa_4^2 \\ &+ 454\kappa_2\kappa_3^3\kappa_4^4 + 454\kappa_2^3\kappa_3\kappa_4^4 + 2304\kappa_2^4\kappa_3\kappa_4^3 + 2304\kappa_2\kappa_3^4\kappa_4^3 + 4400\kappa_2^3\kappa_3^4\kappa_4 \\ &+ 4400\kappa_2^4\kappa_3^3\kappa_4 + 6096\kappa_2^3\kappa_3^3\kappa_4^2 + 3280\kappa_2^2\kappa_3^3\kappa_4^3 + 3280\kappa_2^3\kappa_3^2\kappa_4^3 + 112\kappa_2^7\kappa_4 \\ &+ 112\kappa_3^7\kappa_4 + 112\kappa_2^7\kappa_3 + 112\kappa_2\kappa_3^7 - 33\kappa_4^8 - 172\kappa_2\kappa_4^7 - 172\kappa_3\kappa_4^7 \\ &- 309\kappa_2^2\kappa_4^6 - 309\kappa_3^2\kappa_4^6 - 90\kappa_2^3\kappa_4^5 - 90\kappa_3^3\kappa_4^5 - 744\kappa_2\kappa_3\kappa_4^6 - 934\kappa_2\kappa_3^2\kappa_4^5 \\ &- 934\kappa_2^2\kappa_3\kappa_4^5 - 460\kappa_1^2\kappa_4^6 - 2760\kappa_1^2\kappa_2\kappa_4^5 - 2760\kappa_1^2\kappa_3\kappa_4^5 - 544\kappa_1^2\kappa_2^5\kappa_3 \\ &- 544\kappa_1^2\kappa_2\kappa_3^5 - 544\kappa_1^2\kappa_2^5\kappa_4 - 544\kappa_1^2\kappa_3^5\kappa_4 - 6252\kappa_1^2\kappa_2^2\kappa_4^4 - 6252\kappa_1^2\kappa_3^2\kappa_4^4 \\ &- 3136\kappa_1^2\kappa_2^4\kappa_3^2 - 3136\kappa_1^2\kappa_2^2\kappa_3^4 - 3200\kappa_1^2\kappa_2^4\kappa_4^2 - 3200\kappa_1^2\kappa_3^4\kappa_4^2 \\ &- 5184\kappa_1^2\kappa_2^3\kappa_3^3 - 6608\kappa_1^2\kappa_2^3\kappa_4^3 - 6608\kappa_1^2\kappa_3^3\kappa_4^3 - 34208\kappa_1^2\kappa_2^2\kappa_3^2\kappa_4^2 \\ &- 19824\kappa_1^2\kappa_2^3\kappa_3\kappa_4^2 - 19824\kappa_1^2\kappa_2\kappa_3^3\kappa_4^2 - 18400\kappa_1^2\kappa_2^3\kappa_3^2\kappa_4 \\ &- 18400\kappa_1^2\kappa_2^2\kappa_3^3\kappa_4 - 6400\kappa_1^2\kappa_2^4\kappa_3\kappa_4 - 6400\kappa_1^2\kappa_2\kappa_3^4\kappa_4 - 25008\kappa_1^2\kappa_2^2\kappa_3\kappa_4^3 \\ &- 25008\kappa_1^2\kappa_2\kappa_3^2\kappa_4^3 - 13800\kappa_1^2\kappa_2\kappa_3\kappa_4^4\big] \end{aligned} \tag{B3c}$$

Here, $\kappa_1 = \tanh K$, $\kappa_2 = \tanh K'$, $\kappa_3 = \tanh K''$ and $\kappa_4 = \tanh K'''$.

Equation (B1) is reduced to:

$$\begin{aligned} &\ln\lambda - \ln 2(\cosh 2K \cosh 2(K'+K''+K'''))^{1/2} \\ &= \frac{1}{2(2\pi)^4}\int_0^\pi\int_0^\pi\int_0^\pi\int_0^\pi \ln[1 - 2\kappa_{3D}\cos\omega' \\ &\quad -2\kappa'_{3D}\big(w_x\cos\omega_x + w_y\cos\omega_y + w_z\cos\omega_z\big)\big]d\omega' d\omega_x d\omega_y d\omega_z \end{aligned} \tag{B4}$$

Here

$$\begin{aligned} \kappa_{3D} &= \frac{\tanh 2K}{2\cosh 2(K'+K''+K''')} \\ &= \frac{\kappa_1\big(1-\kappa_2^2-\kappa_3^2-\kappa_4^2+\kappa_2^2\kappa_3^2+\kappa_3^2\kappa_4^2+\kappa_2^2\kappa_4^2-\kappa_2^2\kappa_3^2\kappa_4^2\big)}{\Gamma}. \end{aligned} \tag{B5}$$

and

$$\kappa'_{3D} = \frac{\tanh 2(K' + K'' + K''')}{2\cosh 2K}$$
$$= \frac{(1-\kappa_1^2)}{\Gamma} \cdot \big(\kappa_2 + \kappa_3 + \kappa_4 + \kappa_2\kappa_3^2 + \kappa_2\kappa_4^2 + \kappa_2^2\kappa_3 + \kappa_3\kappa_4^2 + \kappa_2^2\kappa_4$$
$$+ \kappa_3^2\kappa_4 + \kappa_2\kappa_3^2\kappa_4^2 + \kappa_2^2\kappa_3\kappa_4^2 + \kappa_2^2\kappa_3^2\kappa_4 + 4\kappa_2\kappa_3\kappa_4\big) \tag{B6}$$

with

$$\Gamma = 1 + F_2 + F_4 + F_6 + F_8 \tag{B7}$$

$$F_2 = \kappa_1^2 + \kappa_2^2 + \kappa_3^2 + \kappa_4^2 + 4\kappa_2\kappa_3 + 4\kappa_3\kappa_4 + 4\kappa_2\kappa_4 \tag{B8a}$$

$$F_4 = \kappa_1^2\kappa_2^2 + \kappa_1^2\kappa_3^2 + \kappa_1^2\kappa_4^2 + \kappa_2^2\kappa_3^2 + \kappa_3^2\kappa_4^2 + \kappa_2^2\kappa_4^2 + 4\kappa_1^2\kappa_2\kappa_3$$
$$+ 4\kappa_1^2\kappa_3\kappa_4 + 4\kappa_1^2\kappa_2\kappa_4 + 4\kappa_2\kappa_3\kappa_4^2 + 4\kappa_2\kappa_3^2\kappa_4 + 4\kappa_2^2\kappa_3\kappa_4 \tag{B8b}$$

$$F_6 = \kappa_1^2\kappa_2^2\kappa_3^2 + \kappa_1^2\kappa_3^2\kappa_4^2 + \kappa_1^2\kappa_2^2\kappa_4^2 + \kappa_2^2\kappa_3^2\kappa_4^2 + 4\kappa_1^2\kappa_2\kappa_3\kappa_4^2 + 4\kappa_1^2\kappa_2\kappa_3^2\kappa_4$$
$$+ 4\kappa_1^2\kappa_2^2\kappa_3\kappa_4 \tag{B8c}$$

$$F_8 = \kappa_1^2\kappa_2^2\kappa_3^2\kappa_4^2 \tag{B8d}$$

Employing the equation $1/(1+x) = 1 - x + x^2 - x^3 + x^4 - \cdots$ to expand $1/$, one obtains:

$$\frac{1}{\Gamma} = 1 - F_2 + \big(F_2^2 - F_4\big) + \big(2F_2F_4 - F_6 - F_2^3\big)$$
$$+ \big(F_4^2 + 2F_2F_6 + F_2^4 - F_8 - 3F_2^2F_4\big) + \cdots \tag{B9}$$

Then, one has:

$$\kappa_{3D} = G_1 - (G_1F_2 + G_3) + \big(G_1F_2^2 - G_1F_4 + G_3F_2 + G_5\big)$$
$$+ \big(2G_1F_2F_4 - G_1F_6 - G_1F_2^3 - G_3F_2^2 + G_3F_4 - G_5F_2 - G_7\big)$$
$$+ \big(G_1F_4^2 + 2G_1F_2F_6 + G_1F_2^4 - G_1F_8 - 3G_1F_2^2F_4 - 2G_3F_2F_4$$
$$+ G_3F_6 + G_3F_2^3 + G_5F_2^2 - G_5F_4 + G_7F_2\big) \tag{B10}$$

with

$$G_1 = \kappa_1 \tag{B11a}$$

$$G_3 = \kappa_1\kappa_2^2 + \kappa_1\kappa_3^2 + \kappa_1\kappa_4^2 \tag{B11b}$$

$$G_5 = \kappa_1\kappa_2^2\kappa_3^2 + \kappa_1\kappa_3^2\kappa_4^2 + \kappa_1\kappa_2^2\kappa_4^2 \tag{B11c}$$

$$G_7 = \kappa_1\kappa_2^2\kappa_3^2\kappa_4^2 \tag{B11d}$$

and

$$\begin{aligned}\kappa'_{3D} = {} & H_1 - (H_1F_2 - H_3) + (H_1F_2^2 - H_1F_4 - H_3F_2 + H_5) \\ & + \left(2H_1F_2F_4 - H_1F_6 - H_1F_2^3 + H_3F_2^2 - H_3F_4 - H_5F_2 + H_7\right) \\ & + \left(H_1F_4^2 + 2H_1F_2F_6 + H_1F_2^4 - H_1F_8 - 3H_1F_2^2F_4 + 2H_3F_2F_4\right. \\ & \left. - H_3F_6 - H_3F_2^3 + H_5F_2^2 - H_5F_4 - H_7F_2\right) \end{aligned} \tag{B12}$$

with

$$H_1 = \kappa_2 + \kappa_3 + \kappa_4 \tag{B13a}$$

$$\begin{aligned} H_3 = {} & \kappa_2\kappa_3^2 + \kappa_2\kappa_4^2 + \kappa_2^2\kappa_3 + \kappa_3\kappa_4^2 + \kappa_2^2\kappa_4 + \kappa_3^2\kappa_4 \\ & + 4\kappa_2\kappa_3\kappa_4 - \kappa_1^2\kappa_2 - \kappa_1^2\kappa_3 - \kappa_1^2\kappa_4 \end{aligned} \tag{B13b}$$

$$\begin{aligned} H_5 = {} & \kappa_2\kappa_3^2\kappa_4^2 + \kappa_2^2\kappa_3\kappa_4^2 + \kappa_2^2\kappa_3^2\kappa_4 - \kappa_1^2\kappa_2\kappa_3^2 - \kappa_1^2\kappa_2^2\kappa_3 \\ & - \kappa_1^2\kappa_2\kappa_4^2 - \kappa_1^2\kappa_2^2\kappa_4 - \kappa_1^2\kappa_3\kappa_4^2 - \kappa_1^2\kappa_3^2\kappa_4 - 4\kappa_1^2\kappa_2\kappa_3\kappa_4 \end{aligned} \tag{B13c}$$

$$H_7 = -\kappa_1^2\kappa_2\kappa_3^2\kappa_4^2 - \kappa_1^2\kappa_2^2\kappa_3\kappa_4^2 - \kappa_1^2\kappa_2^2\kappa_3^2\kappa_4 \tag{B13d}$$

Then, one can calculate the high-order terms $\kappa_{3D}^2, \kappa_{3D}^4, \kappa_{3D}^6, \ldots; \kappa_{3D}'^2, \kappa_{3D}'^4, \kappa_{3D}'^6, \ldots; \kappa_{3D}^2\kappa_{3D}'^2, \kappa_{3D}^4\kappa_{3D}'^2, \ldots; \kappa_{3D}^2\kappa_{3D}'^4, \kappa_{3D}^4\kappa_{3D}'^4, \ldots; \ldots$

The left side of the equation above for the partition function is re-written as:

$$\begin{aligned} & \ln\lambda - \ln\left[2\cosh K\cosh K'\cosh K''\left(\frac{\Gamma}{1-\kappa_4^2}\right)^{1/2}\right] \\ & = \ln\lambda - \ln[2\cosh K\cosh K'\cosh K''(1 + \Omega_1 + \Omega_2 + \Omega_3 \ldots)] \end{aligned} \tag{B14}$$

with

$$\Omega_1 = \frac{1}{2}\left(F_2 + \kappa_4^2\right) \tag{B15a}$$

$$\Omega_2 = \frac{1}{2}F_4 + \frac{1}{4}F_2\kappa_4^2 + \frac{3}{8}\kappa_4^4 - \frac{1}{8}F_2^2 \tag{B15b}$$

$$\Omega_3 = \frac{1}{2}F_6 + \frac{1}{4}F_4\kappa_4^2 + \frac{3}{16}F_2\kappa_4^4 + \frac{5}{16}\kappa_4^6 - \frac{1}{4}F_2F_4 - \frac{1}{16}F_2^2\kappa_4^2 + \frac{1}{16}F_2^3 \tag{B15c}$$

Expanding the expression on the right-hand side of the expression for the partition function and integrating each term yields:

$$\begin{aligned} & -\left[\frac{1}{2}\left(\kappa_{3D}^2 + \kappa_{3D}'^2\right) + f^2\kappa_{3D}'^2\right] \\ & -\left[\frac{3}{4}\left(\kappa_{3D}^4 + \kappa_{3D}'^4\right) + 3\kappa_{3D}^2\kappa_{3D}'^2 + 6f^2\left(\kappa_{3D}^2\kappa_{3D}'^2 + \kappa_{3D}'^4\right) + 4.5f^4\kappa_{3D}'^4\right] \end{aligned}$$

$$- \left[\frac{5}{3}\left(\kappa_{3D}^{6} + \kappa_{3D}^{\prime 6}\right) + 15\left(\kappa_{3D}^{4}\kappa_{3D}^{\prime 2} + \kappa_{3D}^{2}\kappa_{3D}^{\prime 4}\right) + 30f^{2}\left(\kappa_{3D}^{4}\kappa_{3D}^{\prime 2} + \kappa_{3D}^{\prime 6}\right)\right.$$
$$\left. + 120f^{2}\kappa_{3D}^{2}\kappa_{3D}^{\prime 4} + 90f^{4}\left(\kappa_{3D}^{2}\kappa_{3D}^{\prime 4} + \kappa_{3D}^{\prime 6}\right) + \frac{100}{3}f^{6}\kappa_{3D}^{\prime 6}\right] - \cdots \tag{B16}$$

Putting the expansions for $\kappa_{3\mathrm{D}}$ and κ'_{3D} (and also high-order terms) into the expression (B16), one arrives, after a little algebra, at:

$$- \Omega_1 + \left[\left(\kappa_1^2\kappa_2^2 + \kappa_2^2\kappa_3^2 + \kappa_1^2\kappa_3^2\right) + \frac{1}{2}\Omega_1^2 - \Omega_2\right]$$
$$+ \left[\left(16\kappa_1^2\kappa_2^2\kappa_3^2 + \kappa_1^4\kappa_2^2 + \kappa_1^2\kappa_2^4 + \kappa_2^4\kappa_3^2 + \kappa_2^2\kappa_3^4 + \kappa_3^4\kappa_1^2 + \kappa_3^2\kappa_1^4\right)\right.$$
$$\left. + \Omega_1\Omega_2 - \Omega_3 - \frac{1}{3}\Omega_1^3\right] \tag{B17}$$

Re-writing this equation in logarithmic form results in:

$$\ln(1 + \Lambda_1 + \Lambda_2 + \Lambda_3 + \cdots) \tag{B18}$$

with

$$\Lambda_1 = -\Omega_1 \tag{B19a}$$

$$\Lambda_2 = \left(\kappa_1^2\kappa_2^2 + \kappa_2^2\kappa_3^2 + \kappa_1^2\kappa_3^2\right) + \Omega_1^2 - \Omega_2 \tag{B19b}$$

$$\Lambda_3 = \left(16\kappa_1^2\kappa_2^2\kappa_3^2 + \kappa_1^4\kappa_2^2 + \kappa_1^2\kappa_2^4 + \kappa_2^4\kappa_3^2 + \kappa_2^2\kappa_3^4 + \kappa_3^4\kappa_1^2 + \kappa_3^2\kappa_1^4\right)$$
$$+ 2\Omega_1\Omega_2 - \Omega_3 - \Omega_1^3 - \Omega_1\left(\kappa_1^2\kappa_2^2 + \kappa_2^2\kappa_3^2 + \kappa_1^2\kappa_3^2\right) \tag{B19c}$$

Then, one obtains from (B14) and (B18):

$$\ln\lambda = \ln[2\cosh K\cosh K'\cosh K''(1 + \Omega_1 + \Omega_2 + \Omega_3 + \cdots)$$
$$\times (1 + \Lambda_1 + \Lambda_2 + \Lambda_3 + \cdots)]$$
$$= \ln\left\{2\cosh K\cosh K'\cosh K''\left[1 + \left(\kappa_1^2\kappa_2^2 + \kappa_2^2\kappa_3^2 + \kappa_3^2\kappa_1^2\right)\right.\right.$$
$$\left.\left.\left(16\kappa_1^2\kappa_2^2\kappa_3^2 + \kappa_1^4\kappa_2^2 + \kappa_1^2\kappa_2^4 + \kappa_2^4\kappa_3^2 + \kappa_2^2\kappa_3^4 + \kappa_3^4\kappa_1^2 + \kappa_3^2\kappa_1^4\right) + \cdots\right]\right\} \tag{B20}$$

This result fits well with the high-temperature series expansion at the high temperature limit [93]:

$$\lambda = Z^{1/n} = 2\cosh K\cosh K'\cosh K''\left[1 + \left(\kappa_1^2\kappa_2^2 + \kappa_2^2\kappa_3^2 + \kappa_3^2\kappa_1^2\right)\right.$$
$$\left. + \left(16\kappa_1^2\kappa_2^2\kappa_3^2 + \kappa_1^4\kappa_2^2 + \kappa_1^2\kappa_2^4 + \kappa_2^4\kappa_3^2 + \kappa_2^2\kappa_3^4 + \kappa_3^4\kappa_1^2 + \kappa_3^2\kappa_1^4\right) + \cdots\right]. \tag{B21}$$

Evidently, (B3a)–(B3c) revert to the first three terms b_0, b_1 and b_2 in (A2) as $K = K' = K''$ (and, thus, $\kappa_1 = \kappa_2 = \kappa_3 = \kappa_4 = \kappa$). One could try to add more terms A_3, $A_4, \ldots$ Certainly, such calculations would be very laborious, tedious, and extremely difficult. Nonetheless, the first three terms look impressive and appear sufficient to illustrate clearly that the same procedure for (A2) can be generalized to the general cases of K,′ K'' and K''' and reveal physical significance as well as some symmetries among the parameters κ_1, κ_2, κ_3 and κ_4. The addition of the higher terms

A_3, A_4, ... would not add more evident physical significance. All efforts are devoted to reveal the possibility of elegantly embodying the opening form of infinite terms of the high-temperature expansion into the square roots of the weights. These weights can vanish, when the temperature is lowered to deviate from the high-temperature limit.

The weights w_y and w_z in the form of the square root embody the opening form of the high-temperature expansion in infinite terms into a closed form. This is a novel and elegant method of dealing with the problem of infinite. The combination of this closed form with the close form of the function in the 4-fold integral produces the closed-form expressions for the free energy of the 3D Ising model from $T=0$ to any finite temperatures and also at infinite temperature.

References

[1] E. Ising, Z. Phys. **31,** 253 (1925).
[2] W.L. Bragg and E.J. Williams, Proc. R. Soc. (Lond.) A **145,** 699 (1934).
[3] W.L. Bragg and E.J. Williams, Proc. R. Soc. (Lond.) A **151,** 540 (1935).
[4] F.C. Nix and W. Shockley, Rev. Mod. Phys. **10** 1 (1938).
[5] W. Shockley, J. Chem. Phys. **6** 130 (1938).
[6] B.L. van der Waerden, Z. Phys. **118** 473 (1941).
[7] J. Ashkin and W.E. Lamb Jr, Phys. Rev. **64,** 159 (1943).
[8] C.N. Yang and T.D. Lee, Phys. Rev. **87,** 404 (1952).
[9] T.D. Lee and C.N. Yang, Phys. Rev. **87,** 410 (1952).
[10] S.L. Sondhi, S.M. Girvin, J.P. Carini, *et al*., Rev. Mod. Phys. **69,** 315 (1997).
[11] D.V. Shopova and D.I. Uzunov, Phys. Rep. **379,** 1 (2003).
[12] P.C. Hohenberg and B.I. Halperin, Rev. Mod. Phys. **49,** 435 (1977).
[13] L. Onsager, Phys. Rev. **65,** 117 (1944).
[14] H.A. Kramers and G.H. Wannier, Phys. Rev. **60,** 252 (1941).
[15] H.A. Kramers and G.H. Wannier, Phys. Rev. **60,** 263 (1941).
[16] E.W. Montroll, J. Chem. Phys. **9,** 706 (1941).
[17] B. Kaufman, Phys. Rev. **76,** 1232 (1949).
[18] B. Kaufman and L. Onsager, Phys. Rev. **76,** 1244 (1949).
[19] L. Onsager, and B. Kaufman, Phys. Soc. Camb. Conf. Report (1947), pp 137.
[20] C.N. Yang, Phys. Rev. **85,** 808 (1952).
[21] C.H. Chang, Phys. Rev. **88,** 1422 (1952).
[22] R.B. Potts, Phys. Rev. **88,** 352 (1952).
[23] G.F. Newell, Phys. Rev. **78,** 444 (1950).
[24] G.H. Wannier, Rev. Mod. Phys. **17,** 50 (1945).
[25] G.H. Wannier, Phys. Rev. **79,** 357 (1950).
[26] G.F. Newell, Phys. Rev. **79,** 876 (1950).
[27] R.M.F. Houtapple, Physica **16,** 425 (1950).
[28] H.N.V. Temperley, Proc. R. Soc. A **202,** 202 (1950).
[29] T. Yamamoto, Prog. Theor. Phys. **6,** 533 (1951).
[30] R.B. Potts, Proc. Phys. Soc. (Lond.) A **68,** 145 (1955).
[31] V.G. Vaks, A.L. Larkin and Y.N. Ovchinnikov, Soviet Phys. JETP **22,** 820 (1966).
[32] M.E. Fisher, Proc. R. Soc. A **254,** 66 (1960).
[33] M.E. Fisher, Proc. R. Soc. A **254,** 502 (1960).

[34] D. Park, Physica **22,** 932 (1956).
[35] M.F. Sykes and M.E. Fisher, Phys. Rev. Lett. **1,** 321 (1958).
[36] I. Syôzi, Prog. Theor. Phys. **6,** 306 (1951).
[37] S. Naya, Prog. Theor. Phys. **11,** 53 (1954).
[38] R.J. Baxter and F.Y. Wu, Phys. Rev. Lett. **31,** 1294 (1973).
[39] E.H. Lieb, Phys. Rev. Lett. **18,** 692 (1967).
[40] E.H. Lieb, Phys. Rev. **162,** 162 (1967).
[41] E.H. Lieb, Phys. Rev. Lett. **18,** 1046 (1967).
[42] E.H. Lieb, Phys. Rev. Lett. **19,** 108 (1967).
[43] B. Sutherland, Phys. Rev. Lett. **19,** 103 (1967).
[44] C.P. Yang, Phys. Rev. Lett. **19,** 586 (1967).
[45] B. Sutherland, C.N. Yang and C.P. Yang, Phys. Rev. Lett. **19,** 588 (1967).
[46] F.Y. Wu, Phys. Rev. Lett. **18,** 605 (1967).
[47] F.Y. Wu, Phys. Rev. **168,** 539 (1968).
[48] F.Y. Wu, Phys. Rev. **183,** 604 (1969).
[49] F.Y. Wu, Phys. Rev. Lett. **22,** 1174 (1969).
[50] C.P. Fan and F.Y. Wu, Phys. Rev. **179,** 560 (1969).
[51] F.Y. Wu, Phys. Rev. Lett. **24,** 1476 (1970).
[52] C.P. Fan and F.Y. Wu, Phys. Rev. B **2,** 723 (1970).
[53] M. Suzuki, Phys. Rev. Lett. **28,** 507 (1972).
[54] A.B. Zamolodchikov, JETP **52,** 325 (1980).
[55] R.J. Barter, Commun. Math. Phys. **88,** 185 (1983).
[56] V.V. Bazhanov and R.J. Barter, J. Stat. Phys. **69,** 453 (1992).
[57] H.Y. Huang, V. Popkov and F.Y. Wu, Phys. Rev. Lett. **78,** 409 (1997).
[58] J.–M. Maillard, Physica A **321,** 28 (2003).
[59] G.F. Newell and E.W. Montroll, Rev. Mod. Phys. **25,** 353 (1953).
[60] M. Kac and J.C. Ward, Phys. Rev. **88,** 1332 (1952).
[61] R. Kikuchi, Phys. Rev. **81,** 988 (1951).
[62] T. Oguchi, J. Phys. Soc. Jpn. **5,** 75 (1950).
[63] T. Oguchi, J. Phys. Soc. Jpn. **6,** 27 (1951).
[64] T. Oguchi, J. Phys. Soc. Jpn. **6,** 31 (1951).
[65] C. Domb, Proc. R. Soc. (Lond.) **A 196** 36 (1949).
[66] C. Domb, Proc. R. Soc. (Lond.) **A 199** 199 (1949).
[67] J.E. Brooks and C. Domb, Proc. R. Soc. (Lond.) **A 207** 343 (1951).
[68] C. Domb and R.B. Potts, Proc. R. Soc. (Lond.) **A 210,** 125 (1951).
[69] E.W. Montroll, Nuovo Cimento Suppl. **6,** 265 (1949).
[70] D. ter Haar, Phys. Rev. **76,** L176 (1949).
[71] D. ter Haar and B. Martin, Phys. Rev. **77,** L721 (1950).
[72] E. Trefftz, Z. Phys. **127,** S371 (1950).
[73] A.J. Wakefield, Proc. Camb. Phil. Soc. **47,** 419 (1951).
[74] A.J. Wakefield, Proc. Camb. Phil. Soc. **47,** 799 (1951).
[75] T.H. Berlin and M. Kac, Phys. Rev. **86,** 821 (1952).
[76] M. Kurata and R. Kikuchi, J. Chem. Phys. **21,** 434 (1953).
[77] G.S. Rushbrooke, Nuovo Cimento Suppl. **6,** 252 (1949).
[78] C. Domb, Nature **163,** 775 (1949).
[79] C. Domb and M.F. Sykes, Proc. R. Soc. A **235,** 247 (1956).
[80] C. Domb and M.F. Sykes, Phil. Mag. **2,** 733 (1957).
[81] C. Domb and M.F. Sykes, Phys. Rev. **108,** 1415 (1957).
[82] C. Domb and M.F. Sykes, Proc. R. Soc. A **240,** 214 (1957).
[83] C. Domb and M.F. Sykes, J. Math. Phys. **2,** 63 (1961).
[84] T. Tanaka, H. Katsumori and S. Toshima, Prog. Theor. Phys. **6,** 17 (1951).

[85] P.W. Kasteleijn, Physica **22,** 387 (1956).
[86] J. Hijmans and J. de Boer, Physica **21,** 471 (1955).
[87] J. Hijmans and J. de Boer, Physica **21,** 485 (1955).
[88] J. Hijmans and J. de Boer, Physica **21,** 499 (1955).
[89] G.S. Rushbrooke and P.J. Wood, Mol. Phys. **1,** 257 (1958).
[90] A. Levitas and M. Lax, Phys. Rev. **110,** 1016 (1958).
[91] M.E. Fisher, Phys. Rev. **113,** 969 (1959).
[92] M.E. Fisher and M.F. Sykes, Phys. Rev. **114,** 45 (1959).
[93] C. Domb, Adv. Phys. **9,** 149 (1960).
[94] C. Domb and D.L. Hunter, Proc. Phys. Soc. (Lond.) **86,** 1147 (1965).
[95] C. Domb and M.F. Sykes, Phys. Rev. **128,** 168 (1962).
[96] G.A. Baker Jr, Phys. Rev. **124,** 768 (1961).
[97] J.W. Essam and M.E. Fisher, J. Chem. Phys. **38,** 802 (1963).
[98] M.E. Fisher, Physica **25,** 521 (1959).
[99] M.E. Fisher, Physica **28,** 172 (1962).
[100] M.E. Fisher, J. Math. Phys. **5,** 944 (1964).
[101] M.E. Fisher and D.S. Gaunt, Phys. Rev. **133,** A 224 (1964).
[102] M.E. Fisher and R.J. Burford, Phys. Rev. **156,** 583 (1967).
[103] M.E. Fisher, Rep. Prog. Phys. **30,** 615 (1967).
[104] S.G. Brush, Rev. Mod. Phys. **39,** 883 (1967).
[105] L.P. Kadanoff, W. Götze, D. Hamblen, *et al*., Rev. Mod. Phys. **39,** 395 (1967).
[106] G. Parisi, *Statistical Field Theory* (Addison–Wesley, New York, 1988).
[107] C. Domb, in *Phase Transitions and Critical Phenomena*, edited by C. Domb and M.S. Green, Vol. 3 (Academic Press, London, 1974).
[108] H. Arisue and K. Tabata, Nucl. Phys. B **435,** 555 (1995).
[109] R.J. Baxter and I.G. Enting, J. Stat. Phys. **21,** 103 (1979).
[110] G. Bhanot, M. Creutz and J. Lacki, Phys. Rev. Lett. **69,** 1841 (1992).
[111] A.J. Guttmann and I.G. Enting, J. Phys. A **26,** 807 (1993).
[112] M.J. Buckingham and J.D. Gunton, Phys. Rev. **178,** 848 (1969).
[113] Z. Salman and J. Adler, Int. J. Mod. Phys. C **9,** 195 (1998).
[114] U. Glässner, G. Bhanot, M. Creutz, *et al*., Nucl. Phys. B Proc. Suppl. **42,** 758 (1995).
[115] M. Campostrini, A. Pelissetto, P. Rossi and E. Vicari, Phys. Rev. E **60,** 3526 (1999).
[116] P. Butera and M. Comi, Phys. Rev. B **58,** 11552 (1998).
[117] H. Shi, Y.C. Xu and B.L. Hao, Acta Phys. Sin. **27,** 47 (1978).
[118] P. Butera and M. Comi, Phys. Rev. B **56,** 8212 (1997).
[119] P. Butera and M. Comi, Phys. Rev. B **62,** 14837 (2000).
[120] J. Zinn–Justin, J. Phys. (Paris) **42,** 783 (1981).
[121] J. Adler, J. Phys. A **16,** 3585 (1983).
[122] A.J. Liu and M.E. Fisher, Physica A **156,** 35 (1989).
[123] A.J. Guttmann and I.G. Enting, J. Phys. A **31,** 8103 (1998).
[124] H. Arisue and T. Fujiwara, Phys. Rev. E **67,** 066109 (2003).
[125] H. Arisue, T. Fujiwara and K. Tabata, Nucl. Phys. B Proc. Suppl. **129,** 774 (2004).
[126] K.G. Wilson, Phys. Rev. B **4,** 3174 (1971).
[127] K.G. Wilson, Phys. Rev. B **4,** 3184 (1971).
[128] K.G. Wilson, Phys. Rev. D **3,** 1818 (1971).
[129] K.G. Wilson, Phys. Rev. Lett. **28,** 548 (1972).
[130] K.G. Wilson and M.E. Fisher, Phys. Rev. Lett. **28,** 240 (1972).
[131] M.E. Fisher, S.K. Ma and B.G. Nickel, Phys. Rev. Lett. **29,** 917 (1972).
[132] F.J. Wegner, Phys. Rev. B **6,** 1891 (1972).
[133] F.J. Wegner, Phys. Rev. B **6,** 4529 (1972).
[134] D.S. Ritchie and M.E. Fisher, Phys. Rev. B **5,** 2668 (1972).

[135] H.B. Tarko and M.E. Fisher, Phys. Rev. B **11,** 1217 (1975).
[136] A. Aharony and M.E. Fisher, Phys. Rev. B **8,** 3323 (1973).
[137] A. Aharony, Phys. Rev. B **8,** 3342 (1973).
[138] A. Aharony, Phys. Rev. B **8,** 3349 (1973).
[139] A. Aharony, Phys. Rev. B **8,** 3358 (1973).
[140] S.K. Ma, Phys. Rev. A **7,** 2172 (1973).
[141] S.K. Ma, Rev. Mod. Phys. **45,** 589 (1973).
[142] K.G. Wilson and J. Kogut, Phys. Rep. **12,** 75 (1974).
[143] M.E. Fisher, Rev. Mod. Phys. **46,** 597 (1974).
[144] K.G. Wilson, Rev. Mod. Phys. **47,** 773 (1975).
[145] L.P. Kadanoff, Phys. Rev. Lett. **16,** 1005 (1975).
[146] L.P. Kadanoff and A. Houghton, Phys. Rev. B **11,** 377 (1975).
[147] G.A. Baker Jr, B.G. Nickel, M.S. Green, *et al.*, Phys. Rev. Lett. **36,** 1351 (1976).
[148] J. Als–Nielsen, Phys. Rev. Lett. **37,** 1161 (1976).
[149] K.G. Wilson, Rev. Mod. Phys. **55,** 583 (1983).
[150] G.A. Baker Jr and N. Kawashima, Phys. Rev. Lett. **75,** 994 (1995).
[151] S.Y. Zinn, S.N. Lai and M.E. Fisher, Phys. Rev. E **54,** 1176 (1996).
[152] M.E. Fisher, Rev. Mod. Phys. **70,** 653 (1998).
[153] H.E. Stanley, Rev. Mod. Phys. **71,** S358 (1999).
[154] A. Pelissetto and E. Vicari, Phys. Rep. **368,** 549 (2002).
[155] R. Swendsen, J.S. Wang and A.M. Ferrenberg, in *The Monte Carlo Method in Condensed Matter Physics*, edited by K. Binder (Springer, Berlin, 1992).
[156] C. Itzykson, *Progress in Gauge Field Theories, Proceedings of the Cargèse Summer School* (Plenum Press, New York, 1983).
[157] C. Itzykson and J.M. Drouffe, *Statistical Field Theory* (Cambridge University Press, Cambridge, 1989).
[158] R.H. Swendsen, in *Real Space Renormalization*, edited by T.W. Burkhardt and J.M.J. van Leeuwen (Springer, Berlin, 1982).
[159] J. Zinn–Justin, Phys. Rep. **344,** 159 (2001).
[160] B.A. Berg, in *Multiscale Phenomena and Their Simulation*, edited by F. Karsch, B. Monien and H. Satz (World Scientific, Singapore, 1997).
[161] H.W.J. Blöte, J. de Bruin, A. Compagner, *et al.*, Europhys. Lett. **10,** 105 (1989).
[162] H.W.J. Blöte, A. Compagner, J.H. Croockewit, *et al.*, Physica A **161,** 1 (1989).
[163] H.W.J. Blöte, E. Luijten and J.R. Heringa, J. Phys. A **28,** 6289 (1995).
[164] H.W.J. Blöte and G. Kamieniarz, Acta Phys. Pol. A **85,** 395 (1994).
[165] Y.J. Deng and H.W.J. Blöte, Phys. Rev. Lett. **88,** 190602 (2002).
[166] Y.J. Deng and H.W.J. Blöte, Phys. Rev. E **70,** 046111 (2004).
[167] J. Kaupuzs, Ann. Phys. **10,** 299 (2001).
[168] A.M. Ferrenberg and D.P. Landau, Phys. Rev. B **44,** 5081 (1991).
[169] K. Chen, A.M. Ferrenberg and D.P. Landau, Phys. Rev. B **48,** 3249 (1993).
[170] R. Gupta and P. Tamayo, Int. J. Mod. Phys. C **7,** 305 (1996).
[171] M. Hasenbusch, Int. J. Mod. Phys. C **12,** 911 (2001).
[172] N. Ito and M. Suzuki, J. Phys. Soc. Jpn. **60,** 1978 (1991).
[173] G.S. Pawley, R.H. Swendsen, D.J. Wallace, *et al.*, Phys. Rev. B **29,** 4030 (1984).
[174] A.L. Talapov and H.W.J. Blöte, J. Phys. A **29,** 5727 (1996).
[175] H.W.J. Blöte and G. Kamieniarz, Physica A **196,** 455 (1993).
[176] Y.J. Deng and H.W.J. Blöte, Phys. Rev. E **68,** 036125 (2003).
[177] C.F. Baillie, R. Gupta, K.A. Hawick, *et al.*, Phys. Rev. B **45,** 10438 (1992).
[178] R.H. Swendsen, Phys. Rev. Lett. **42,** 859 (1979).
[179] R.H. Swendsen and J.S. Wang, Phys. Rev. Lett. **58,** 86 (1987).
[180] F. Livet, Europhys. Lett. **16,** 139 (1991).

[181] D.P. Landau, Physica A **205,** 41 (1994).
[182] A.M. Ferrenberg, D.P. Landau and K. Binder, J. Stat. Phys. **63,** 867 (1991).
[183] S. Wansleben and D.P. Landau, Phys. Rev. B **43,** 6006 (1991).
[184] D. Stauffer and R. Knecht, Int. J. Mod. Phys. C **7,** 893 (1996).
[185] D. Stauffer, Physica A **244,** 344 (1997).
[186] H.W.J. Blöte, L.N. Shchur and A.L. Talapov, Int. J. Mod. Phys. C **10,** 1137 (1999).
[187] R. Guida and J. Zinn–Justin, Nucl. Phys. B **489,** 626 (1997).
[188] R. Guida and J. Zinn–Justin, J. Phys. A **31,** 8103 (1998).
[189] J.C. Le Guillou and J. Zinn–Justin, Phys. Rev. B **21,** 3976 (1980).
[190] B. Li, N. Madras and A.D. Sokal, J. Stat. Phys. **80,** 661 (1995).
[191] A.J.F. Desouza and F.G.B. Moreira, Phys. Rev. B **48,** 9586 (1993).
[192] K. Binder, Adv. Phys. **23,** 917 (1974).
[193] K. Binder, in *Phase Transitions and Critical Phenomena*, edited by C. Domb and M.S. Green, Vol. 5b [(Academic Press, London, 1976).
[194] K. Binder (editor). *Monte Carlo Methods in Statistical Physics* (Springer, Berlin, 1979).
[195] K. Binder, Rep. Prog. Phys. **60,** 487 (1997).
[196] K. Binder and D.W. Heermann, *Monte Carlo Simulation Statistical Physics – An Introduction* (Springer, Berlin, 1988).
[197] D.P. Landau, in *The Monte Carlo Method in Condensed Matter Physics*, edited by K. Binder (Springer, Berlin, 1992).
[198] D.P. Landau and K. Binder, *A Guide to Monte Carlo Simulation in Statistical Physics* (Cambridge University Press, Cambridge, 2000).
[199] B. Dünweg, in *Monte Carlo and Molecular Dynamics of Condensed Matter Systems*, edited by K. Binder and G. Ciccotti (Italian Physical Society, Bologna, 1996).
[200] W. Janke, in *Computational Physics. Selected Methods, Simple Exercises, Serious Applications*, edited by K.H. Hoffmann and M. Schreiber (Springer, Berlin, 1996).
[201] M.E. Fisher, in *Critical Phenomena*, edited by M.S. Green (Academic Press, London, 1971).
[202] K. Binder, in *Computational Methods in Field Theory*, edited by H. Gausterer and C.B. Lang (Springer, Berlin, 1992).
[203] J. Garcia and J.A. Gonzalo, Physica A **326,** 464 (2003).
[204] H.J. Elmers, J. Hauschild, H. Höche, *et al.*, Phys. Rev. Lett. **73,** 898 (1994).
[205] Z.B. Li, L. Schülke and B. Zheng, Phys. Rev. Lett. **74,** 3396 (1995).
[206] Z.B. Li, U. Ritschel and B. Zheng, J. Phys. A **27,** L837 (1994).
[207] Y.J. Deng and H.W.J. Blöte, Phys. Rev. E **67,** 066116 (2003).
[208] K. Huang, *Statistical Mechanics* (Wiley, New York, 1963).
[209] D.M. Burley, in *Phase Transitions and Critical Phenomena*, edited by C. Domb and M.S. Green, Vol. 2 (Academic Press, New York, 1972).
[210] L.P. Kadanoff, in *Phase Transitions and Critical Phenomena*, edited by C. Domb and M.S. Green, Vol. 5a (Academic Press, New York, 1976).
[211] C. Domb and M.S. Green (editors), *Phase Transitions and Critical Phenomena*, Vol. 6 (Academic Press, New York, 1976).
[212] J.J. Binney, N.J. Dowrick, A.J. Fisher, *et al.*, *The Theory of Critical Phenomena, An Introduction to the Renormalization Group* (Clarendon Press, Oxford, 1992).
[213] K. Binder and E. Luijten, Phys. Rep. **344,** 179 (2001).
[214] B. Widom, in *Fundamental Problems in Statistical Mechanics*, edited by E.C.G. Cohen (North–Holland, Amsterdam, 1975).
[215] D.J. Wallace and R.K. Zia, Rep. Prog. Phys. **41,** 1 (1978).
[216] S.C. Greer and M.R. Moldover, Annu. Rev. Phys. Chem. **32,** 233 (1981).
[217] C. Domb, *The Critical Point: A Historical Introduction to the Modern Theory of Critical Phenomena* (Taylor and Francis, London, 1996).

[218] R.J. Creswick, H.A. Farach and C.P. Poole Jr, *Introduction to Renormlization Group Methods in Physics* (Wiley, New York, 1990).
[219] B.M. McCoy and T.T. Wu, *The Two-Dimensional Ising Model* (Harvard University Press, Cambridge, MA, 1973).
[220] R.J. Baxter, *Exactly Solved Models in Statistical Mechanics* (Academic Press, London, 1982).
[221] H.E. Stanley, *An Introduction to Phase Transitions and Critical Phenomena* (Oxford University Press, Oxford, 1971).
[222] S.K. Ma, *Modern Theory of Critical Phenomena* (Addison–Wesley, Redwood, CA, 1976).
[223] P. Pfeuty and G. Toulouse, *Introduction to the Renormalization Group and to Critical Phenomena* (Wiley, London, 1977).
[224] D.J. Amit, *Field Theory, the Renormalization Group and Critical Phenomena* (World Scientific, Singapore, 1984).
[225] J. Zinn–Justin, *Quantum Field Theory and Critical Phenomena* (Oxford University Press, Oxford, 1996).
[226] L.D. Landau, Phys. Z. Sowjetunion **11,** 26 (1937).
[227] L.D. Landau, Phys. Z. Sowjetunion **11,** 545 (1937).
[228] H.A. Bethe, Proc. R. Soc. A **150,** 552 (1935).
[229] J.G. Kirkwood, J. Chem. Phys. **6,** 70 (1938).
[230] A. Rosengren, J. Phys. A **19,** 1709 (1986).
[231] M.E. Fisher, J. Phys. A **28,** 6323 (1995).
[232] D.S. Gaunt, in *Phase Transitions* (Cargèse, 1980), edited by M. Levy, J.C. Le Guillou and J. Zinn–Justin (Plenum, New York, 1982).
[233] R.B. Pearson, Phys. Rep. **103,** 185 (1981).
[234] M.N. Barber, R.B. Pearson, D. Toussaint, *et al*., Phys. Rev. B **32,** 1720 (1985).
[235] J.K. Kim, A.J. de Souza and D.P. Landau, Phys. Rev. E **54,** 2291 (1996).
[236] F.J. Wegner, in *Phase Transitions and Critical Phenomena*, edited by C. Domb and M.S. Green, Vol. 6 (Academic Press, London, 1976).
[237] T.D. Schultz, D.C. Mattis and E.H. Lieb, Rev. Mod. Phys. **36,** 856 (1964).
[238] G. Bhanot, M. Creutz, I. Horvath, *et al*., Phys. Rev. E **49,** 2445 (1994).
[239] R.B. Potts and J.C. Ward, Prog. Theor. Phys. **13,** 38 (1955).
[240] S. Sherman, J. Math. Phys. **1,** 202 (1960).
[241] S. Sherman, J. Math. Phys. **4,** 1213 (1963).
[242] P.N. Burgoyne, J. Math. Phys. **4,** 1320 (1963).
[243] L.P. Kadanoff, Nuovo Cimento **44,** 276 (1966).
[244] C.A. Hurst and H.S. Green, J. Chem. Phys. **33,** 1059 (1960).
[245] P.W. Kasteleyn, Physica **27,** 1209 (1961).
[246] P.W. Kasteleyn, J. Math. Phys. **4,** 287 (1963).
[247] M.E. Fisher, Phys. Rev. **124,** 1664 (1961).
[248] H.N.V. Temperley and M.E. Fisher, Phil. Mag. **6,** 1061 (1961).
[249] E.W. Montroll, R.B. Potts and J.C. Ward, J. Math. Phys. **4,** 308 (1963).
[250] J. Stephenson, J. Math. Phys. **5,** 1009 (1964).
[251] K. Kano, Progr. Theor. Phys. **35,** 1 (1966).
[252] T.T. Wu, Phys. Rev. **149,** 380 (1966).
[253] G. Szego, Communications du seminaire mathematique de l'université de Lund, tome supplementaire. dedié a Marcel Riesz (1952), p. 228.
[254] V. Grenander and G. Szego, *Toeplitz Forms and Their Applications* (University of California Press, Berkeley, CA, 1958).
[255] M.E. Fisher and J.H. Chen, J. Phys. **46,** 1645 (1985).
[256] J. Als–Nielsen and R.J. Birgeneau, Am. J. Phys. **45,** 554 (1977).

[257] A. Aharony and B.I. Halperin, Phys. Rev. Lett. **35,** 1308 (1975).
[258] G.S. Rushbrooke, J. Chem. Phys. **39,** 842 (1963).
[259] B. Widom, J. Chem. Phys. **43,** 3898 (1965).
[260] G. Stell, Phys. Rev. Lett. **20,** 533 (1968).
[261] R.B. Griffiths, Phys. Rev. Lett. **14,** 623 (1965).
[262] G.V. Ryazanov, Soviet Phys. JETP **22,** 789 (1966).
[263] E. Brézin, J.C. Le Guillou and J. Zinn–Justin, in *Phase Transitions and Critical Phenomena*, edited by C. Domb and M.S. Green, Vol. 6 (Academic Press, London, 1976).
[264] L.P. Kadanoff, in *Phase Transitions and Critical Phenomena*, edited by C. Domb and M.S. Green, Vol. 5a (Academic Press, London, 1976).
[265] J. Kaupuzs, Euro Phys. J. B **45,** 459 (2005).
[266] R. Mahnke, J. Kaupuzs and I. Lubashevsky, Phys. Rep. **408,** 1 (2005).
[267] J. Kaupuzs and E. Klotins, Ferroelectron. **296,** 239 (2003).
[268] M. Vicentini–Missoni, in *Phase Transitions and Critical Phenomena*, edited by C. Domb and M.S. Green, Vol. 2 (Academic Press, London, 1972).
[269] P. Weiss and R. Forrer, Ann. Phys. (Paris) **5,** 153 (1926).
[270] J.S. Kouvel and J.B. Comly, Phys. Rev. Lett. **20,** 1237 (1968).
[271] C.O. Graham Jr, J. Appl. Phys. **36,** 1135 (1965).
[272] J.T. Ho and J.D. Litster, Phys. Rev. Lett. **22,** 603 (1969).
[273] J.T. Ho and J.D. Litster, J. Appl. Phys. **40,** 1270 (1969).
[274] M. Vicentini–Missoni, J.M.H. Levelt–Sengers and M.S. Green, J. Res. Natl. Bur. Stand. A **73,** 563 (1969).
[275] M. Vicentini–Missoni, R.I. Joseph, M.S. Green, *et al.*, Phys. Rev. B **1,** 2312 (1970).
[276] J.M.H. Levelt–Sengers, M.S. Green and M. Vicentini–Missoni, Phys. Rev. Lett. **22,** 389 (1969).
[277] B. Widom, in *Phase Transitions and Critical Phenomena*, edited by C. Domb and M.S. Green, Vol. 2 (Academic Press, London, 1972).
[278] F.P. Buff and R.A. Lovett, in *Simple Dense Fluids*, edited by H. Frisch and Z.W. Salzburg (Academic Press, New York, 1968).
[279] A.M. Wims, J.V. Sengers, D. McIntyre and J. Shereshefsky, J. Chem. Phys. **52,** 3042 (1970).
[280] J.S. Huang and W.W. Webb, J. Chem. Phys. **50,** 3677 (1969).
[281] T. Shirane, T. Moriya, T. Bitoh, *et al.*, J. Phys. Soc. Jpn. **64,** 951 (1995).
[282] M. Seeger, S.N. Kaul, H. Kronmüller, *et al.*, Phys. Rev. B **51,** 12585 (1995).
[283] D.P. Belanger and H. Yoshizawa, Phys. Rev. B **35,** 4823 (1987).
[284] B.H. Chen, B. Payandeh and M. Robert, Phys. Rev. **E 62,** 2369 (2000).
[285] B.H. Chen, B. Payandeh and M. Robert, Phys. Rev. **E 64,** 042401 (2001).
[286] K. Hamano, T. Kawazura, T. Koyama, *et al.*, J. Chem. Phys. **82,** 2718 (1985).
[287] K. Hamano, N. Kuwahara, I. Mitsushima, *et al.*, J. Chem. Phys. **94,** 2172 (1991).
[288] D.T. Jacobs, Phys. Rev. A **33,** 2605 (1986).
[289] J. Lee, Phys. Rev. Lett. **71,** 211 (1993).
[290] S. Limberg, L. Belkoura and D. Woermann, J. Mol. Liq. **73/74,** 223 (1997).
[291] O. Müller and J. Winkelmann, Phys. Rev. **E 59,** 2026 (1999).
[292] H. Sato, N. Kuwahara and K. Kubota, Phys. Rev. **E 53,** 3854 (1996).
[293] A.M. Strydom, P.D. du Plessis, D. Kaczorowski, *et al.*, Physica B **186/188,** 785 (1993).
[294] M.W. Pestak and M.H.W. Chan, Phys. Rev. B **30,** 274 (1984).
[295] S. Shimofure, K. Kubota, R. Kita, *et al.*, J. Chem. Phys. **111,** 4199 (1999).
[296] T. Takada and T. Watanabe, J. Low. Temp. Phys. **49,** 435 (1982).
[297] B.R. Greene, *The Elegant Universe: Superstrings, Hidden Dimensions, and the Quest for the Ultimate Theory* (Vintage Press, New York, 1999).

[298] L. Smolin, *Three Roads to Quantum Gravity* (Weidenfeld & Nicolson/Orion Publishing, London, 2000).
[299] R.G. Littlejohn and M. Reinsch, Rev. Mod. Phys. **69,** 213 (1997).
[300] J.P. Uzan, Rev. Mod. Phys. **75,** 403 (2003).
[301] T. Kaluza, Sitzungsber. Preuss. Akad. Wiss. Phys. Math. Kl. **LIV,** 966 (1921).
[302] O. Klein, Z. Phys. **37,** 875 (1926).
[303] L. Randall and R. Sundrum, Phys. Rev. Lett. **83,** 4690 (1999).
[304] N. Arkani–Hamed, S. Dimopoulos and G. Dvali, Phys. Lett. B **429,** 263 (1998).
[305] I. Antoniadis, N. Arkani–Hamed, S. Dimopoulos, *et al*., Phys. Lett. B **436,** 257 (1998).
[306] G. Shiu and S.H.H. Tye, Phys. Rev. D **58,** 106007 (1998).
[307] J.L. Hewett, Phys. Rev. Lett. **82,** 4765 (1999).
[308] J. Garriga and T. Tanaka, Phys. Rev. Lett. **84,** 2778 (2000).
[309] J. Polchinski, *Superstring Theory* (Cambridge University Press, Cambridge, England, 1997).
[310] S.W. Hawking, *A Brief History of Time: From the Big Bang to Black Holes* (Bantam Books, New York, 1988).
[311] P. de Bernardis, P.A.R. Ade, J.J. Bock, *et al*., Nature **404,** 955 (2000).
[312] Z. Lao, Waley's English translation (Hunan Publishing House, Dao De Jing, Changsha, China, 1992).
[313] L. Smolin, Phys. Rev. **D 62**, 086001 (2000).
[314] F. Markopoulou, Nuclear Phys. B Proc. Suppl. **88,** 308 (2000); and also see gr–qc/9704013.
[315] M. Wortis, in *Phase Transitions and Critical Phenomena*, edited by C. Domb and M.S. Green, Vol. 3 (Academic Press, London, 1974).
[316] D.S. Gaunt and A.J. Guttmann, in *Phase Transitions and Critical Phenomena*, edited by C. Domb and M.S. Green, Vol. 3 (Academic Press, London, 1974).
[317] K. Knopp, *Theory of Functions: Parts I and II* (Dover Publications, New York, 1996).
[318] K.G. Wilson, in *Phase Transitions and Critical Phenomena*, edited by C. Domb and M.S. Green, Vol. 6 (Academic Press, London, 1976).
[319] A.J. Guttmann, J. Phys. C **2,** 1900 (1969).
[320] C. Domb and A.J. Guttmann, J. Phys. C **3,** 1652 (1970).
[321] H. Müller–Krumnhaar and K. Binder, J. Stat. Phys. **8,** 1 (1973).
[322] E. Stoll, K. Binder and T. Schneider, Phys. Rev. B **8,** 3266 (1973).
[323] D. Knuth, *The Art of Computer Programming*, Vol. 2 (Addison–Wesley, Reading, MA, 1979).
[324] G.A. Marsaglia, in *Computer Science and Statistics: The Interface*, edited by L. Billard (Elsevier, Amsterdam, 1985).
[325] L.N. Shchur and H.W.J. Blöte, Phys. Rev. E **55,** R 4905 (1997).
[326] D. Stauffer, Int. J. Mod. Phys. C **10,** 807 (1999).
[327] P. Heller, Rep. Prog. Phys. **30,** 731 (1967).
[328] M. Vicentini–Missoni, in *Critical Phenomena*, edited by M.S. Green (Academic Press, New York, 1971).
[329] H.G. Ballesteros, L.A. Fernández, V. Martin–Mayor, *et al*., Phys. Lett. B **441,** 330 (1998).
[330] R.H. Swendsen, Phys. Rev. B **20,** 2080 (1979).
[331] L.P. Kadanoff, Physics **2,** 263 (1966).
[332] T.L. Bell and K.G. Wilson, Phys. Rev. B **10,** 3935 (1974).
[333] C. Di Castro and G. Jona–Lasinio, in *Phase Transitions and Critical Phenomena*, edited by C. Domb and M.S. Green, Vol. 6 (Academic Press, Lond., 1976).
[334] K. Symanzik, J. Math. Phys. **7,** 510 (1966).
[335] M. Kac, *Enigmas of Chance* (Harper and Row, New York, 1985).

[336] C.A. Hurst, J. Math. Phys. **6,** 11 (1965).
[337] F. Barahona, J. Phys. A. Math. Gen. **15,** 3241 (1982).
[338] S. Istrail, *Proceedings of the 32nd ACM Symposium on the Theory of Computing (STOC00)*, May 21–23 (ACM Press, Portland, OR, 2000), p. 87–96.
[339] B.A. Cipra, Science **288,** 1562 (2000).
[340] B.A. Cipra, SIAM News **33,** 6 (2000).
[341] R. Feynman, *Lectures on Statistical Mechanics* (Addison–Wesley, New York, 1972).
[342] P.W. Kasteleyn, in *Graph Theory and Theoretical Physics*, edited by F. Harary (Academic Press, New York, 1967).
[343] H.N.V. Temperley, in *Phase Transitions and Critical Phenomena*, edited by C. Domb and M.S. Green, Vol. 1 [(Academic Press, New York, 1974).
[344] M. Livio, *The Golden Ratio* (Random House, New York, 2002).